UNIVERSITÉ DE STRASBOURG

ÉCOLE DOCTORALE des Science de la Vie et de la Santé

Institut de Génétique et de Biologie Moléculaire et Cellulaire (IGBMC)

CNRS UMR 7104 - INSERM U964 – Université de Strasbourg

THÈSE DE DOCTORAT

Présentée par : **Naimah ZEIN**

Soutenue le 14 **Décembre 2018**

Pour obtenir le grade de : **Docteur de l'université de Strasbourg**

Discipline : Sciences de la Vie et de la Santé

Spécialité : Aspects Moléculaires et Cellulaires de la Biologie

"CpdX", a non-steroidal Selective Glucocorticoid Receptor Agonistic Modulator (SEGRAM) selectively triggers the beneficial anti-inflammatory activity of glucocorticoids, but not their long-term debilitating effects

Directeurs de Thèse : **Pr. CHAMBON Pierre** (IGBMC - Université de Strasbourg)

Dr. JESSEL Nadia (Faculté de Médecine - Université de Strasbourg)

RAPPORTEURS : **Pr. SOUMELIS Vassili** (CHU de Paris Diderot, Paris)

Pr. SELLAM Jérémie (Hôpital Saint-Antoine, AP-HP, Paris)

Examinateur interne : Dr. FROSSARD Nelly (Faculté de Pharmacie - Université de Strasbourg)

CONFIDENTIEL

À mes parents

À mes frères

Remerciements

En premier lieu, je tiens à remercier mon directeur de thèse, monsieur le Professeur PIERRE CHAMBON, pour la confiance qu'il m'a accordée en acceptant d'encadrer ce travail doctoral, pour ses multiples conseils et pour toutes les heures qu'il a consacrées à diriger cette recherche. J'aimerais également lui dire à quel point j'ai apprécié sa grande disponibilité et son respect sans faille des délais serrés de relecture des documents que je lui ai adressés. J'ai été extrêmement sensible à ses qualités humaines d'écoute et de compréhension tout au long de ce travail doctoral.

Je tiens également à remercier ma co-directrice de thèse, Mme le Docteur NADIA JESSEL, pour sa confiance en moi, son aide et son support scientifique et moral. Ainsi, je la remercie pour ses multiples encouragements et sa gentillesse.

Je souhaite remercier les membres de mon jury de thèse, le Professeur Vassili SOUMELIS, le Professeur Jérémie SELLAM et la Docteur Nelly FROSSARD, d'avoir accepté d'évaluer mon travail de thèse.

Je tiens à remercier Dr. Catherine Schuster, Directrice de l'école Doctorale des Science de la Vie et de la Santé de Strasbourg, ainsi que le Dr. Serge Potier.

Je suis particulièrement reconnaissante à Katell MORVAN, pour son aide administratif et son support moral qu'elle a accordé à l'égard de ma thèse.

Je souhaiterais aussi adresser ma gratitude à Valérie, pour son assistance et son aide.

Je souhaite exprimer ma gratitude aux membres de l'équipe Chambon. Merci à Jacky HUA pour son encadrement et ses aides scientifiques et techniques. Un grand Merci à Laetitia, Nisha, Manohar et Atish pour leur aide leur support.

Ma reconnaissance va aussi à ma Famille et mes amis.

TABLE OF CONTENTS

RESUMÉ des principaux résultats en Français

Caractérisation *in vitro* et *in vivo* de ligands non-stéroïdiens du récepteur des glucocorticoïdes dotés d'activités anti-inflammatoires bénéfiques, mais dépourvus des effets secondaires indésirables des glucocorticoïdes de synthèse

Les glucocorticoïdes (GC) sont les principales hormones du stress. Ils sont nécessaires à tous les stades de la vie et contrôlent de nombreux processus physiologiques, en se liant à leur propre récepteur, le récepteur des glucocorticoïdes (GR), qui appartient à la superfamille des récepteurs nucléaires. Il est présent dans toutes les cellules des vertébrés, et contrôle l'expression de nombreux gènes impliqués dans de multiples processus physiologiques, tels que le développement, le métabolisme et la réponse immunitaire.

Du point de vue structural, le GR est une protéine modulaire composée de plusieurs domaines:

(i) un domaine de transactivation et de transrepression N-terminal (NTD, dénommé "domaine A/B"); **(ii)** un domaine de liaison à l'ADN (DBD, dénommé "domaine C") qui se lie à des séquences d'ADN cibles, appelées éléments de réponse aux glucocorticoïdes (GRE); **(iii)** une région charnière flexible, le "domaine D"; **(iv)** un domaine de liaison à des ligands glucocorticoïdiques (LBD, dénommé "domaine E") et **(v)** un domaine C-terminal (CTD, le "domaine F").

Lors de la liaison d'un glucocorticoïde au LBD, le récepteur cytoplasmique est transloqué dans le noyau, où il exerce l'une des trois fonctions de régulation de la transcription :

(1) La transactivation ''directe'', par la liaison directe du GR associé à son ligand à un élément GRE ''positif'' [(+)GRE], activant ainsi l'expression des gènes cibles.

(2) La transrépression ''directe'', par la liaison directe du GR ''ligandé'' à un GRE négatif (nGRE), et réprimant ainsi directement les gènes cibles.

(3) La transrépression indirecte, par interaction physique du GR associé à son ligand (GR ''ligandé'') à des facteurs de transcription pro-inflammatoires tels que AP-1 et NF-κB, pour bloquer leur activité.

Les propriétés anti-inflammatoires de GCs naturels (cortisone chez l'homme, corticostérone chez les rongeurs) ont été démontrées il y a plus de 60 ans. Depuis, des molécules synthétiques dotées d'activité glucocorticoïdiques ont été largement utilisés pour traiter des multiples affections aigues ou chroniques. Malheureusement, ces traitements sont souvent accompagnés d'une variété d'effets secondaires pathologiques, tels qu'un diabète de type 2, une augmentation du poids corporel, une stéatose hépatique, une ostéoporose, une hypertension et/ou une atrophie cutanée. Ces effets secondaires surviennent durant des traitements au long cours (supérieur à quelques semaines), quelle que soit la dose et la voie d'administration.

Avant que notre laboratoire ne découvre en 2011 la fonction de transrépression directe exercée par le GR ‘’ligandé’’, les effets anti-inflammatoires bénéfiques des glucocorticoïdes étaient attribués à la voie de transrépression indirecte, alors que nombre d’effets secondaires pathologiques paraissaient attribuées à la voie de transactivation directe.

Au cours des quinze dernières années, de multiples travaux ont été consacrés au développement de nouveaux ligands du GR, appelés «dissociés» ou «selectifs» agonistes du GR, (SEGRAs pour SElective GR Agonists), conservant un profil de transrépression, tout en étant dépourvus de leur propriétés de transactivation. Un certain nombre de SEGRAs éventuels ont été synthétisés, mais très peu ont fait l’objet d’essais *in vivo* chez l’animal. Un tel ligand, RU24858, présentait un profil dissocié *in vitro*, mais, des études physiopathologiques n'ont pas confirmé cette dissociation *in vivo*.

Plus récemment, un ligand non-stéroïdien synthétique, ZK245186 (dénommé ultérieurement, Mapracorat), a été décrit comme étant un agent anti-inflammatoire dans le traitement d’affections cutanées. Un effet anti-inflammatoire sur des cellules épithéliales cornéennes soumises à un stress osmotique a aussi été démontré *in vitro*, et également *in vivo* dans des modèles expérimentaux d'inflammation de l'œil sec, avec une activité comparable à celle d’un glucocorticoïde synthétique «traditionnel», [la Dexaméthasone (Dex)], mais avec des effets secondaires réduits. Le Mapracorat a également fait l’objet d’essais cliniques entre juin 2009 et juillet 2013 pour différentes applications. En fait, depuis avril 2018, aucun résultat positif issu de ces essais n'a été rapporté et aucune autorisation de la mise sur le marché n'a été accordée, ce qui suggére que l’administration du Mapracorat pourrait créer des problèmes d'efficacité et/ou des effets secondaires.

Ensuite, des études dans notre propre laboratoire ayant démontré en 2011 que la fonction de ‘’transrépression directe’’ médiée par liaison des glucocorticoïdes au GR est également impliquée dans les effets secondaires indésirables, il est apparu que seule l’utilisation de ligand ne possédant que la fonction de transrépression indirecte serait efficace dans la prévention des effets secondaires indésirables des glucocorticoïdes. Par conséquent, il apparaissait nécessaire de développer des SEGRAs qui n’induiraient ni la fonction de transactivation directe, ni celle de la transrépression directe du GR, tout en induisant son activité de transrépression indirecte et ses propriétés anti-inflammatoires *in vivo*.

A la fin des années 1990, Schering AG, (maintenant Bayer HealthCare Pharmaceuticals), avait développé de nouveaux composés non-stéroïdiens (brevet US 6 245 804), et revendiqué une éventuelle activité bénéfique anti-inflammatoire partiellement dissociée des effets métaboliques indésirables. En 2016, des études propres à notre laboratoire ont montré que parmi de nombreux composés synthétisés par Shering AG, l’un d’entre eux que nous avons dénommé CpdX ne présentait *in vitro* (dans les cellules en culture), ni la fonction de transactivation, ni celle de transrépression directe du GR, tout en stimulant son activité de transrépression indirecte. Depuis, nous avons également testé un dérivé du CpdX qui nous est propre, et que nous avons dénommé CpdX-D3.

L’objet de notre projet de thèse a consisté à caractériser le composé CpdX, ainsi que son dérivé CpdX-D3, quant à leurs activités thérapeutiques et, à démontrer qu’elles sont semblables à

celles des glucocorticoïdes synthétiques couramment utilisés, tout en étant débarrassées de leurs effets secondaires débilitants.

Résultats

Afin de déterminer les effets anti-inflammatoires *in vivo* des composés CpdX et CpdX-D3, dans diverses affections inflammatoires, nous les avons testés chez la souris dans divers modèles pathologiques:

1) Une inflammation cutanée de type ''dermatite atopique'' induite par une application locale d'un analogue de la vitamine D3 (MC903) (**Tableau 1**).
2) Une inflammation cutanée de type ''dermatite de contacte'' induite par une application locale du 12-O-tetradecanoylphorbol-13-acetate (TPA) (**Tableau 2**).
3) Un ''Psoriasis'' expérimental induit par une application locale d'Aldara (en crème) (**Tableau 3**).
4) Un ''syndrome asthmatique'' créé par une application intranasale de ''House Dust Mite'' (HDM) (**Tableau 4**).
5) Un ''syndrome arthritique'' induit par une injection sous-cutanée de collagène dans la queue de la souris (**Tableau 5**).
6) Une ''colite'' induite par administration orale de Dextran Sulfate Sodium (DSS) (**Tableau 6**).
7) Une inflammation oculaire de type ''conjonctivite'' induite dans les yeux de la souris par une application locale d'ovalbumine (**Tableau 7**).

Dans toutes ces affections, nos résultats ont montrés que le traitement par les composés CpdX ou CpdX-D3 réduit l'inflammation avec la même efficacité que la Dexaméthasone (glucocorticoïde synthétique). Encore plus intéressant, dans tous les cas, des traitements à court et à long terme ont montré que CpdX, de même que CpdX-D3, n'entraine pas les effets indésirables caractéristiques des traitements par les glucocorticoïdes de synthèse, notamment un syndrome métabolique, une ostéoporose et/ou une atrophie cutanée. (**Tableau 8**).

Tableau 1: L'inflammation cutanée de type ''dermatite atopique'', induite chez la souris par application locale de ‘’MC903’’, est efficacement réduite par application des SEGRAs CpdX ou CpdX-D3, sans entrainer une atrophie marquée de l’épiderme, semblable à celle qui accompagne l’application d’un corticoïde synthétique, tel que la Dexaméthasone.

Symptômes	Traitement		
	Dexaméthasone	CpdX	CpdX-D3
Aspect de la peau			
Épaississement	Diminué	Diminué	Diminué
Rougeur	Diminuée	Diminuée	Diminuée
Lésions croûteuses	Diminuées	Diminuées	Diminuées
Anomalies cellulaires sur coupes histologiques			
Hyperplasie de l'épiderme	Diminuée de 50-60%	Diminuée de 50-60%	Diminuée de 50-60%
Infiltration de cellules inflammatoires	Diminuée de 70%	Diminuée de 70%	Diminuée de 70%
Diagnostic moléculaire			
Augmentation de l'expression des gènes pro-inflammatoires (mesurée par RT-PCR): IL1β, IL6, COX2, MMP13, TSLP*, IL10* et IL13*	Diminuée de 50-70%	Diminuée de 50-70%	Diminuée de 50-70%

*: Cytokines spécifiques d'une inflammation de type Th2

Tableau 2: L'inflammation cutanée de type ''dermatite de contact'' (induite chez la souris par une application locale de ‘’TPA’’) est efficacement réduite par application locale de CpdX ou de CpdX-D3, sans entrainer une atrophie marquée de l’épiderme, semblable à celle qui accompagne l’application d’un corticoïde synthétique, tel que la Dexaméthasone.

Symptômes	Traitement		
	Dexaméthasone	CpdX	CpdX-D3
Aspect de la peau			
Épaississement	Diminué	Diminué	Diminué
Rougeur	Diminuée	Diminuée	Diminuée
Lésions croûteuses	Diminuées	Diminuées	Diminuées
Anomalies cellulaires sur coupes histologiques			
Hyperplasie de l'épiderme	Diminuée de 50-60%	Diminuée de 50-60%	Diminuée de 50-60%
Infiltration de cellules inflammatoires	Diminuée de 70%	Diminuée de 70%	Diminuée de 70%
Diagnostic moléculaire			
Augmentation de l'expression des gènes pro-inflammatoires (mesurée par RT-PCR): IL1β, IL6, COX2, CCL4, MMP13, TNFα*, TSLP**, IL22*** et IL23***	Diminuée de 40-70%	Diminuée de 40-70%	Diminuée de 40-70%

*: Cytokines spécifiques d'une inflammation de type Th1

**: Cytokines spécifiques d'une inflammation de type Th2

***: Cytokines spécifiques d'une inflammation de type Th17

Tableau 3: L'inflammation cutanée de type ''Psoriasis'', induite chez la souris par une application locale d'Aldara (crème), est efficacement réduite par application locale de CpdX ou de CpdX-D3, sans entrainer l'atrophie marquée de l'épiderme, qui accompagne l'application d'un corticoïde synthétique, tel que la Dexaméthasone.

Symptômes	Traitement		
	Dexaméthasone	CpdX	CpdX-D3
Aspect de la peau			
Épaississement	Diminué	Diminué	Diminué
Rougeur	Diminuée	Diminuée	Diminuée
Lésions croûteuses	Diminuées	Diminuées	Diminuées
Anomalies cellulaires sur coupes histologiques			
Hyperplasie de l'épiderme	Diminuée de 50-60%	Diminuée de 50-60%	Diminuée de 50-60%
Infiltration de cellules inflammatoires	Diminuée de 70%	Diminuée de 70%	Diminuée de 70%
Diagnostic moléculaire			
Augmentation de l'expression des gènes pro-inflammatoires de type Th17 (mesurée par RT-PCR): IL17a, IL17c, IL17f et IL22	Diminuée de 40-70%	Diminuée de 40-70%	Diminuée de 40-70%

Tableau 4: Le syndrome asthmatique, créé chez la souris par une application intranasale de ''House Dust Mite'' (HDM), est efficacement réduit par application de CpdX ou de CpdX-D3, sans entrainer les effets pathologiques qui accompagnent l'application d'un corticoïde synthétique, tel que la Dexaméthasone.

Symptômes	Traitement		
	Dexaméthasone	CpdX	CpdX-D3
Anomalies cellulaires sur coupes histologiques			
Augmentation du nombre des cellules inflammatoires présentes dans le fluide de lavage broncho-alvéolaire (BAL)	Diminué de 60-70%	Diminué de 60-70%	Diminué de 60-70%
Infiltration de cellules inflammatoires péribronchiques et périvasculaires	Diminuée	Diminuée	Diminuée
Présence des cellules caliciformes	Absence	Absence	Absence
Diagnostic moléculaire			
Augmentation de l'expression des gènes pro-inflammatoires (mesurée par RT-PCR): IL1β, IL6, Eotaxin, CCL4, IL4*, IL5* et IL13*	Diminuée de 50-70%	Diminuée de 50-70%	Diminuée de 50-70%
Déclenchement d'une crise déterminée par le test de la fonction des poumons à l'aide de l'appareil ''Flexivant''			
Hyperréactivité des voies respiratoires	Diminuée de 60-70%	Diminuée de 60-70%	-

*: Cytokines spécifiques d'une inflammation de type Th2

Tableau 5: Un syndrome arthritique (créé chez la souris par une injection sous-cutanée de collagène dans la queue) est efficacement réduit par injection intra-péritonéale de CpdX ou de CpdX-D3, sans entrainer les effets pathologiques qui accompagnent l'application d'un corticoïde synthétique, tel que la Dexaméthasone.

Symptômes	Traitement		
Aspect de l'inflammation des pattes	**Dexaméthasone**	**CpdX**	**CpdX-D3**
Gonflement	Diminué	Diminué	Diminué
Rougeur	Diminuée	Diminuée	Diminuée
Epaisseur au niveau de la cheville	Diminuée	Diminuée	Diminuée
Diagnostic moléculaire			
Augmentation de l'expression des gènes pro-inflammatoires (mesurée par RT-PCR): IL1β, IL6, TNFα, IL17a* et IL17f*	Diminuée de 50-70%	Diminuée de 50-70%	Diminuée de 50-70%

*: Cytokines spécifiques d'une inflammation de type Th17

Tableau6: Le syndrome de colite aiguë, créé chez la souris par une administration orale de Dextran Sulfate Sodium (DSS), est efficacement réduit par injection intra-péritonéale de CpdX ou de CpdX-D3, sans entrainer les effets pathologiques qui accompagnent l'application d'un corticoïde synthétique, tel que la Dexaméthasone.

Symptômes	Traitement		
Symptômes observés chez la souris	**Dexaméthasone**	**CpdX**	**CpdX-D3**
Diarrhée	Diminuée	Diminuée	Diminuée
Saignement rectal	Diminué	Diminué	Diminué
Diagnostic moléculaire			
Augmentation de l'expression des gènes pro-inflammatoires (mesurée par RT-PCR): IL1β, IL6, MMP13, TSLP*, IL17a** et IL17f**	Diminuée de 40-50%	Diminuée de 40-50%	Diminuée de 40-50%
Anomalies cellulaires sur coupes histologiques			
Structure des villosités intestinales et de crypte du côlon détruite	Rétablie	Rétablie	Rétablie
Infiltration de cellules inflammatoires de la muqueuse	Diminuée	Diminuée	Diminuée

*: Cytokines spécifiques d'une inflammation de type Th2

**: Cytokines spécifiques d'une inflammation de type Th17

Tableau 7: Une inflammation oculaire de type ''conjonctivite'', induite par une application locale topique d'ovalbumine dans les yeux de la souris, est efficacement réduite par application des SEGRAs CpdX ou CpdX-D3, sans entrainer les effets pathologiques qui accompagnent l'application d'un corticoïde synthétique, telle que la Dexaméthasone.

Symptômes	**Traitement**		
Aspect de l'inflammation des yeux	**Dexaméthasone**	**CpdX**	**CpdX-D3**
Fermeture de l'œil	Non	Non	Non
Épaississement des paupières	Normal	Normal	Normal
Rougeur	Non	Non	Non
Prurit	diminué	diminué	diminué
larmoiement réflexe	diminué	diminué	diminué

Tableau 8: Des traitements à court et à long terme d'affections inflammatoires par CpdX ou CpdX-D3, n'entrainent pas les effets pathologiques induits par les glucocorticoïdes synthétiques tels que la Dexaméthasone.

Effets secondaires pathologiques des glucocorticoïdes	**Traitement**		
Effets à court terme	**Dexaméthasone**	**CpdX**	**CpdX-D3**
Atrophie cutanée			
Aspect de la peau	Atrophiée	Normale	Normale
Epaisseur de l'épiderme (coupes histologiques)	Couche unicellulaire	Couche multicellulaire	Couche multicellulaire
Augmentation de l'expression (mesurée par RT-PCR) du gène Redd1 et diminution de l'expression du gène Kindlin1, pathognomonique d'une atrophie de l'épiderme	Oui	Non	Non
Effets à long terme			
Ostéoporose			
Ostéoporose mesurée par microCT (volume osseux, densitométrie osseuse et épaisseur corticale)	Oui	Non	Non
Expression (mesurée par RT-PCR) du gène marqueur de l'ostéoporose WNT16	Diminuée de 50%	Normale	Normale
Changement dans la composition corporelle			
Poids des souris	Diminué	Normal	Normal
Masse lipidique abdominale	Augmentée	Normale	Normale
Apoptose du thymus	Oui	Non	Non
Changement des glandes surrénales			

Poids des glandes surrénales	Diminué de 50%	Augmenté de 10%	Augmenté de 10%
Taux sanguin de la corticostérone le matin	Diminué de 85%	Augmenté de 400%	Augmenté de 400%
Taux sanguin de la corticostérone le soir	Diminué de 40%	Augmenté de 10%	Augmenté de 10%
Taille de zone Fasciculata (Coupes histologiques)	70% diminuée	10% augmentée	10% augmentée
Expression (mesurée par RT-PCR) des gènes: Cyp11A/Cpy11B/HSD3B impliqués dans la synthèse de la corticostérone	Diminuée de 50%	Augmentée de 10%	Augmentée de 10%
Syndrome métabolique (Diabète de type 2)			
Hyperglycémie	Oui	Non	Non
Hyperinsulinémie (Résistance à l'insuline)	Oui	Non	Non
Taux sanguin du cholestérol et des acides biliaires	Augmentés	Normaux	Normaux
Dépôts de lipides dans le foie (coupes histologiques)	Oui	Non	Non
Expression (mesurée par RT-PCR) des gènes FASN et SCD1 impliqués dans la lipogenèse hépatique	Augmentée de 50%	Normale	Normale

Conclusions

Pour conclure, les composés CpdX et CpdX-D3 se sont révélés très efficace dans le traitement d'affections inflammatoires majeures, sans entrainer les effets secondaires qui limitent très sérieusement l'utilisation des glucocorticoïdes de synthèse à long terme, en induisant en particulier un syndrome métabolique accompagné de l'apparition d'un syndrome diabétique de type 2 et d'une ostéoporose associée à des fractures spontanées.

MAIN ABREVIATIONS

A

ACTH:	Adrenocorticotrophic hormone
AD:	Atopic dermatitis
AP-1:	Activator protein 1

C

CCL:	C-C motif ligand
CD:	Crohn's disease
CDSN:	Corneodesmosin
CD4+:	Cluster of differentiation 4+
CRF:	Corticotropin-releasing factor
CRH:	Corticotropin-releasing hormone
COX-2:	Cyclooxygenase-2
CTD:	C-terminal domain

D

DBD:	DNA-binding domain

F

FLG:	Fillagrin

G

GC:	Glucocorticoid
GH:	Growth hormone
GR:	Glucocorticoid receptor
GRE:	Glucocorticoid-responsive element
(+)GRE:	Positive glucocorticoid-responsive element
GSK-3:	Glycogen synthase kinase 3

H

HDAC3:	Histone deacetylase 3
HDM:	House Dust Mite
HPA:	Hypothalamic-pituitary-adrenal
HSD11β:	Hydroxysteroid 11-beta dehydrogenase
Hsp:	Heat shock proteins

I

IBD:	Inflammatory bowel diseases
IFN-γ:	Interferon gamma
Ig:	Immunoglobulin
IGF-1:	Insulin-like growth factor-1
IL:	Interleukin
IR:	Inverted repeat

J

JNK:	JUN N-terminal kinase

L

LBD:	Ligand binding domain

M

MAPK:	Mitogen protein kinase

N

NAFLD:	Non-alcoholic fatty liver disease
NCoR1:	Nuclear receptor corepressor 1
NF-κB:	Nuclear factor-kappa B
nGRE:	Negative glucocorticoid-responsive element
NR:	Nuclear receptor
NR3C1:	Nuclear receptor subfamily 3, group C, member 1
NTD:	N-terminal domain

P

PTM:	Post-translational modification

R

RA:	Rheumatoid arthritis
RXR:	Retinoid X receptor

S

SAID:	Steroidal anti-inflammatory drug
SEGRAM:	Selective Glucocorticoid Receptor Agonistic Modulator
SMRT:	Silencing mediator for retinoid and thyroid-hormone receptor
SRC:	Steroid receptor coactivator
SUMO:	Small ubiquitin-related modifier

T

TF:	Transcription factor
Th:	T helper
TIF2:	Transcriptional mediators/intermediary factor 2
TLR7:	Toll-like receptor 7
TNF-α:	Tumor necrosis factor-α
TSLP:	Thymic stromal Lymphopoietin

U

UC:	Ulcerative colitis

INDEX OF FIGURES

INTRODUCTION

1. Glucocorticoids (GCs) and their receptor

1.1. Glucocorticoids

Glucocorticoids (GCs) are steroid hormones necessary at all stages of the vertebrate life. They regulate numerous physiological processes by binding to their cognate receptor, the glucocorticoid receptor (GR), in an effort to maintain homeostasis, particularly under stress conditions.

Due to their multiple functions in development and homeostasis, GCs are described as consummate multi-taskers. They play important physiological roles in the central nervous and immune systems and during the perinatal maturation of lungs. Alterations of GC homeostasis may result in long-lasting effects under physiological and pathological conditions.

GCs mediate communication between the hypothalamus and peripheral tissues, and coordinate physiological and mental responses to stress, for example by increasing the level of glucose in the blood through promoting hepatic gluconeogenesis and catabolism of fat reserves. Along with increase of blood pressure and alteration of cognitive functions, these changes elevate readiness to combat stress. Importantly, in the immune system, GCs exert important homeostatic functions, in order to prevent excessive and harmful responses to antigens and infections, *see* (Clark & Belvisi, **2012**) *for review*.

1.1.1. **Biosynthesis of glucocorticoids and its regulation**

1.1.1.1. The Hypothalamic-pituitary-adrenal (HPA) axis controls the synthesis of glucocorticoids

The Hypothalamic-pituitary-adrenal (HPA) axis comprises three structures: the hypothalamus, the pituitary gland and the adrenal cortex. The HPA axis activity is mediated by the secretion of the Corticotropin-Releasing Factor (CRF, also referred to as Corticotropin-Releasing Hormone (CRH)) in the hypothalamus. The CRF stimulates the corticotropic cells of the anterior pituitary gland to release the adrenocorticotrophic hormone (ACTH), which in its turn activates the secretion of the glucocorticoids in the zona fasciculata of the adrenal cortex. Glucocorticoids inhibit the secretion of CRF in the hypothalamus, and of ACTH in the pituitary gland, which is called the feedback inhibition of GCs synthesis (**Figure 1**), *see* (Clark & Belvisi, **2012**) *for review*.

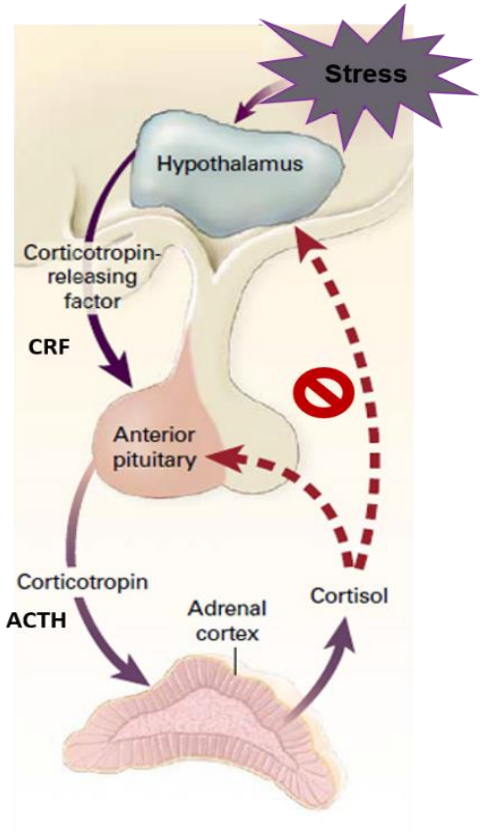

Figure 1: Schematic representation of the mechanism involved in the control of cortisol levels by the HPA axis.

1.1.1.2. The pathway of glucocorticoids synthesis from cholesterol

Glucocorticoids are synthetized from cholesterol (**Figure 2**), in the zona fasciculata of the adrenal cortex, where its synthesis and release into systemic circulation is controlled by the HPA axis. Under normal conditions, the endogenous GC levels in the blood display circadian variations that are regulated by the central clock located in the suprachiasmatic nucleus of the hypothalamus, with a peak at the beginning of the period of greatest activity (the morning in humans, nightfall in mice and in many other rodents), *see* (Clark & Belvisi, **2012**) *for review*.

The level of active GCs in tissues (brain, muscles, lung, pancreas, skin, etc…) is controlled by two enzymes: the hydroxysteroid 11-beta dehydrogenases (HSD11β) 1 and 2 (Draper & Stewart, **2005**). HSD11B1 transforms the inactive cortisone to cortisol, while HSD11B2 catalyzes the opposite reaction. The sensitization or desensitization of cells to GCs effects is mediated by modulation of the expression of genes encoding these two enzymes, *see* (Clark & Belvisi, **2012**) *for review*.

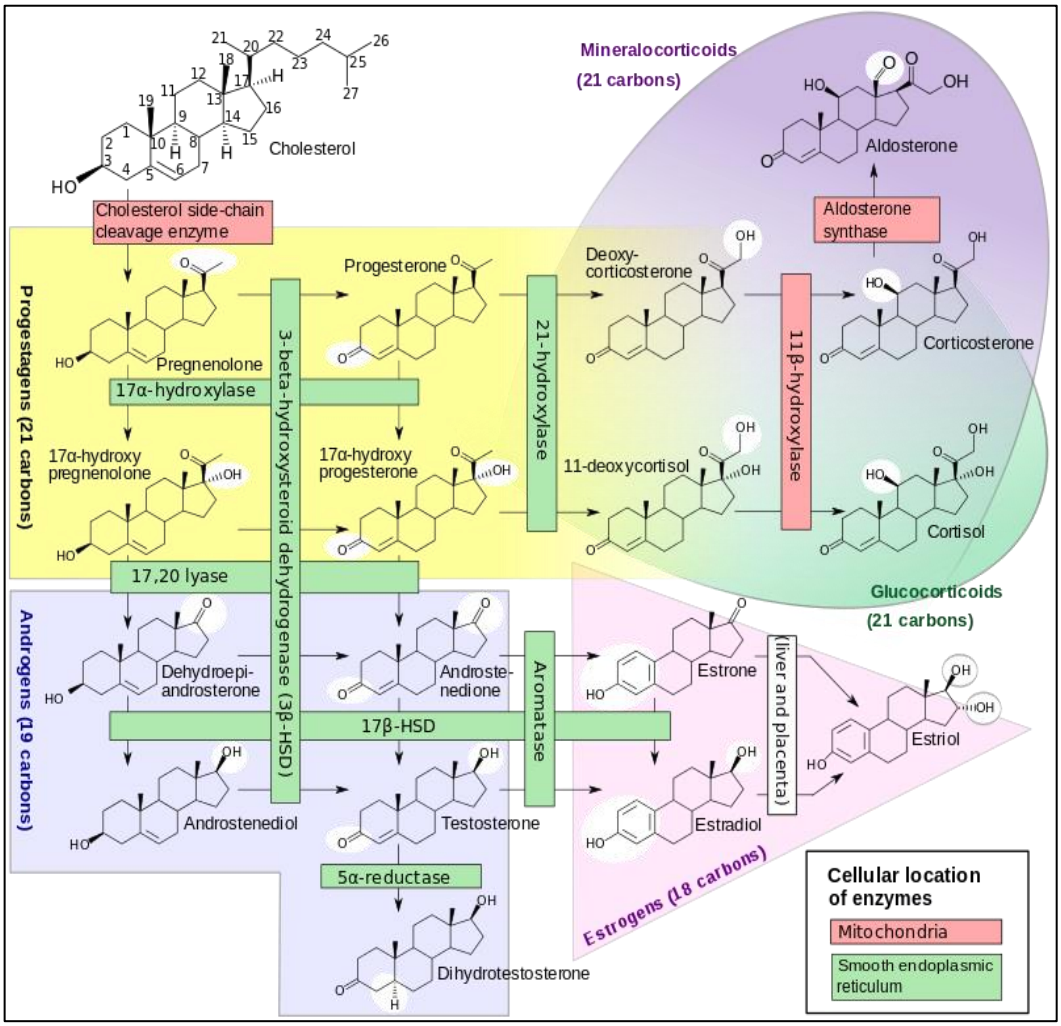

Figure 2: The pathway of glucocorticoids and mineralocorticoids synthesis from cholesterol. (WikiJournal of Medecine, **2014**)

1.2. The glucocorticoid receptor (GR)

1.2.1. Structure

The glucocorticoid receptor (GR) is a transcription factor (TF) which belongs to the superfamily of nuclear receptors (NR); it is also known as NR3C1 (nuclear receptor subfamily 3, group C, member 1). The GR is encoded in the NR3C1 gene, which is located on chromosome 5 in humans, and comprises 9 exons, *see* (Clark & Belvisi, **2012**) *for review*.

In most cell types, the GR is a protein of 777 amino acids. It is composed of several domains (**Figure 3**):

- an N-terminal transactivation and transrepression domain (NTD, or "A/B domain");
- a central DNA-binding domain (DBD, called the "C domain"). This C domain is the most conserved domain across the nuclear receptor superfamily and contains two zinc finger motifs that recognize and bind target DNA sequences, called glucocorticoid-responsive elements (GREs);
- a flexible hinge region (the "D domain");
- a C-terminal ligand binding domain (LBD, or "E domain"). This domain forms a hydrophobic pocket for GCs binding;
- and a C-terminal domain (CTD or "F domain").

Alternative splicing events give rise to 3 GR isoforms (GRα, GRβ and GRγ), GRα is the predominant isoform. GR isoforms differ at the C-terminus (GRβ) or within the DNA-binding domain (GRγ). In addition, alternative sites of translation initiation generate isoforms lacking some or all of AF1. GCs sensitivity can be modulated by the relative levels of expression of these isoforms in a cell specific manner. For example GRβ may function as a dominant negative, GC-independent regulator of transcription in cells in which its expression is sufficiently high.

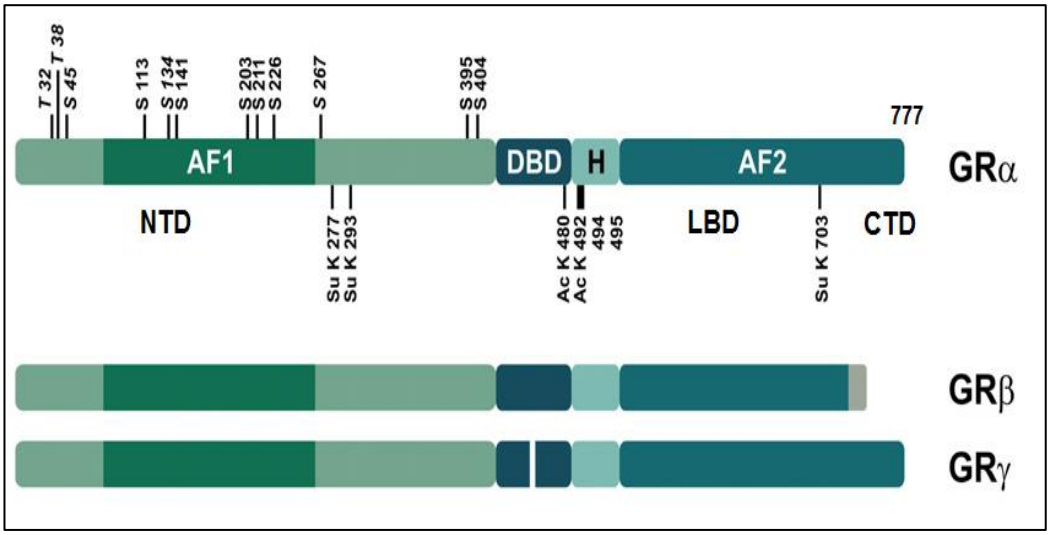

Figure 3: Glucocorticoid receptor (GR) gene structure and GR isoforms, *see* (Clark & Belvisi, **2012**) *for review*.

1.2.2. Modes of action of GCs

In the absence of ligand, the GR primary resides in the cytoplasm (Hua, Ganti, & Chambon, **2016**), where it is associated with a complex of heat shock proteins (hsp90, hsp56, hsp40) and other immunophilins (FKBP51, FKBP52, cyp44, pp5). These proteins maintain the receptor in an appropriate conformation to promote ligand binding within a hydrophobic pocket in the C terminus. Upon binding of a GC to the GR LBD, the GR undergoes a conformational change that results in the exposition of two nuclear localization signals located at the DBD/hinge region junction and within the LBD, respectively. GR is then rapidly translocated into the nucleus through nuclear pores, where it can exert one of its three transcriptional regulatory functions (**Figure 4**).

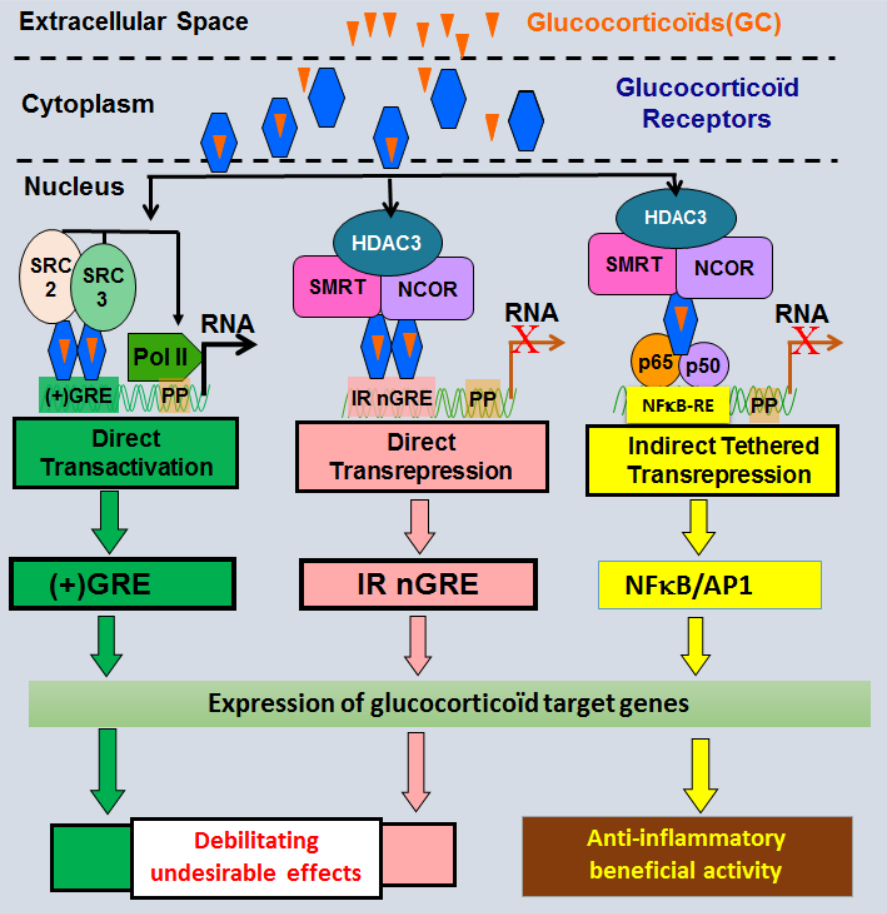

Figure 4: Scheme showing the three transcriptional regulatory functions of the glucocorticoid receptor (GR) upon binding of a glucocorticoid (GC).

1.2.2.1. Transcriptional direct transactivation through binding of the GR to (+)GREs

Homodimers of GR recognize directly *cis*-acting positive GC response elements GREs ((+)GREs), thereby activating the expression of target genes. The consensus palindromic (+)GRE sequence, GGAACANNNTGTTCT (with N being any of A, T, C or G), is often an imperfect palindrome comprising two 6-base pair half sites separated by 3 base pairs, hence termed "IR3" (for "inverted repeat 3"), see (Clark & Belvisi, **2012**) for review.

It has been shown that the transactivation by the agonist-liganded GR is mediated through the association with the coactivators of the steroid receptor coactivator (SRC) family, such as (SRC1, TIF2/SRC2 and SRC3) (Surjit et al., **2011**).

1.2.2.2. Transcriptional direct transrepression through binding of the GR to nGREs

Direct transrepression is mediated by the interaction of the GR with negative GC response elements (nGREs), which mediate the direct repression of specific genes. The consensus nGRE sequence, $CTCC(N)_{0\text{-}2}GGAGA$ (with N being any of A, T, C or G), is also palindromic, but differs from the classic (+)GRE in sequence and spacer length (and is therefore named IR0, IR1 or IR2, as the case may be) (Surjit et al., **2011**).

The IR nGRE-mediated direct repression requires the formation of a repressive complex at the IR nGRE DBS. This complex comprises one or both of the corepressors SMRT (silencing mediator for retinoid or thyroid-hormone receptors) and NCoR1 (nuclear receptor corepressor 1), as well as the histone deacetylase (HDAC3) (Hua, Paulen, & Chambon, **2016**).

1.2.2.3. Transcriptional indirect transrepression through binding of the GR to NF-κB, AP-1 or STAT3

The indirect transrepression activity of GCs is an important negative regulatory mechanism, which is also called “tethered transrepression”, and arises from the physical interaction of GC-bound GR with pro-inflammatory transcription factors: the activator protein-1 (AP-1), the nuclear factor-kappa B (NF-κB) and STAT3. Through binding to the Jun subunit of AP-1, the p65 subunit of NF-κB and STAT3, The GR antagonizes their activity and interferes with the transcriptional activation function of these three proteins (Clark & Belvisi, **2012**).

Moreover, the GC-induced tethered indirect transrepression requires the NCoR1 and/or the SMRT corepressors; however, these corepressors are not required for the tethered association of the GR to NF-κB or AP1 bound to their cognate DNA binding

sites. It was also shown that HDAC3 plays an essential role in GC-induced tethered transrepression *in vivo* (Hua, Ganti, et al., **2016**).

1.2.3. Post-translational modifications (PTMs) of the GR

The GR is subject to a number of post-translational modifications (PTMs), such as phosphorylation, sumoylation and ubiquitylation. PTMs play important roles in the stability and the subcellular distribution of the GR, the DNA binding, the ligand response, as well as the transcriptional activities.

1.2.3.1. Phosphorylation

Phosphorylation (generally on Serine, Threonine or Tyrosine residues) has been shown to modulate dimerization of GR, its DNA binding, nuclear localization, coregulator interaction, and ligand binding affinity, all of which alter the transcriptional activities. Generally, phosphorylation of the GR increases its protein half-life.

To date, seven phosphorylation sites on GR have been experimentally confirmed and are clustered within the NTD: (Ser113, Ser134, Ser141, Ser203, Ser211, Ser226 and Ser404). These serine residues are conserved among humans, mice and rats. The enzymes responsible for the phosphorylation of the GR *in vivo* are the mitogen protein kinases (MAPKs), the JUN N-terminal kinases (JNKs) and the glycogen synthase kinase 3 (GSK-3).

It has been reported that the phosphorylation of Ser203, Ser211 and Ser226 residues, which are located in the AF1, plays an essential role in the exposure of protein surfaces, which is critical for cofactor interactions.

Upon ligand binding, Ser203 is phosphorylated and the GR is translocated into the nucleus; it has been shown that the mutation of this site precludes nuclear accumulation and subsequent GR-dependent gene regulation. However, the Ser226

phosphorylation via the JNK signaling pathway, results in elevated nuclear export, thus decreasing gene regulation through GR.

Furthermore, our laboratory has shown that the phosphorylation at the two serine residues (Ser226 and Ser404) may boost the Sumoylation of the GR, which is mandatory for the transrepression (Hua, Paulen, et al., **2016**; Tan & Wahli, **2016**).

1.2.3.2. Sumoylation

Small ubiquitin-related modifier 1 (SUMO-1) is a polypeptide, that can be covalently ligated to lysine residues of a variety of target proteins, and can alter their stability, localization or transcription regulatory activity. The GR can be sumoylated at three lysine residues: K277 and K293 located in the NTD and K703 in the LBD. GR sumoylation at specific lysine residue triggers molecular transrepression pathways that are linked to inflammation (Hua, Ganti, et al., **2016**; Hua, Paulen, et al., **2016**).

Studies in our laboratory have shown that Sumoylation of a lysine residue in human and mouse GR (K293 of human GR) located in the NTD, is indispensable for either form of transrepression *in vitro* and *in vivo*. These studies have also reported that lysine K579 of the human GR LBD was mandatory for NCoR1 binding to Sumoylated GR and for the IR nGRE-mediated repression; no such dependency was reported for the SMRT binding and repression.

More interestingly, the SMRT/NCoR1 corepressors associated with HDAC3 and the repressive complexes of sumoylated GR neither bound to a (+)GRE nor inhibited (+)GRE-mediated transactivation. This showed that recruitment and formation of the repressive complexes were specific to IR nGREs (Hua, Paulen, et al., **2016**; Tan & Wahli, **2016**).

Seemingly, the sumoylation of the GR, the recruitment and the formation of the SMRT/NCoR1-HDAC3 repressing complex, is required for its binding to IR nGREs. In addition, *in vitro* and *in vivo* studies have shown a similar dependence on a

Sumoylated GR NTD for corepressor recruitment (SMRT/NCoR1) in the tethered indirect transrepression.

However, the sumoylation was dispensable for the binding of GR to DNA bound TFs (NF-κB/AP-1/STAT3); instead, the GR LBD was needed to interact with NF-κB or AP1, as proven by the loss of DNA-bound c-Jun or p65, to a LBD-deleted GR (Hua, Paulen, et al., **2016**; Tan & Wahli, **2016**).

2. Inflammation

An inflammatory reaction (inflammation) is the biological response of the vascularized tissues to harmful stimuli, such as pathogens, irritants or damaged cells. This protective response is mediated by blood vessels, immune cells, and molecular mediators. The role of inflammation is to remove the cause of cell injury, to eliminate necrotic cells, lesions and tissues damaged, and to initiate tissue repair.

The classical signs of inflammation are: fever, pain, redness, swelling, and loss of function. Inflammation is considered as a mechanism of innate and adaptive immunity. Indeed, a properly mounted immune response is essential for recognizing and eliminating pathogens arising from foreign invaders and tissue trauma.

Inflammatory cells respond to foreign molecules and inflammatory stimulus by producing bioactive substances such as prostanoids, cytokines and chemokines. These mediators have pleiotropic effects and interact with many immune cell types to initiate the inflammatory response. The dysregulation of these reactions can lead to acute and chronic inflammatory disorders. Indeed, pharmacological intervention is essential to attenuate cellular inflammation controls. The key enzyme responsible for the induction and the production of mediators is the Cyclooxygenase-2 (COX-2) and the NF-κB activation pathway, which controls the transcription of inflammatory genes. These two pathways are considered as attractive targets for developing anti-inflammatory therapeutics, as they are activated by several inflammatory stimuli.

2.1. Inflammatory diseases

2.1.1. Allergic inflammation

Allergy is the susceptibility of some people to react upon an exposition to certain antigens (allergens). One of the common features of allergic disorders is the production of allergen-specific IgE and expansion of allergen-specific T helper 2 (Th2) cells. Allergic inflammation like asthma, atopic dermatitis and rhinitis are becoming more frequent in the developed countries.

In the environment, different types of allergens exist, such as House Dust Mite (HDM) or eggs (ovalbumin) witch can induce the production of IgE. There are some other substances, which can induce an adaptive immune reaction independently of immunoglobulins, as it is the case for the nickel-induced contact dermatitis.

An allergic inflammation can develop depending on the type and concentration of the allergen, as well as the frequency of exposure to the same allergen that promote a Th2 immune response. It has been shown that a defective epidermal barrier function is a critical factor in the initiation of an atopic dermatitis (AD), and also in the progression from this disease to asthma (J. G. Li et al., **2016**).
The epithelium permeability to allergens is influenced by the expression of some genes, for example CDSN and FLG. CDSN, which is a gene coding for a protein of corneodesmosomes (the corneodesmosin), is responsible for the maturation and adhesion of corneocytes in the stratum corneum of the epidermis. Mutations in this gene are associated with chronic dermatitis or infection in the skin in atopic diseases and allergies. FLG is a gene coding for fillagrin, a protein of the epidermis that regulates the structure of the stratum corneum. It has been reported that mutations in this gene are associated with the development of allergic diseases.

2.1.1.1. Atopic dermatitis

Atopic dermatitis (AD), also known as atopic eczema, is a chronic inflammatory skin disease. It is characterized by eczematous skin lesions (red patches with blistering and crusting that can lead to scaling, cracking and thickening of the skin), and intense itching (**Figure 5**) (Brunello, **2018**).

The phenotype of AD patients is variable with age, ethnicity and severity. Usually, AD lesions are distributed in the skin body areas in an age-manner; they are found on the face and trunk in infants, on the body folds in children (2 of 10 children) and on hands and eyelid in adults (prevalence of 10%) (**Figure 5**). AD can be a reason of psychological burden on patients and their relatives, and can lead to some other atopic diseases (food allergy, asthma, allergic rhinitis and allergic conjunctivitis), and mental disorders (Weidinger & Novak, **2016**).

Prevention to reduce AD may involve early consummation of some foods by infants, such as peanuts, milk and hen eggs that can decrease the risk of the sensitization (Brunello, **2018**).

AD presents the same immunological characteristics as other atopic diseases, including Th2 inflammation with Th2 cytokine production, lesional eosinophilia and IgE high level. Skin lesions in atopic diseases are the results of the interactions between IgE antigen presenting cells, T cells activation eosinophils and keratinocytes. These diseases are associated with mast cells degranulation and eosinophilia (Galli et al., **2007**).

The expression of the thymic stromal lymphopoietin (TSLP) is considered as a key regulator of Th2 allergies, such as AD and asthma (Liu, **2006**). Studies in our laboratory have shown that keratinocyte selective ablation of the Retinoid X Receptors (RXRα and RXRβ) in the epidermis (RXRαβ ep-/- mutant mice) induces a high expression of TSLP in keratinocytes of an human AD-like in mice. A topical treatment with vitamin D3 or with its low calcemic analogue (MC903), induces

increased expression of TSLP in keratinocytes of mice and leads to an AD-like phenotype in a TSLP dependent manner (M. Li et al., **2006**). GCs are presently used for the treatment of AD, due to their beneficial anti-inflammatory effects.

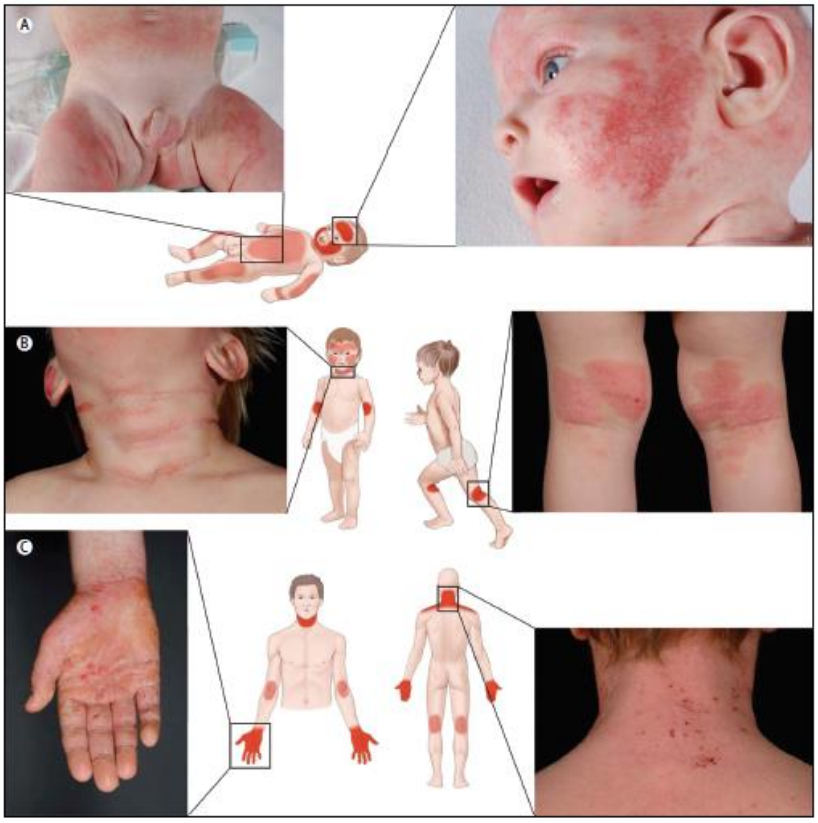

Figure 5: Typical clinical appearance and locations of atopic dermatitis at different ages. (A) In infants, AD is generally acute. (B) From age 1–2 years, polymorphous manifestations with different types of skin lesions are seen. (C) Adolescents and adults often present lichenified and excoriated plaques (Weidinger & Novak, **2016**).

2.1.1.2. Asthma

Asthma is an inflammatory disease, that affects the airways (**Figure 6**), and is characterized by an increased bronchoconstriction and a highly sensitivity to an inhaled antigen. In modern society, asthma is becoming very prevalent and it represents a global health problem. As today, antihistamines and steroids are the most effective drugs used for treating asthma; they act by targeting signaling pathways and by suppressing different types of immune cells.

However, certain biological therapies have been developed to treat resistant patients. Prominently, antibodies targeting IgE are prescribed in case of the fall of the usual therapies. In addition to the anti-IgE, several antibodies are in development in order to target other cytokines and their receptors (such as IL-2, IL-13, IL-5, IL-1, and TNF-α) to treat severe asthma patients.

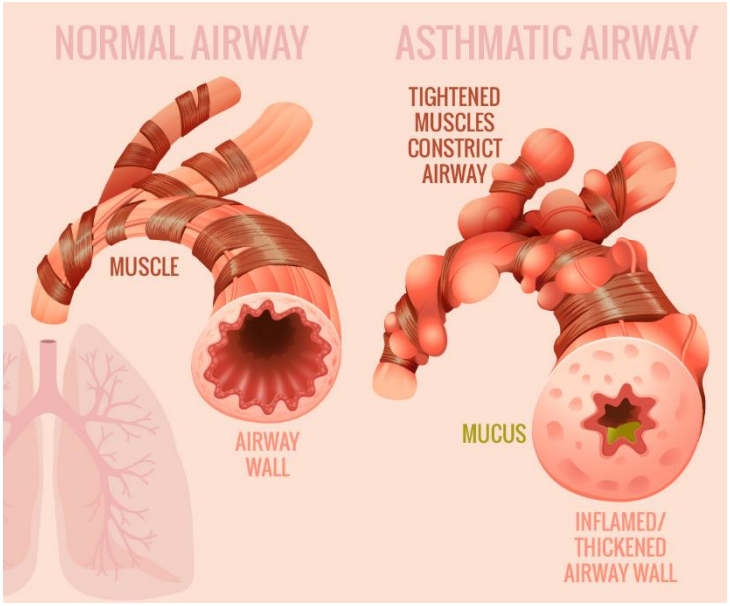

Figure 6: Normal and asthmatic airways. (National Heart, Lung, and Blood Institute, **2014**, http://www.nhlbi.nih.gov/health/health-topics/topics/asthma/#).

2.1.1.3. Allergic conjunctivitis

Allergic conjunctivitis is a common form of ocular allergy. It is characterized by two phase responses: early and late-phase responses, and it is usually associated with type 1 hypersensitivity reactions. Patients suffering from conjunctivitis present some common symptoms, such as hyperemia, tearing, itching and chemosis. The early-phase response is developed directly after exposure to the allergen, and it is characterized by mast cell degranulation. After 6 to 10 hours, the late-phase response appears, it is characterized by an infiltration of some inflammatory cells in the conjunctiva, such as, eosinophils, neutrophils and lymphocytes (Bielory et al., **2014**). This leads to the secretion of cytokines, chemokines and inflammatory molecules

witch contribute to a serious chronic disorder. Recruitment of eosinophils and other immune cells is mediated by the chemokines C-C motif ligand 5 (CCL5) and 11 (CCL11) (Bisset & Schmid-Grendelmeier, **2005**). This recruitment of immune cells leads to the production of several cytokines, such as tumor necrosis factor-α (TNF-α) and interleukin-1β (IL-1β) and chemokines like interleukin-8 (IL-8).

Glucocorticoids are the most potent treatments used for allergic eye disease, they have the capacity to inhibit the secreted cytokines and chemokines that lead to the eosinophils activation. However, treatment with GCs is associated with several side effects, such as increase in the intraocular pressure, decreased resistance to infections and risk of cataract.

2.1.2. Psoriasis

Psoriasis is a chronic, systemic, immune-mediated disease, associated with severe cutaneous manifestations and negative effects on patient quality of life. It affects the skin and the joints, and can be manifested by different phenotypes, (the most common form of psoriasis is the psoriasis vulgaris). Psoriasis is characterized by soreness and skin lesions with burning and itching (Greb et al., **2016**).

During the different phases of the disease, the innate and adaptive immune systems are chronically activated, then pro-inflammatory cytokines are released in the blood, which this leads to the damage of different tissues and organs for a long-term period. Psoriasis is associated with some other complications: ‘’rheumatological type’’ in case of the psoriatic arthritis, or cardiovascular and psychiatric in some other cases. This contribute to a bad quality of life of the patients.

Psoriasis can be initiated by many factors, such as heritable predisposition, endocrine hormones, infection or mechanical trauma, as well as some medicines (β-blockers or lithium) and imiquimod (a Toll-like receptor 7 (TLR7) agonist) (Ogawa, Sato, Minagawa, & Okuyama, **2018**).

It has been reported that a topical treatment with imiquimod in mice skin induce a psoriasis-like inflammation through the IL-23/IL-17 axis with the activation of a variety of immune cells. Cells involved in this disorder are keratinocytes, dendritic and T cells (especially $CD4^+$ Th1 and Th17 cells). Dendritic cells are responsible for the secretion of IL-12 and IL-23, and then to the activation of T cells. Activated Th1 cells, Th17 cells and Th22 cells produce IFN-γ, IL-17 and IL-22 respectively (**Figure 7**).

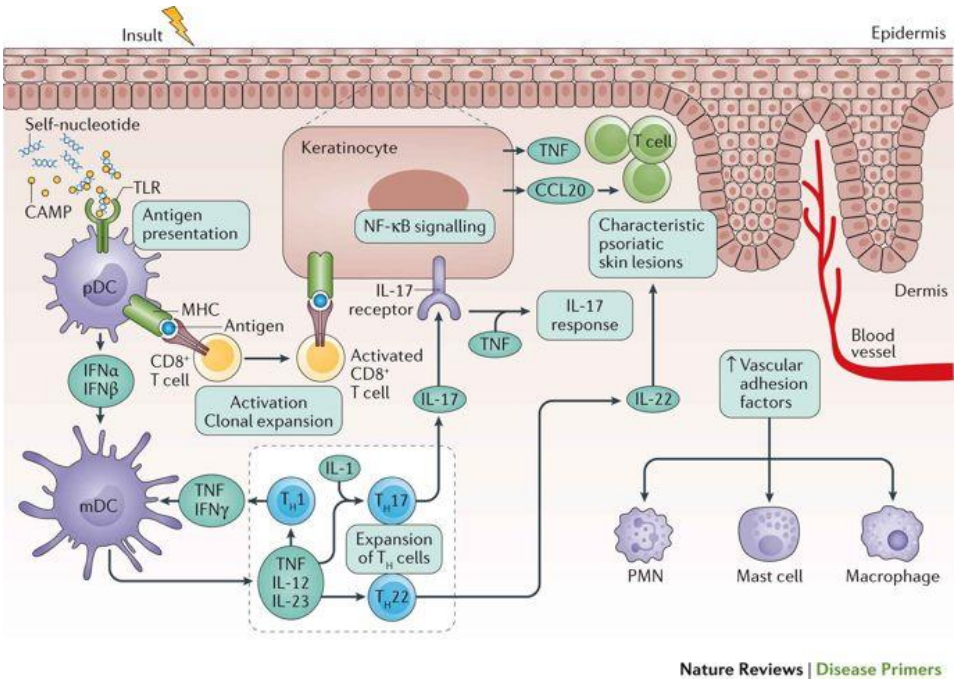

Figure 7: Mechanisms of psoriasis (Greb et al., **2016**).

2.1.3. Rheumatoid arthritis

Rheumatoid arthritis (RA) is a chronic, autoimmune inflammatory disease. It is characterized by an alteration of the synovial membrane, the cartilage and the bone tissue (**Figure 8**). Leading to hard pain, impaired joint function and decrease in the mobility.

The regulation and the resolution of the inflammation in RA are leading by cytokine-mediated processes, for example, the activation of Th2 cells by interleukins IL-4 and IL-13, the induction of inflammation by IL-9, the eosinophil expansion by IL-5-induction, the IL-33-mediated macrophage polarization, the IL-10 production by the

inflammatory B cells and the IL-27-mediated suppression of lymphoid follicle formation (Chen, Bozec, Ramming, & Schett, **2018**).

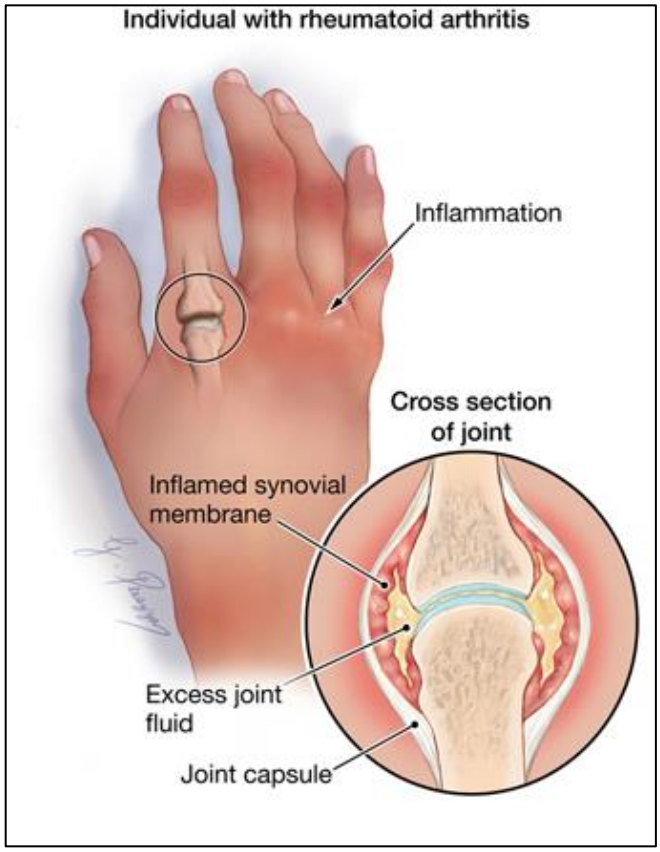

Figure 8: Signs of rheumatoid arthritis.

RA is treated by GCs, since they are still the most potent anti-inflammatory drugs used for immune-mediated disorders. However, their long-term use is associated with osteoporosis. Studies have shown that more than 50% of patients develops vertebral fracture after long-term treatment with GCs. Importantly, it has been reported that mice treated with collagen develop a Th17 rheumatoid arthritis-like inflammation which is widely used as model (Chen et al., **2018**).

2.1.4. Ulcerative colitis

Ulcerative colitis (UC) is a chronic disorder that affects the gastrointestinal tract. (Matusiewicz, Neubauer, Bednarz-Misa, Gorska, & Krzystek-Korpacka, **2017**). It is characterized by diarrhea and severe abdominal pain. Patients with UC can develop complications, such as tissue fibrosis, colon cancer and stenosis (Wirtz et al., **2017**). In UC, the inflammation in colon is observed in the mucosal and the submucosal parts.

Regulation of the immune process in gastrointestinal tract is mediated by T-lymphocytes, especially CD4+ T-cell. In the case of UC disease, the cytokine production is a Th17-related response, with high production of IL-17a and IL-17 f interleukins.

Studies have shown that oral administration of dextran sulfate sodium (DSS) to mice via drinking water induces severe ulcerative colitis, characterized by loss of weight, bloody diarrhea, loss of epithelial cells and infiltrations, which mimic some features in human UC (Wirtz et al., **2017**).

3. Therapeutic uses of glucocorticoids

Glucocorticoids became clinically used after the pioneering work of Philip Hench and other scientists since in the 1930s-1940s. The anti-inflammatory effects of GCs were discovered in 1948 after a treatment of a rheumatoid arthritis patient with cortisone, which was considered as a revolution in medicine. This was followed by the synthesis of potential GCs for the treatment of several chronic inflammatory affections (**Figure 9**). GCs are considered as important therapies in many inflammatory disorders, such as asthma (Barnes, **2006**) and rheumatoid arthritis. Moreover, GCs are used in transplantation for their immunosuppressive effects, and in hematological malignancies for their anti-proliferative properties (Fardet, Petersen, & Nazareth, **2011**). Total GC usage is growing constantly, due to increased prevalence of chronic disorders in ageing populations and to longer treatments.

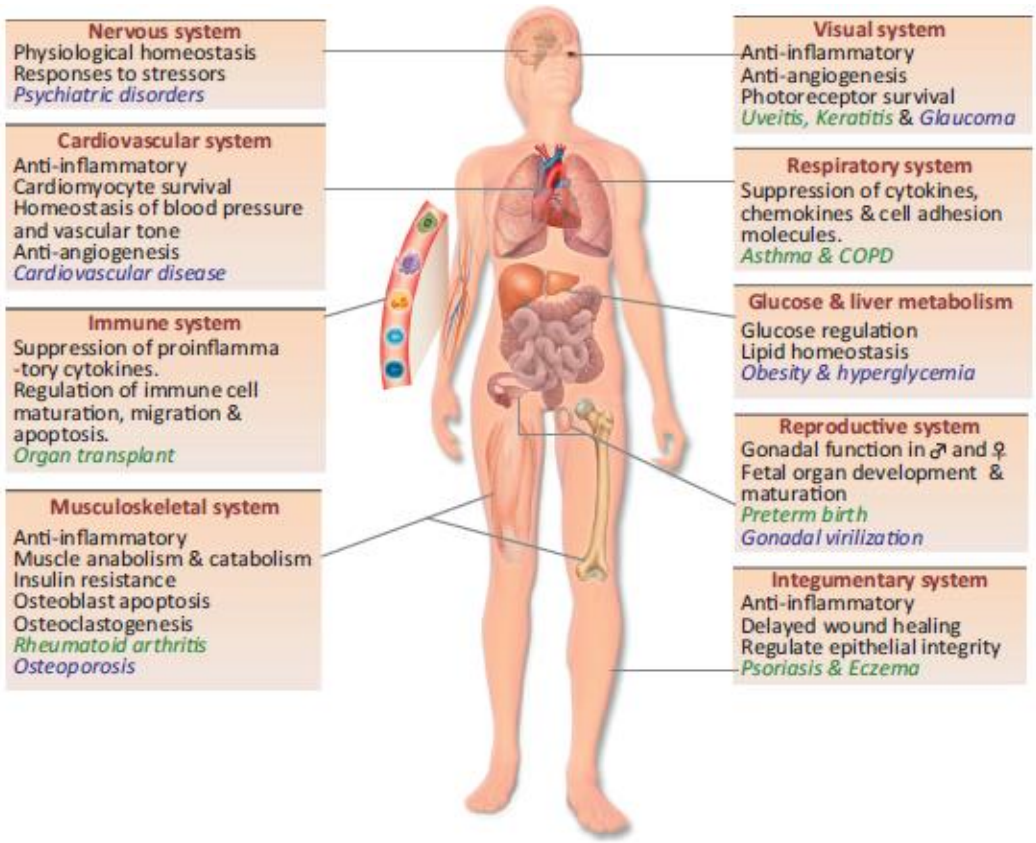

Figure 9: Role of glucocorticoids in health and disease.

4. Debilitating undesirable side-effects of GCs

The anti-inflammatory properties of natural GCs were demonstrated more than 60 years ago (Carryer et al., **1950**). Since then, synthetic GCs derivatives have been widely used in treatments aimed at suppressing or alleviating acute and chronic inflammatory and allergic disorders in various diseases. Unfortunately, GCs treatments are associated with a variety of serious debilitating side effects (Oray, Abu Samra, Ebrahimiadib, Meese, & Foster, **2016**), such as skin atrophy, osteoporosis, hepatic steatosis, type 2 diabetes, dyslipidemia, weight gain, gastritis, hypertension, ischemic heart disease, dermatoporosis, cataract, glaucoma, mydriasis or suppression of cell-mediated immunity (**Figure 10**). Different side effects may occur in up to 90% of patients who take GCs for more than 60 days, regardless of the dose and route of administration. Some of these side effects may even occur in patients taking low (≤ 7.5 mg/day) dosages.

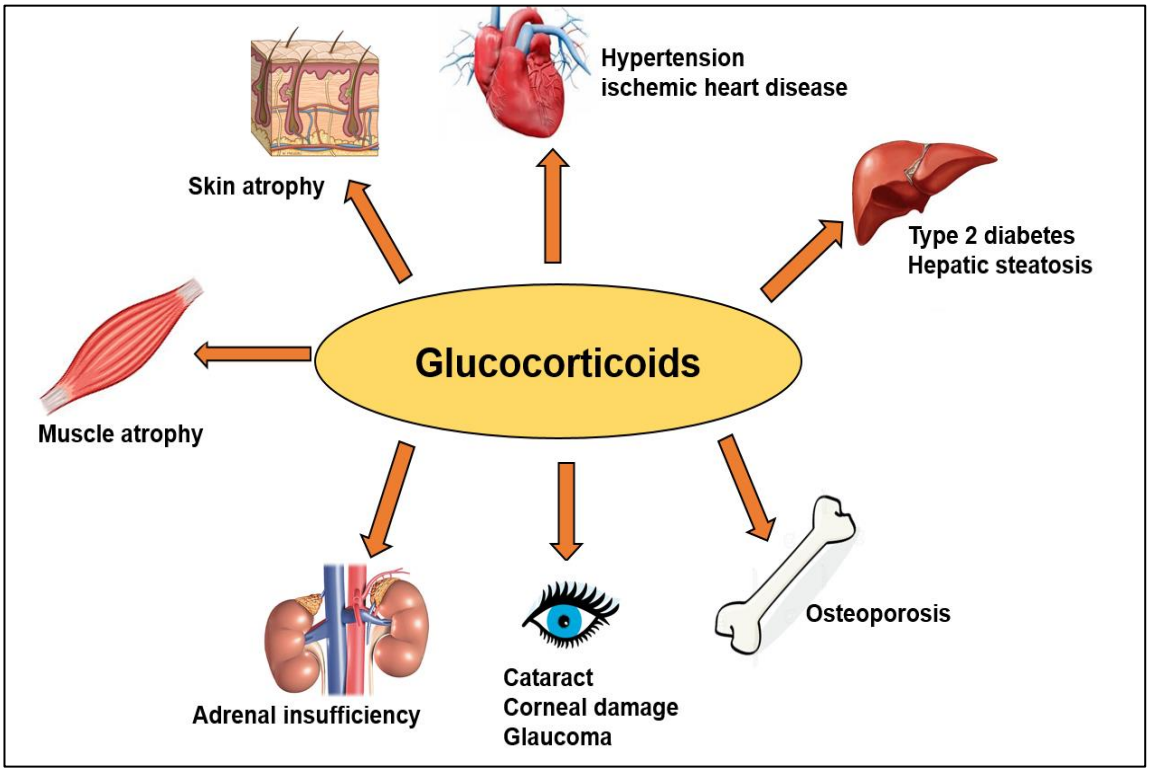

Figure 10: Glucocorticoids debilitating side-effects

4.1. Epidermal skin atrophy

Epidermal skin atrophy is a severe limitation of topical treatments with GCs (Schoepe, Schacke, May, & Asadullah, **2006**). It consists of a reduction of the epidermal part of the skin. Epidermal skin atrophy is detected when the tissue becomes shiny, thinner, and more susceptible to environmental and mechanical aggression. Several mechanisms are responsible for the induction of epidermal skin atrophy, such as suppressive effects on skin cell proliferation (mainly keratinocytes) and synthesis of some proteins and molecules (Sevilla & Perez, **2018**). Suppression of proliferation of keratinocytes could be related to reduce biosynthesis of macromolecules and mitotic rates in these cells. In addition, this alteration of proliferation may result in epidermal structural defect, and thinning of the stratum corneum. The ultimate consequences are an increased permeability and an elevation in trans-epidermal water loss, which indicates disrupted skin barrier function (Schoepe et al., **2006**).

4.2. Osteoporosis

Osteoporosis is a common undesirable side effect of a long-term glucocorticoid clinical treatment (Hildebrandt et al., **2018**). Patients under a high dose of GCs treatment represent a high risk for developing osteoporosis, and bone fracture (Weinstein, **2012**). Osteoporosis is a progressive disease characterized by a low bone mass, microarchitecture deterioration of bone tissue, bone fragility, and as a consequent an increase in fracture risk. Secondary osteoporosis, as the consequence of systemic drug use, such as steroidal anti-inflammatory drugs (SAIDs), is one of the most debilitating complications of glucocorticoid therapy, which has been recognized since 1940. The cumulative dose as well as the duration of SAID's exposure are the key determinants in the development of osteoporosis. Bone loss starts promptly after the initiation of SAID therapy and is mainly taking place in the first six months of treatment. In addition to bone loss, SAID therapy can also result in changes in the architectural integrity of the bone.

GCs affect bone metabolism via different mechanisms:

(1) The suppression of osteoblast proliferation and activity leads to the inhibition of bone formation.

(2) The decrease of the gastrointestinal Ca2+ absorption and the increase of the urinary Ca2+ excretion, which leads to a high osteoclastic bone resorption.

(3) Reduction of the number of osteoblasts and osteoclasts by inducing apoptosis in bone cells.

(4) Suppression of the critical mediators for the bone homeostasis: insulin-like growth factor-1 (IGF-1) and the growth hormone (GH)

(5) Suppression of bone formation via inhibition of Wnt16 expression (Hachemi et al., **2018**; Hildebrandt et al., **2018**).

4.3. Metabolism and endocrine system

4.3.1. Metabolic syndrome- Type 2 diabetes

Upon a long-term glucocorticoid administration, hyperglycemia is a common undesirable side effect (Clore & Thurby-Hay, **2009**). Hyperglycemia is detected when an excessive amount of glucose circulates in the blood plasma, such as, e.g., higher than 11.1 mmol of glucose per L of blood (200 mg of glucose per dL of blood). The American Diabetes Association guidelines classifies subjects in several subgroups, from slightly hyperglycemic (with a glucose level ranging from about 5.6 to about 7 mmol/L of blood, *i.e.*, from about 100 to about 126 mg/dL of blood), to diabetic (with a glucose level above 7 mmol/L of blood, *i.e.*, above 126 mg/dL of blood). The effect of SAIDs on glucose metabolism is dose-dependent and causes a mild increase in fasting blood glucose levels and a larger increase in postprandial blood glucose in patients without preexisting diabetes mellitus. SAID-induced hyperglycemia is multifactorial in origin and can be explained by the augmentation of hepatic gluconeogenesis, inhibition of glucose uptake in adipose tissue and/or alteration of receptor and post-receptor functions.

The second sign of metabolic syndrome is hyperinsulinemia. It corresponds to an excessive amount of insulin circulating in the blood plasma. Hyperinsulinemia is associated with hypertension, obesity, and dyslipidemia and glucose intolerance. All these factors are known as the “metabolic syndrome”. A chronic exposure of humans to GCs is well known to result in whole-body insulin-resistance and decreased β-cell insulin production (Geer, Islam, & Buettner, **2014**).

Moreover, hepatic steatosis is also a sign of the metabolic syndrome. It is a condition were large droplets of triglyceride fat accumulate in liver cells via the process of steatosis (i.e., abnormal retention of lipids within a cell). This accumulation of fat may also be accompanied by a progressive inflammation of the liver (hepatitis), called steatohepatitis. In addition, hypercholesterolemia is a main cause of non-alcoholic fatty liver diseases (NAFLDs), in which Cholesterol is converted into bile acids in liver

(Kim et al., **2014**). Accordingly, a high level of bile acids was also observed in patients exhibiting fatty liver diseases (Aranha et al., **2008**).

4.3.2. Adrenal insufficiency

After a long-term GCs treatment, the HPA axis is affected, leading to the induction of an adrenal insufficiency, in which the adrenal glands do not produce adequate amounts of cortisol. The use of high-dose of steroids for more than a week results in an involution of the adrenal glands because the exogenous glucocorticoids suppress the secretion of the hypothalamic CRH and the pituitary ACTH hormones, and inhibits the syntheses of adrenal corticosterone (cortisol) synthesizing enzymes. With prolonged suppression, there is an atrophy of the adrenal glands and it may take months to recover their full function after the glucocorticoid therapy has been stopped. During this recovery time, patients are vulnerable to adrenal insufficiency when under stress (e.g. illness), due to both adrenal atrophy and suppression of CRH and ACTH release.

5. SElective GR Agonistic Modulators (SEGRAMs)

Before the 2011 discovery of the GR direct transrepression pathway by our laboratory (Surjit et al., **2011**), the beneficial anti-inflammatory effects of GCs were ascribed to the indirect tethered transrepression pathway, while many of the undesirable side effects arising from GC treatments were thought to be related selectively to the direct transactivation pathway (Clark & Belvisi, **2012**).

Intense efforts have therefore been made over the past two decades to develop novel GR ligands, termed “dissociated” or “SElective” GR Agonistic Modulators (SEGRAMs) that would retain a transrepression profile, while having lost partially or, most ideally, entirely, their transactivation properties.

In this regard, a number of putative SEGRAMs have been developed, but few have made it to clinical trials. Such a ligand, RU24858, was found to exhibit such an

expected dissociated profile *in vitro* (Vayssiere et al., **1997**). However, upon administration *in vivo*, pathophysiological studies failed to confirm this dissociation (Belvisi et al., **2001**).

Later, another synthetic non-steroidal ligand, namely Mapracorat (also named ZK245186 or BOL-303242-X), was described as an anti-inflammatory agent for treating skin disorders (Schacke et al., **2009**). *In vitro* studies have shown that Mapracorat acts as an anti-inflammatory agent in corneal epithelial cells challenged with osmotic stress (Cavet, Harrington, Ward, & Zhang, **2010**), and *in vivo* in experimental models of dry eye and postoperative inflammation (Shafiee, Bucolo, Budzynski, Ward, & Lopez, **2011**), with an activity comparable to that of the synthetic "traditional" steroid dexamethasone, but reduced side effects in intraocular pressure and body weight. Mapracorat has also been the study product of several clinical trials between June 2009 and July 2013. However, as today, no study results of these trials are available and no marketing authorization has been granted, suggesting that Mapracorat might have revealed problems of efficacy and/or side effects.

As in 2011, the GC-bound GR-mediated direct transrepression function was also shown to be involved in undesirable side effects (Surjit et al., **2011**), it appeared that targeting exclusively the indirect tethered transrepression pathway would be efficient in preventing side effects.

There remained thus a need for the development of SEGRAMs which cannot induce efficiently neither the direct transactivation, nor the direct transrepression functions of GR, while still inducing its indirect tethered transrepression activity and anti-inflammatory properties *in vivo*.

6. The compound X (CpdX) and its deuterated derivatives

In the late 1990's, Schering AG, now Bayer HealthCare Pharmaceuticals, developed novel nonsteroidal compounds, claiming an anti-inflammatory activity dissociated from their metabolic effects. By 2015, our laboratory discovered that among these compounds, one of them which was named "CpdX", does not induce the transactivation and direct transrepression functions of the GR, while still inducing its indirect tethered transrepression activity (Hua, Ganti, et al., **2016**).

Contrary to the putative SEGRAMs previously described (such as Mapracorat), CpdX and its deuterated form (CpdX-D3) and their enantiomers, selectively induce the GR "indirect tethered transrepression activity", being thus a *bona fide* SEGRAMs selectively exhibiting the GR indirect transrepression function, whereas Mapracorat exhibits all three GR functions. Most importantly, we now demonstrate that, upon long-term administration to mice, CpdX and its derivatives are therapeutically as effective as the synthetic glucocorticoid Dexamethasone (Dex), while being devoid of the well-established debilitating side-effects of synthetic glucocorticoids.

7. References

Aranha, M. M., Cortez-Pinto, H., Costa, A., da Silva, I. B., Camilo, M. E., de Moura, M. C., & Rodrigues, C. M. (2008). Bile acid levels are increased in the liver of patients with steatohepatitis. Eur J Gastroenterol Hepatol, 20(6), 519-525. doi:10.1097/MEG.0b013e3282f4710a

Barnes, P. J. (2006). Transcription factors in airway diseases. Lab Invest, 86(9), 867-872. doi:10.1038/labinvest.3700456

Belvisi, M. G., Wicks, S. L., Battram, C. H., Bottoms, S. E., Redford, J. E., Woodman, P., . . . Foster, M. L. (2001). Therapeutic benefit of a dissociated glucocorticoid and the relevance of in vitro separation of transrepression from transactivation activity. J Immunol, 166(3), 1975-1982. Retrieved from http://www.ncbi.nlm.nih.gov/pubmed/11160246

Bielory, L., Skoner, D. P., Blaiss, M. S., Leatherman, B., Dykewicz, M. S., Smith, N., . . . Allen-Ramey, F. (2014). Ocular and nasal allergy symptom burden in America: the Allergies, Immunotherapy, and RhinoconjunctivitiS (AIRS) surveys. Allergy Asthma Proc, 35(3), 211-218. doi:10.2500/aap.2014.35.3750

Bisset, L. R., & Schmid-Grendelmeier, P. (2005). Chemokines and their receptors in the pathogenesis of allergic asthma: progress and perspective. Curr Opin Pulm Med, 11(1), 35-42.

Brunello, L. (2018). Atopic dermatitis. Nat Rev Dis Primers, 4(1), 2. doi:10.1038/s41572-018-0004-9

Carryer, H. M., Koelsche, G. A., Prickman, L. E., Maytum, C. K., Lake, C. F., & Williams, H. L. (1950). Effects of cortisone on bronchial asthma and hay fever occurring in subjects sensitive to ragweed pollen. Proc Staff Meet Mayo Clin, 25(17), 482-486. Retrieved from http://www.ncbi.nlm.nih.gov/pubmed/15440926

Cavet, M. E., Harrington, K. L., Ward, K. W., & Zhang, J. Z. (2010). Mapracorat, a novel selective glucocorticoid receptor agonist, inhibits hyperosmolar-induced cytokine release and MAPK pathways in human corneal epithelial cells. Mol Vis, 16, 1791-1800. Retrieved from http://www.ncbi.nlm.nih.gov/pubmed/20824100

Chen, Z., Bozec, A., Ramming, A., & Schett, G. (2018). Anti-inflammatory and immune-regulatory cytokines in rheumatoid arthritis. Nat Rev Rheumatol. doi:10.1038/s41584-018-0109-2

Clark, A. R., & Belvisi, M. G. (2012). Maps and legends: the quest for dissociated ligands of the glucocorticoid receptor. Pharmacol Ther, 134(1), 54-67. doi:10.1016/j.pharmthera.2011.12.004

Clore, J. N., & Thurby-Hay, L. (2009). Glucocorticoid-induced hyperglycemia. Endocr Pract, 15(5), 469-474. doi:10.4158/EP08331.RAR

Draper, N., & Stewart, P. M. (2005). 11beta-hydroxysteroid dehydrogenase and the pre-receptor regulation of corticosteroid hormone action. J Endocrinol, 186(2), 251-271. doi:10.1677/joe.1.06019

Fardet, L., Petersen, I., & Nazareth, I. (2011). Prevalence of long-term oral glucocorticoid prescriptions in the UK over the past 20 years. Rheumatology (Oxford), 50(11), 1982-1990. doi:10.1093/rheumatology/ker017

Galli, E., Gianni, S., Auricchio, G., Brunetti, E., Mancino, G., & Rossi, P. (2007). Atopic dermatitis and asthma. Allergy Asthma Proc, 28(5), 540-543. doi:10.2500/aap2007.28.3048

Geer, E. B., Islam, J., & Buettner, C. (2014). Mechanisms of glucocorticoid-induced insulin resistance: focus on adipose tissue function and lipid metabolism. Endocrinol Metab Clin North Am, 43(1), 75-102. doi:10.1016/j.ecl.2013.10.005

Greb, J. E., Goldminz, A. M., Elder, J. T., Lebwohl, M. G., Gladman, D. D., Wu, J. J., . . . Gottlieb, A. B. (2016). Psoriasis. Nat Rev Dis Primers, 2, 16082. doi:10.1038/nrdp.2016.82

Hachemi, Y., Rapp, A. E., Picke, A. K., Weidinger, G., Ignatius, A., & Tuckermann, J. (2018). Molecular mechanisms of glucocorticoids on skeleton and bone regeneration after fracture. J Mol Endocrinol, 61(1), R75-R90. doi:10.1530/JME-18-0024

Hildebrandt, S., Baschant, U., Thiele, S., Tuckermann, J., Hofbauer, L. C., & Rauner, M. (2018). Glucocorticoids suppress Wnt16 expression in osteoblasts in vitro and in vivo. Sci Rep, 8(1), 8711. doi:10.1038/s41598-018-26300-z

Hua, G., Ganti, K. P., & Chambon, P. (2016). Glucocorticoid-induced tethered transrepression requires SUMOylation of GR and formation of a SUMO-SMRT/NCoR1-HDAC3 repressing complex. Proc Natl Acad Sci U S A, 113(5), E635-643. doi:10.1073/pnas.1522826113

Hua, G., Paulen, L., & Chambon, P. (2016). GR SUMOylation and formation of an SUMO-SMRT/NCoR1-HDAC3 repressing complex is mandatory for GC-induced IR nGRE-mediated transrepression. Proc Natl Acad Sci U S A, 113(5), E626-634. doi:10.1073/pnas.1522821113

Kim, C., Kim, M. Y., Kang, D. R., Kim, J. Y., Park, J. B., & investigators, K. M. s. (2014). The Efficacy of Fimasartan for Cardiovascular Events and Metabolic Syndrome (K-MetS Study): Rationale, Design and Participant Characteristics. Pulse (Basel), 1(3-4), 177-185. doi:10.1159/000360965

Li, J. G., Leyva-Castillo, J. M., Hener, P., Eisenmann, A., Zaafouri, S., Jonca, N., . . . Li, M. (2016). Counterregulation between thymic stromal lymphopoietin- and IL-23-driven immune axes shapes skin inflammation in mice with epidermal barrier defects. Journal of Allergy and Clinical Immunology, 138(1), 150-+. doi:10.1016/j.jaci.2016.01.013

Li, M., Hener, P., Zhang, Z., Kato, S., Metzger, D., & Chambon, P. (2006). Topical vitamin D3 and low-calcemic analogs induce thymic stromal lymphopoietin in mouse keratinocytes and trigger an atopic dermatitis. Proc Natl Acad Sci U S A, 103(31), 11736-11741. doi:10.1073/pnas.0604575103

Liu, Y. J. (2006). Thymic stromal lymphopoietin: master switch for allergic inflammation. J Exp Med, 203(2), 269-273. doi:10.1084/jem.20051745

Matusiewicz, M., Neubauer, K., Bednarz-Misa, I., Gorska, S., & Krzystek-Korpacka, M. (2017). Systemic interleukin-9 in inflammatory bowel disease: Association with mucosal healing in ulcerative colitis. World J Gastroenterol, 23(22), 4039-4046. doi:10.3748/wjg.v23.i22.4039

Ogawa, E., Sato, Y., Minagawa, A., & Okuyama, R. (2018). Pathogenesis of psoriasis and development of treatment. J Dermatol, 45(3), 264-272. doi:10.1111/1346-8138.14139

Oray, M., Abu Samra, K., Ebrahimiadib, N., Meese, H., & Foster, C. S. (2016). Long-term side effects of glucocorticoids. Expert Opin Drug Saf, 15(4), 457-465. doi:10.1517/14740338.2016.1140743

Schacke, H., Zollner, T. M., Docke, W. D., Rehwinkel, H., Jaroch, S., Skuballa, W., . . . Asadullah, K. (2009). Characterization of ZK 245186, a novel, selective glucocorticoid receptor agonist for the topical treatment of inflammatory skin diseases. Br J Pharmacol, 158(4), 1088-1103. doi:10.1111/j.1476-5381.2009.00238.x

Schoepe, S., Schacke, H., May, E., & Asadullah, K. (2006). Glucocorticoid therapy-induced skin atrophy. Exp Dermatol, 15(6), 406-420. doi:10.1111/j.0906-6705.2006.00435.x

Sevilla, L. M., & Perez, P. (2018). Roles of the Glucocorticoid and Mineralocorticoid Receptors in Skin Pathophysiology. Int J Mol Sci, 19(7). doi:10.3390/ijms19071906

Shafiee, A., Bucolo, C., Budzynski, E., Ward, K. W., & Lopez, F. J. (2011). In vivo ocular efficacy profile of mapracorat, a novel selective glucocorticoid receptor agonist, in rabbit

models of ocular disease. Invest Ophthalmol Vis Sci, 52(3), 1422-1430. doi:10.1167/iovs.10-5598

Surjit, M., Ganti, K. P., Mukherji, A., Ye, T., Hua, G., Metzger, D., . . . Chambon, P. (2011). Widespread negative response elements mediate direct repression by agonist-liganded glucocorticoid receptor. Cell, 145(2), 224-241. doi:10.1016/j.cell.2011.03.027

Tan, C. K., & Wahli, W. (2016). A trilogy of glucocorticoid receptor actions. Proc Natl Acad Sci U S A, 113(5), 1115-1117. doi:10.1073/pnas.1524215113

Vayssiere, B. M., Dupont, S., Choquart, A., Petit, F., Garcia, T., Marchandeau, C., . . . RescheRigon, M. (1997). Synthetic glucocorticoids that dissociate transactivation and AP-1 transrepression exhibit antiinflammatory activity in vivo. Molecular Endocrinology, 11(9), 1245-1255. doi:DOI 10.1210/me.11.9.1245

Weidinger S. & Novak N., (2016). Atopic dermatitis. Lancet. 387(10023):1109-1122. doi: 10.1016/S0140-6736(15)00149-X.

Weinstein, R. S. (2012). Glucocorticoid-induced osteonecrosis. Endocrine, 41(2), 183-190. doi:10.1007/s12020-011-9580-0

Wirtz, S., Popp, V., Kindermann, M., Gerlach, K., Weigmann, B., Fichtner-Feigl, S., & Neurath, M. F. (2017). Chemically induced mouse models of acute and chronic intestinal inflammation. Nat Protoc, 12(7), 1295-1309. doi:10.1038/nprot.2017.044

OBJECTIVES OF MY THESIS WORK

Earlier studies performed in our laboratory have revealed that Compound X (CpdX), cannot induce the direct transactivation and direct transrepression functions of the GR, while still inducing its tethered indirect transrepression activity and some of its anti-inflammatory properties *in vivo*. These results suggested that CpdX could be a *bona fide* Selective Glucocorticoid Receptor Agonistic Modulator (SEGRAM) which is devoid of most of the undesirable effects of glucocorticoids, while keeping their therapeutically beneficial properties.

My thesis research was aimed at further characterizing Compound X and some of its derivatives, as clinically effective anti-inflammatory compounds, similar to glucocorticoids, but exempt of their deleterious side-effects.

My thesis work was focused on two **objectives**:

1- To investigate whether CpdX and some of its derivatives, exhibit an efficient anti-inflammatory activity in diseases which are presently treated with synthetic glucocorticoids.

2- To explore whether the administration of CpdX and some of its derivatives, is devoid of the debilitating pathological side-effects of a synthetic glucocorticoid therapy, such as a metabolic syndrome, a skin atrophy or an osteoporosis.

My results are described and discussed in two parts:

(I) CpdX and CpdX-D3 and their respective enantiomers are *bona fide* Selective Glucocorticoid Receptor Agonistic Modulators (SEGRAMs). *(Manuscript in preparation)*

(II) CpdX and CpdX-D3 and their respective enantiomers do not exhibit the multiple long-term undesirable effects of present day synthetic glucocorticoids, such as Dexamethasone, while keeping their beneficial anti-inflammatory functions. *(Manuscript in preparation)*

PART I

(Manuscript in preparation)

CpdX and CpdX-D3 and their respective enantiomers are *bona fide* Selective Glucocorticoid Receptor Agonistic Modulators (SEGRAMs)

CpdX and CpdX-D3 and their respective enantiomers are *bona fide* Selective Glucocorticoid Receptor Agonistic Modulators (SEGRAMs)

Guoqiang Hua[a,1], Naimah Zein[a,1], François Daubeuf[b], Nadia Jessel[c], and Pierre Chambon[a,d,e,2]

[a]Institut de Génétique et de Biologie Moléculaire et Cellulaire, CNRS UMR7104, INSERM U964, Illkirch, 67404, France;
[b]Laboratoire d'Innovation Thérapeutique, Unité Mixte de Recherche 7200, Centre National de la Recherche Scientifique-Université de Strasbourg, Faculté de Pharmacie, F-67400 Illkirch, France;
[c]INSERM (French National Institute of Health and Medical Research), UMR 1260, Regenerative Nanomedicine laboratory, Faculté de Médecine, FMTS, Strasbourg Cedex F-67085, France;
[d]University of Strasbourg Institute for Advanced Study, Illkirch, 67404, France;
[e]Collège de France, Illkirch, 67404, France;

[1] G.H. and N.Z. contributed equally to this work

[2]Correspondance: chambon@igbmc.fr (P.C.)

PART I:

CpdX and CpdX-D3 and their respective enantiomers are *bona fide* Selective Glucocorticoid Receptor Agonistic Modulators (SEGRAMs)

1. Introduction

Glucocorticoids (GCs) belong to a class of steroid hormones found in vertebrates (cortisol in humans and corticosterone in rodents). They regulate numerous physiological processes by binding to their cognate receptor, the glucocorticoid receptor (GR), in an effort to maintain homeostasis, particularly under stress conditions. Synthetic GCs (e.g. Dexamethasone) are used in clinical treatments to suppress inflammatory and allergic disorders (1). However, their long-term use is associated with a variety of serious pathological side-effects.

Upon GC binding, the GR regulates the expression of target genes either by (i) direct transactivation through direct binding to conserved positive response element named "(+)GRE" DNA binding sites (DBS) (2), (ii) direct transrepression through binding to conserved inverted repeated negative response element named "IR nGRE" DBSs (3), or (iii) tethered indirect transrepression mediated through interaction with transactivators, such as NFkB, AP1 or STAT3 bound to their cognate DBSs (4). We recently reported that Sumoylation of the GR NTD and the subsequent formation of a NCoR1/SMRT/HDAC3 repressing complex is mandatory for both GC-induced IR nGRE-mediated direct transrepression (5) and tethered indirect transrepression (6).

It is widely accepted that most of the beneficial anti-inflammatory effects of GCs are ascribed to tethered transrepression (1), while many of their long-term undesirable side-effects are due to transactivation and/or direct transrepression (3). This has led to searches for dissociated ligands that would selectively induce tethered transrepression and be devoid of both direct transactivation and direct transrepression activities. Along these lines, we recently discovered that a non-steroidal compound that we named CpdX, is selectively lacking both the direct transactivation and the direct transrepression functions *in vitro*, while still exerting

the indirect transrepression activity (6), which suggested that CpdX might be a true *bona fide* Selective Glucocorticoid Receptor Agonistic Modulator (SEGRAM).

We now report that the racemic CpdX is a *bona fide* SEGRAM which, in several mouse inflammation models, represses the inflammatory processes, as efficiently as Dexamethasone. Of note, in two of these inflammation models, the anti-inflammatory activity was selectively associated with one of the CpdX enantiomers. As it was reported that replacing some hydrogen atoms by deuterium atoms may improve the efficiency of various drugs (7), we also investigated whether the anti-inflammatory activity of CpdX and of its enantiomers could be similarly improved by replacing some of the hydrogen atoms by deuterium.

2. Results

CpdX and CpdX-D3, and their respective enantiomers, are as efficient as Dexamethasone (Dex) at decreasing the skin inflammations generated in models of atopic dermatitis and contact dermatitis

To investigate the skin anti-inflammatory activity of CpdX, CpdX-D3 and their enantiomers (see Materials and Methods), three inflammation mouse models have been used: (i) a Calcipotriol (MC903)- induced atopic dermatitis-like T_h2 inflammation (Fig. 1A) (8), (ii) a TPA-induced irritant contact dermatitis-like $T_h1/T_h2/T_h17$ inflammation (Fig. S1A) (9), (iii) an Aldara-induced psoriasis-like T_h17 inflammation (Fig. S1B) (10).

Q-RT-PCR analyses of ear extracts from the MC903-induced atopic dermatitis model demonstrated that CpdX and CpdX-D3 repressed, as efficiently as Dex, the MC 903-induced transcription of a variety of pro-inflammatory genes (MMP13, COX2, IL-1β, IL-6, IL-10, IL-13 and TSLP) which includes genes characteristic of a T_h2 inflammation (IL-10, IL-13 and TSLP) (Fig. 1B). Histological analyses revealed an MC 903-induced epidermal hyperplasia and a dermal cell infiltration were also decreased upon a treatment with either Dex, CpdX or CpdX-D3 and their respective enantiomers (Fig. 1C). Immunohistochemistry analyses (with a TSLP-specific antibody) of MC903-treated mouse epidermis showed that the expression of the TSLP lymphokine was

decreased by either Dex, CpdX or CpdX-D3 treatments. Similar results were obtained with either CpdX(eA), CpdX(eB), CpdX-D3(eA) or CpdX-D3(eB) (data not shown).

Transcript analyses of mouse ear extracts from the TPA-induced irritant contact dermatitis-like inflammation model (Fig.1D) indicated that CpdX, as well as CpdX-D3, repressed as efficiently as Dex, the TPA-induced transcription of pro-inflammatory genes, including those of a T_h1 inflammation (TNFα), a T_h2 inflammation (TSLP) or a T_h17 inflammation (IL17a and IL22).

Using the Aldara-induced psoriasis-like inflammation model, transcript analyses revealed a similar repression of the induced expression of the T_h17 inflammatory genes IL17a, IL17c, IL17f and IL22 (Fig.1E).

Histological analyses of mouse ear skin showed that both an Aldara-induced (psoriasis-like), or a TPA-induced irritant dermatitis-like ear skin inflammation was significantly decreased by treatment with either Dex, CpdX or deuterated (CpdX-D3), as compared to control mice (Fig.S1C, and data not shown).

Taken all together, the above results demonstrated that CpdX, its deuterated form CpdX-D3, as well as their enantiomers, are as efficient as Dexamethasone (Dex) at decreasing the skin inflammations generated in atopic dermatitis-like and a psoriasis-like models, as well as in a TPA-induced inflammation.

CpdX, CpdX(eA), CpdX-D3 and CpdX-D3(eA), but not CpdX(eB) nor CpdX-D3(eB), are as efficient as Dexamethasone (Dex) at decreasing a house dust mite (HDM)-induced asthma-like lung allergic Th2 inflammation

To investigate the anti-inflammatory activity of CpdX, CpdX-D3 and of their enantiomers in a lung inflammation, mice were intranasally-sensitized with 1 µg HDM from D0 to D4, and further intranasally sensitized with 10 µg HDM on D14 and D21. Mice were then subdivided into 8 different groups, and on D29, D30 and D31, each mouse was again intranasally challenged with 1 µg HDM without or together with 0.5

mg/kg of body weight of either Dex, CpdX, CpdX(eA), CpdX(eB), CpdX-D3, CpdX-D3(eA) or CpdX-D3(eB) (Fig. 2A).

To assess the lung allergic inflammation, the fluid of bronchoalveolar lavages (BAL) was analyzed at Day 32 (D32). Upon treatment with either Dex, CpdX or CpdX-D3, the total number of BAL cells, eosinophils and lymphocytes were significantly decreased, as compared to the control group; however, no significant change was observed in the number of neutrophils and macrophages (Fig. 2B). RT-PCR analyses of lung samples showed that the expression of IL-1β, IL-6 and of the T_h2 pro-inflammatory genes (IL-4, IL-5, IL-13), as well as those of the eosinophil chemotactic chemokines Eotaxin and CCL4, were significantly and similarly decreased by either a Dex, a CpdX or a CpdX-D3 treatment (Fig. 2C).

Histological analyses of lung paraffin sections revealed that the HDM-induced peribronchiolar and perivascular inflammatory cell infiltration was strongly decreased upon either a Dex, a CpdX or a CpdX-D3 treatment (Fig. 2D). Immunohistochemistry staining using the eosinophil-specific antibodies MBP confirmed that eosinophils were decreased upon either Dex, CpdX or CpdX-D3 treatment (Fig. S2A), while no significant change was observed using the neutrophil-specific antibody R14 (Fig. S2B).

Pulmonary functional tests of mouse airway responsiveness were invasively performed using a computer-controlled small animal ventilator (FlexVent® system, SCIREQ Technologies). Airway resistance and elastance were measured by their responses to methacholine (50mg/ml). Upon Dex, CpdX or CpdX-D3 administration, the HDM-induced airway hyperresponsiveness (AHR) was found similarly and significantly reduced (Fig. 2E).

Of note, a treatment with CpdX(eA) or CpdX-D3(eA), but not with CpdX(eB) nor CpdX-D3(eB), efficiently decreased the number of total BAL cells, eosinophils and lymphocytes (Fig. 2B), as well as the expression of pro-inflammatory genes (Fig. 2C). Histological analyses of lung paraffin sections also revealed that the peribronchiolar and perivascular inflammatory cell infiltrations were decreased by either a CpdX(eA)

or a CpdX-D3(eA) treatment, but not by a CpdX(eB) nor a CpdX-D3(eB) treatment (Fig. 2D). Furthermore, immunohistochemistry staining using the eosinophil-specific antibodies MBP clearly showed that eosinophils were decreased by either a CpdX(eA) or a CpdX-D3(eA) treatment, but not by CpdX(eB) or CpdX-D3(eB) treatments (Fig. S2A). In keeping with these data, the mouse lung airway resistance and elastance measured by FlexVent® demonstrated that administration of CpdX(eA), but not of CpdX(eB), reduced the HDM-induced airway hyperresponsiveness (AHR) (Fig. 2E).

Taken altogether, the above results demonstrate that CpdX and CpdX-D3 repressed, as efficiently as Dex, an HDM-induced lung inflammation, indicating their potential usefulness for the treatment of T_h2-related inflammatory disorders, such as asthma. Of note, CpdX(eA) and CpdX-D3(eA), but neither CpdX(eB) nor CpdX-D3(eB), did efficiently repress the HDM-induced lung inflammation, indicating a remarkable "enantiomeric" selectivity for CpdX and CpdX-D3 in their ability to "cure" an asthma-like syndrome.

CpdX, CpdX(eA), CpdX-D3 and CpdX-D3(eA), but not CpdX(eB) nor CpdX-D3(eB), are as efficient as Dexamethasone (Dex) at decreasing a collagen-induced arthritis (CIA) Th17 inflammation

Male mice (DBA-1 strain) were subcutaneously-injected in the tail with 100 µg collagen per mouse on D0 to create a collagen-induced arthritis (11). The hind paw thickness at the ankle level was measured twice a week with a caliper. When the ankle thickness had reached ≈ 4 mm (T0, *i.e.*, 30 to 50 days after the collagen injection on D0), mice were daily intraperitoneally-injected for 10 days (T0 to T10) with either vehicle (NaCl 0,9%), Dex, CpdX, CpdX(eA), CpdX(eB), CpdX-D3, CpdX-D3(eA) or CpdX-D3(eB) (1 mg/kg body weight diluted in NaCl 0,9%), and the hind paw thickness was daily measured at the ankle level with a caliper (Fig. 3A).

The initial hind paw thickness (≈ 3 mm) was increased to ≈ 4 mm within 30-50 days following the collagen injection, at which time (T0) the administration of Dex, CpdX or CpdX-D3 resulted within 10 days into a rapid decrease of this thickness (Figs. 3B

and 3C, left panels). A similar decrease in hind paw thickness was observed in mice treated with CpdX(eA) or CpdX-D3(eA), whereas, in marked contrast, no such a decrease was observed upon a CpdX(eB) or a CpdX-D3(eB) treatment (Fig. 3C right panel).

Most notably, the RNA transcripts of the pro-inflammatory genes (IL-1β, IL-6, IL-17a, IL-17f and TNFα) expressed in the hind paws of mice which developed a CIA, were similarly repressed by either a dexamethasone, a CpdX, a CpdX(eA), a CpdX-D3 or a CpdX-D3(eA) treatment, but most notably not by a CpdX(eB) nor a CpdX-D3(eB) treatment (Fig. 3D).

These results demonstrate that both CpdX and CpdX-D3, as well as their enantiomers CpdX(eA), CpdX-D3(eA), but not their CpdX(eB) nor CpdX-D3(eB) enantiomers, are as efficient as Dex at decreasing a rheumatoid arthritis-like T_h17 inflammatory.

CpdX, CpdX-D3 and their enantiomers are as efficient as Dexamethasone at curing a Dextran Sodium Sulfate (DSS)-induced Th17 ulcerative colitis

To investigate the anti-inflammatory activity of CpdX and CpdX-D3 and of their respective enantiomers on a T_h17 ulcerative colitis (12), Balb/C mice were treated with 3% DSS in drinking water for 13 days, with or without an intraperitoneal administration of either Dex, CpdX, CpdX(eA), CpdX(eB), CpdX-D3, CpdX-D3(eA) or CpdX-D3(eB) (1 mg/kg of body weight) on D11, D12 and D13 (Fig.4A). At D14, RNA transcripts were extracted from mouse colons. IL-1β, IL-6, IL-17a, IL-17f, TSLP and MMP13 transcripts were analyzed by q-RT-PCR. Colon samples were also harvested for histological analyses (H&E staining).

Histological analyses (H&E stained paraffin sections) (Fig. 4B, and data not shown) showed dramatic damages in DSS-treated mouse colon as compared to control mice (no DSS treatment): the regular colonic villus/crypt structure was highly disorganized or absent in DSS-treated mice. In addition, ulcerations (arrow head), as well as cell infiltrations into the colonic mucosal (solid arrows) and submucosal (dotted arrows)

layers were also observed. Most notably, in mice treated for 3 days with either Dex, CpdX, CpdX-D3 or their two enantiomers CpdX(eA), CpdX(eB), CpdX-D3(eA) and CpdX-D3(eB), the colonic villus/crypt structure was almost re-established, and both the mucosal and the submucosal cell infiltrations were significantly decreased. Transcriptional analyses showed that the pro-inflammatory genes which were overexpressed in DSS-induced ulcerative colitis were similarly repressed by either Dex, CpdX, CpdX(eA), CpdX(eB), CpdX-D3, CpdX-D3(eA) or CpdX-D3(eB) (Fig.4C).

Taken altogether, these results demonstrate that CpdX, CpdX-D3 and their enantiomers CpdX(eA), CpdX(eB), CpdX-D3(eA) and CpdX-D3(eB) are as efficient as Dex for the treatment of a T_h17-related inflammatory intestinal disorder, such as an ulcerative colitis.

Instillations of either CpdX, CpdX(eA), CpdX(eB), CpdX-D3, CpdX-D3(eA) or CpdX-D3(eB) alleviate, as efficiently as Dexamethasone (Dex), an ovalbumin (OVA)-induced allergic conjunctivitis

To investigate the possible anti-inflammatory effects of either CpdX or CpdX-D3 and of their respective enantiomers on an allergic conjunctivitis, Balb/C mice were intraperitoneally sensitized with 50 µg OVA with alum on both days D0 and D7, and then challenged from D14 to D20 with 250 µg OVA in 5 µL of sterilized vehicle (0.9% NaCl) which were directly instilled onto the conjunctival sac. From D21 to D23, mice were divided into several groups, which received eye instillations with either OVA alone, OVA together with 0.1% of either Dex, CpdX, CpdX(eA), CpdX(eB), CpdX-D3, CpdX-D3(eA) or CpdX-D3(eB) (Fig. 5A). The clinical appearance of mouse eyes was evaluated 20 minutes after the last instillation on D24.

Three clinical signs (conjunctival hyperemia, lid edema and tearing) were scored, as described to evaluate the occurrence and severity of the conjunctivitis (13). Parameters were graded on a scale ranging from 0 to 3 (0 = absence, 1 = mild, 2 = moderate, and 3 = severe symptoms), each animal receiving a total clinical score ranging from 0 to 9. Twenty minutes after the last OVA challenge, eyes from all OVA-

treated mice presented obvious pathological signs of allergic conjunctivitis, as compared to control mice (Vehicle) (Fig.5B). As expected, these signs were considerably reduced by Dex treatment and, most interestingly, similary reduced by either CpdX, CpdX(eA), CpdX(eB), CpdX-D3, CpdX-D3(eA) or CpdX-D3(eB) treatments (Fig. 5C).

These results demonstrate that CpdX, CpdX-D3 and their enantiomers CpdX(eA), CpdX(eB), CpdX-D3(eA) and CpdX-D3(eB) reduce, as efficiently as Dex, an ovalbumin (OVA)-induced allergic conjunctivitis.

3. Discussion

We have demonstrated here that CpdX and its deuterated derivative CpdX-D3 are *bona fide* SEGRAMs, which repress as efficiently as the synthetic glucocorticoid Dexamethasone, a MC903-induced atopic dermatitis-like inflammation, a TPA-induced irritant contact dermatitis, an Aldara-induced psoriasis-like skin inflammation, an HDM-induced asthma-like allergic lung inflammation, a collagen-induced arthritis, a DSS-induced ulcerative colitis and an ovalbumin-induced allergic conjunctivitis.

It is known that, individual enantiomers could have markedly different biological effects (14, 15). We have revealed in this study that two mouse inflammation models, the HDM-induced asthma-like lung allergic inflammation and the collagen-induced arthritis, were efficiently reduced by administration of the CpdX(eA) and CpdX-D3(eA) enantiomers, whereas in marked contrast, the CpdX(eB) and CpdX-D3(eB) enantiomers were inefficient. These results indicate that the enantiomer CpdX(eA) or CpdX-D3(eA) should be preferentially used in the treatment of these two diseases.

Deuterium-carbon bonds are generally about six to ten times more stable than the corresponding hydrogen-carbon bond (17, 18). In this regard, deuterated compounds have been described to have a longer half-life and a significant lower rate of metabolic degradation, and therefore could be more powerful and efficient (17, 18). However, we did not observe any significant difference in anti-inflammatory properties of CpdX and its two enantiomers when compared to their deuterated counterparts. Dose response studies comparing CpdX and CpdX-D3 are required to compare the anti-inflammatory properties of CpdX and CpdX-D3 at lower concentrations. Further investigations should also be carried out to precisely characterize the *in vivo* metabolites of CpdX and CpdX-D3 to possibly design novel anti-inflammatory drugs.

In conclusion, we report here that for both local therapy treatments (skin inflammations, lung inflammation and eye inflammation) and systemic therapy (arthritis and ulcerative colitis), CpdX, its enantiomers and their deuterated counterparts, are potentially future anti-inflammatory drugs, as they are as efficient

as the most currently used synthetic glucocorticoids (e.g. Dexamethasone), but remarkably devoid of their debilitating side-effects which limit their long-term use, most notably at high doses.

4. Materials & Methods

CpdX and its enantiomers

The racemic mixture of CpdX {(R/S)-5-[4-(5-fluoro-2-methoxyphenyl)-2-hydroxy-4-methyl-2-(trifluoromethyl)pentylamino]isobenzofuran-1(3H)-one} was run through a preparative supercritical fluid chromatography (SFC) AD column (250 mm * 30 mm * 5 µm; mobile phase: Neu-MeOH; B%: 20%-20%, 2.3 minutes).

The collected fractions corresponding to the first elution peak were then concentrated under reduced pressure at 30°C, lyophilized and further purified through a Phenomenex Synergi C18 column chromatography [150 mm * 25mm * 10 µm; mobile phase: water (0.1 % TFA)-ACN; B%: 50%-80%, 10 minutes]. The collected fractions were concentrated under reduced pressure at 30°C and lyophilized as a white solid, the identity of which was confirmed by LCMS (MS+1=442.1) and SFC (retention time (RT) = 1.084 mins), and named as the "CpdX(eA)" enantiomer (97.6 % purity).

The collected fractions corresponding to the second elution peak were similarly concentrated under reduced pressure at 30°C, lyophilized and further purified by Phenomenex Synergi C18 column chromatography [150 mm * 25 mm * 10 µm); mobile phase: water (0.1 % TFA)-ACN; B%: 51%-81%, 12 minutes]. The collected fractions were concentrated under reduced pressure at 30°C and lyophilized as a white solid, the identity of which was confirmed by LCMS (MS+1=442.1) and SFC (RT = 1.147 minutes), and named as the "CpdX(eB)" enantiomer with a 98% purity.

CpdX-D3 and its enantiomers

The racemic mixture of the deuterated compound CpdX-D3, {(R/S)-5-{4-[2-(methoxy-D3)-5-fluorophenyl]-2-hydroxy-4-methyl-2-(trifluoromethyl)pentylamino}isobenzofuran-1(3H)-one} was run through a preparative supercritical fluid chromatography (SFC) DAICEL CHIRALPAK AD-H column (250 mm * 30 mm * 5 µm; mobile phase: 0.1% NH_3H_2O-MEOH; B%: 20%-20%, 2.3 minutes).

The collected fractions corresponding to the first elution peak were concentrated under reduced pressure at 30°C and lyophilized as a white solid, the identity of which was confirmed by LCMS (MS+1=445) and SFC (RT = 1.082 minutes), and named as the enantiomer "CpdX-D3(eA)" with a 98.7 % purity.

The collected fractions corresponding to the second elution peak were concentrated under reduced pressure at 30°C and lyophilized as a white solid, the identity of which was confirmed by LCMS (MS+1=445) and SFC (RT = 1.149 minutes), and named as the "CpdX-D3(eB)" enantiomer with a 99.1% purity.

Mice

Wild type BALB/c female mice and DBA/1J male mice were purchased from Charles River Laboratories. They were maintained under institutional guidelines, in a temperature and humidity-controlled animal facility, with a 12 hours light/dark cycle and free access to water and food. Experimental manipulation of mice was approved by the animal care and use committee of the IGBMC/ICS.

Materials

Dexamethasone (Dex), 12-O-Tetradecanoylphorbol-13-acetate (TPA), Calcipotriol (MC903), Ovalbumin (chicken) and Dextran Sodium Sulfate (DSS) were from Sigma Aldrich. Aldara® Cream is provided from MEDA AB (Sweden). Immunization Grade Chick Type II Collagen (7009) was from Chrondrex. House dust mite extract from dermatopha goides pteronyssinus was from Greer source material. Biotinylated goat polyclonal anti-TSLP was from R&D Systems. Anti-Neutrophil antibody [NIMP-

R14] (ab2557) was from Abcam. Anti-Eosinophil antibody (MBP) was a gift kindly provided by Dr. Mei LI (IGBMC, Illkirch, France).

Histology

Mouse samples were fixed overnight at 4°C in 4% paraformaldehyde and embedded in paraffin. Sections (5µm) were stained with hematoxylin and eosin.

Immunohistochemistry staining

For immunohistochemistry (IHC) staining of major basic protein (MBP) in eosinophils and NIMP-R14 in neutrophils, ears or lungs paraffin sections were treated with 0.6% H_2O_2 (in PBS) to block the endogenous peroxidase activity before antigen retrieval with pepsin (Invitrogen) incubated for 10 min at 37°C. Slides were then blocked with 1.5% of normal rabbit serum (Vector Laboratories, Burlingame, Calif) and incubated with monoclonal anti-mouse MBP primary antibody (dilution 1:2000) (for IHC of MBP), or with rat monoclonal anti-NIMP-R14 primary antibody (anti-neutrophil antibody, Abcam, AB2557, dilution 1:500) (for IHC of R14),overnight at 4°C, followed by incubation with biotinylated rabbit anti-rat IgG (Vector Laboratories) for 1h at RT (room temperature) and treatment of AB complex (Vector Laboratories) for 30 min at RT. Staining was then visualized with AEC+ high-sensitivity substrate chromogen solution (Dako, Glostrup, Denmark).

For immunohistochemistry (IHC) staining of TSLP, ears paraffin sections were treated with citric buffer (10mmol/L citric acid, PH6) boiled in the microwave (700W, for 2x5 min) for antigen retrieval. Slides were then blocked with Streptavidin and then Biotin solution (Vector Laboratories) and incubated with goat polyclonal anti-TSLP antibody (Bio-TSLP, dilution 1/50), overnight at 4°C. Slides were then washed and incubated with biotinylated secondary antibody (Strep-CY3, dilution 1/400) for 1 hour at RT. For nucleus staining, a Dapi-Mounting medium is added (Dapi 1/100) to the slides. Staining was then visualized under a UV microscope.

RNA extraction and quantitative RT-PCR

Total RNA was extracted from either mouse ears, lungs, paws or colon with Trizol reagent (Invitrogen) according to standard protocol. RNA was reverse transcribed by using random oligonucleotide hexamers and amplified by means of quantitative PCR with a LightCycler 480 (Roche Diagnostics) and the SYBR Green kit (Roche), according to manufacturer's instructions. Relative RNA levels were calculated with hypoxanthine phosphoribosyl- transferase (HPRT) as an internal control. For analysis of each set of gene expression, an arbitrary value of 1 was given to the samples exhibiting the highest level, and the remaining samples were plotted relative to this value. PCR primers are available upon request.

Analysis of BAL cells.

Mouse lungs were lavaged with saline containing 1 mg/mL EDTA. The lavage fluid was centrifuged, and BAL cells were counted with a hemocytometer (Neubauer's chamber; VWR). Differential cell counts were determined using cytospin preparations stained with Microscopy Hemacolor (Merck).

Measurement of airway responsiveness

Airway responsiveness was invasively determined using a computer-controlled small animal ventilator (FlexVent® system, SCIREQ Technologies). Mice were anesthetized with xylazine (15 mg/kg, i.p.), followed 15 minutes later by an i.p. injection of pentobarbital sodium (54 mg/kg). An 18-gauge metal needle was then inserted into the trachea and each mouse was connected to the FlexVent® ventilator, and quasi-sinusoidally ventilated with a tidal volume of 10 mL/kg at a frequency of 150 breaths/minute and a positive end-expiratory pressure of 2 cm H_2O in order to achieve a mean lung volume close to spontaneous breathing. After baseline measurement, mice were challenged for 10 seconds with a saline aerosol and, at 4.5-minute intervals, with 50 mg/mL methacholine. Airway resistance and elastance were expressed as cm$H_2$0.s/mL and cmH_2O/mL respectively.

5. References:

1. Clark AR, Belvisi MG (2012) Maps and legends: the quest for dissociated ligands of the glucocorticoid receptor. *Pharmacol Ther* 134(1):54–67.

2. Meijsing SH, et al. (2009) DNA binding site sequence directs glucocorticoid receptor structure and activity. *Science* 324(5925):407–410.

3. Surjit M, et al. (2011) Widespread negative response elements mediate direct repression by agonist-liganded glucocorticoid receptor. *Cell* 145(2):224–241.

4. Ratman D, et al. (2013) How glucocorticoid receptors modulate the activity of other transcription factors: a scope beyond tethering. *Mol Cell Endocrinol* 380(1–2):41–54.

5. Hua G, Paulen L, Chambon P (2016) GR SUMOylation and formation of an SUMO-SMRT/NCoR1-HDAC3 repressing complex is mandatory for GC-induced IR nGRE-mediated transrepression. *Proc Natl Acad Sci USA* 113(5):E626-634.

6. Hua G, Ganti KP, Chambon P (2016) Glucocorticoid-induced tethered transrepression requires SUMOylation of GR and formation of a SUMO-SMRT/NCoR1-HDAC3 repressing complex. *Proc Natl Acad Sci USA* 113(5):E635-643.

7. Sanderson K (2009) Big interest in heavy drugs. *Nature* 458(7236):269.

8. Li M, et al. (2006) Topical vitamin D3 and low-calcemic analogs induce thymic stromal lymphopoietin in mouse keratinocytes and trigger an atopic dermatitis. *Proc Natl Acad Sci USA* 103(31):11736–11741.

9. Stanley PL, Steiner S, Havens M, Tramposch KM (1991) Mouse skin inflammation induced by multiple topical applications of 12-O-tetradecanoylphorbol-13-acetate. *Skin Pharmacol* 4(4):262–271.

10. Vinter H, Iversen L, Steiniche T, Kragballe K, Johansen C (2015) Aldara®-induced skin inflammation: studies of patients with psoriasis. *Br J Dermatol* 172(2):345–353.

11. Trentham DE, Townes AS, Kang AH (1977) Autoimmunity to type II collagen an experimental model of arthritis. *J Exp Med* 146(3):857–868.

12. Chassaing B, Aitken JD, Malleshappa M, Vijay-Kumar M (2014) Dextran sulfate sodium (DSS)-induced colitis in mice. *Curr Protoc Immunol* 104:Unit 15.25.

13. Gimenes AD, et al. (2015) Beneficial effect of annexin A1 in a model of experimental allergic conjunctivitis. *Exp Eye Res* 134:24–32.

14. Smith SW (2009) Chiral toxicology: it's the same thing...only different. *Toxicol Sci* 110(1):4–30.

15. Chhabra N, Aseri ML, Padmanabhan D (2013) A review of drug isomerism and its significance. *Int J Appl Basic Med Res* 3(1):16–18.

16. Barker M, et al. (2005) Design and synthesis of new nonsteroidal glucocorticoid modulators through application of an “agreement docking” method. *J Med Chem* 48(14):4507–4510.

17. Uttamsingh V, et al. (2015) Altering metabolic profiles of drugs by precision deuteration: reducing mechanism-based inhibition of CYP2D6 by paroxetine. *J Pharmacol Exp Ther* 354(1):43–54.

18. Mullard A (2017) FDA approves first deuterated drug. *Nat Rev Drug Discov* 16(5):305.

6. Figures & legends

Fig. 1 CpdX and CpdX-D3 and their respective enantiomers are as efficient as Dexamethasone (Dex) at decreasing skin inflammations generated in atopic dermatitis-like and psoriasis-like models, and in a TPA-induced irritant contact dermatitis.

(A) Experimental protocol for a MC903-induced atopic dermatitis-like skin inflammation.

(B) Q-RT-PCR for RNA transcripts of pro-inflammatory genes in mouse ears treated as indicated. Data are represented as mean ± SEM of at least three independent experiments with at least three mice per treatment.

(C) Hematoxylin and eosin staining of ear sections. Scale bar represents 20 µm.

(D) Q-RT-PCR for RNA transcripts of pro-inflammatory genes in ears of mouse treated, as indicated. T_h1, T_h2, T_h17-specific pro-inflammatory interleukins are highlighted. Data are represented as mean ± SEM of at least three independent experiments with at least three mice per treatment.

(E) Q-RT-PCR for transcripts of pro-inflammatory genes in mouse ears treated as indicated. Data are represented as mean ± SEM of at least three independent experiments with at least three mice per treatment.

Fig. 1

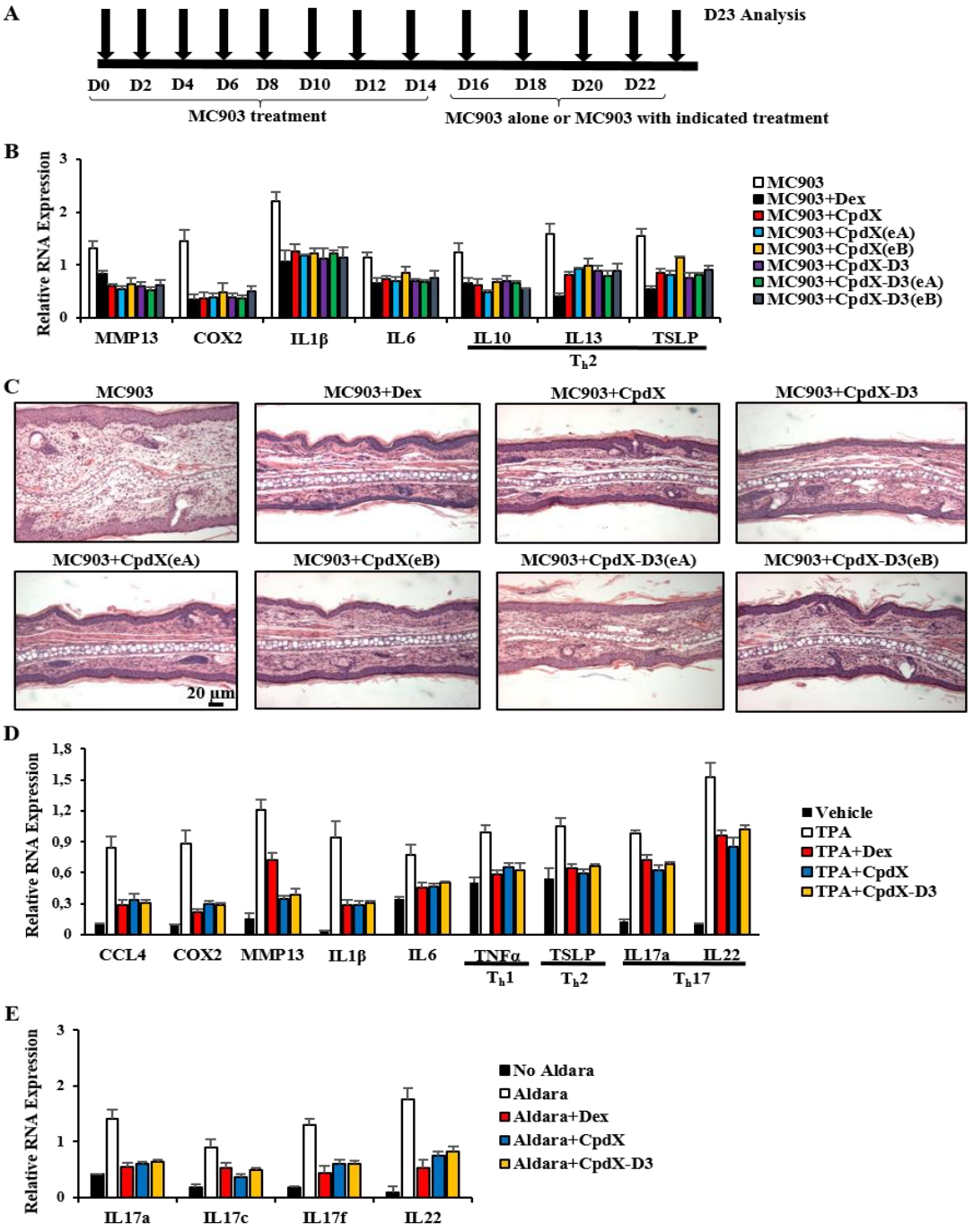
A
D23 Analysis
D0 D2 D4 D6 D8 D10 D12 D14 D16 D18 D20 D22
MC903 treatment
MC903 alone or MC903 with indicated treatment
B
Relative RNA Expression
MC903
MC903+Dex
MC903+CpdX
MC903+CpdX(eA)
MC903+CpdX(eB)
MC903+CpdX-D3
MC903+CpdX-D3(eA)
MC903+CpdX-D3(eB)
MMP13 COX2 IL1β IL6 IL10 IL13 TSLP
Th2
C
MC903
MC903+Dex
MC903+CpdX
MC903+CpdX-D3
MC903+CpdX(eA)
MC903+CpdX(eB)
MC903+CpdX-D3(eA)
MC903+CpdX-D3(eB)
20 µm
D
Relative RNA Expression
Vehicle
TPA
TPA+Dex
TPA+CpdX
TPA+CpdX-D3
CCL4 COX2 MMP13 IL1β IL6 TNFα TSLP IL17a IL22
Th1 Th2 Th17
E
Relative RNA Expression
No Aldara
Aldara
Aldara+Dex
Aldara+CpdX
Aldara+CpdX-D3
IL17a IL17c IL17f IL22

Fig. 2 CpdX, CpdX(eA), CpdX-D3 and CpdX-D3(eA), but not CpdX(eB) nor CpdX-D3(eB), are as efficient as Dexamethasone (Dex) at decreasing an HDM-induced asthma-like lung allergic inflammation.

(A) Experimental protocol for generating an HDM-induced asthma-like lung allergic inflammation.

(B) Cell counting from the fluid of bronchoalveolar lavage (BAL). Data are represented as mean ± SEM of at least three independent experiments with at least four mice per treatment. The statistical significance compared to the HDM treatment was calculated by student t test; (*) $p<0,05$; (**) $p<0,01$; (***) $p<0,001$; (ns) not significant.

(C) Q-RT-PCR for RNA transcripts of pro-inflammatory genes in lungs of mice treated as indicated. T_h2-specific pro-inflammatory interleukins are highlighted. Data are represented as mean ± SEM of at least three independent experiments with at least four mice per treatment. The statistical significance compared to the HDM treatment was calculated by student t test; (*) $p<0,05$; (**) $p<0,01$; (***) $p<0,001$; (ns) not significant.

(D) Hematoxylin and eosin staining of lung sections. Peribronchiolar (B) and perivascular (V) regions are indicated. Scale bar represents 40 µm.

(E) Airway hyperresponsiveness determined using the FlexVent® system after exposure to 50 mg/mL of methacholine. Data are represented as mean ± SEM with at least eight mice per treatment. The statistical significance as compared to the HDM treatment was calculated through Two-way ANOVA followed by Bonferroni multiple comparisons; (**) $p<0,01$; (***) $p<0,001$; (****) $p<0,0001$; (ns) not significant.

Fig. 2

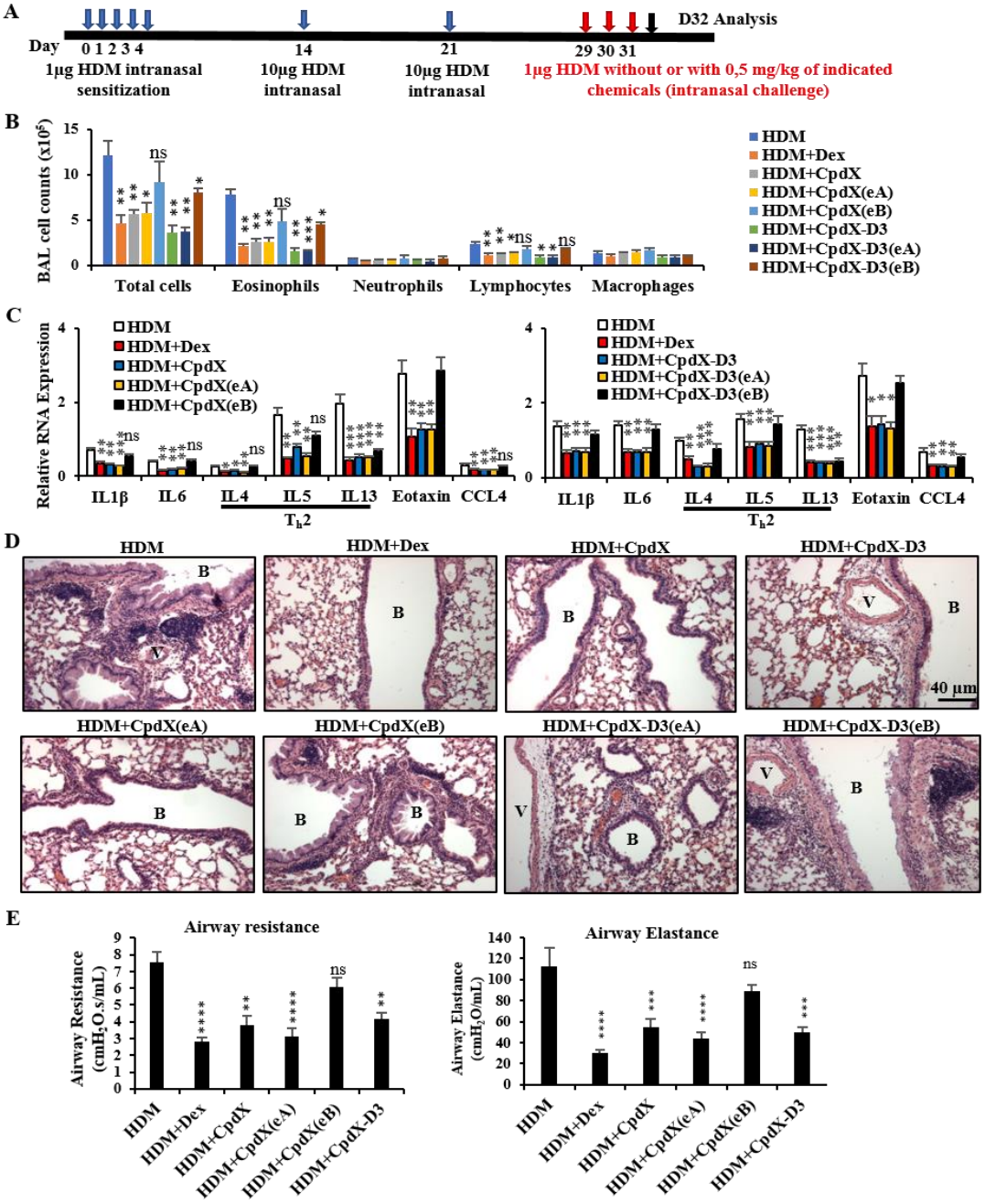
A
Day 0 1 2 3 4
1µg HDM intranasal sensitization
14
10µg HDM intranasal
21
10µg HDM intranasal
29 30 31
D32 Analysis
1µg HDM without or with 0,5 mg/kg of indicated chemicals (intranasal challenge)
B
BAL cell counts (x10⁵)
Total cells
Eosinophils
Neutrophils
Lymphocytes
Macrophages
HDM
HDM+Dex
HDM+CpdX
HDM+CpdX(eA)
HDM+CpdX(eB)
HDM+CpdX-D3
HDM+CpdX-D3(eA)
HDM+CpdX-D3(eB)
C
Relative RNA Expression
IL1β
IL6
IL4
IL5
IL13
Eotaxin
CCL4
Th2
D
HDM
HDM+Dex
HDM+CpdX
HDM+CpdX-D3
HDM+CpdX(eA)
HDM+CpdX(eB)
HDM+CpdX-D3(eA)
HDM+CpdX-D3(eB)
B
V
40 µm
E
Airway resistance
Airway Resistance (cmH2O.s/mL)
Airway Elastance
Airway Elastance (cmH2O/mL)

Fig. 3 CpdX, CpdX(eA), CpdX-D3 and CpdX-D3(eA), but not CpdX(eB) nor CpdX-D3(eB), are as efficient as Dexamethasone (Dex) at decreasing a collagen-induced arthritis (CIA) Th17 inflammation.

(A) Experimental protocol for collagen-induced arthritis.

(B) Photographs of the hind paws of mice in which a collagen-induced arthritis-like inflammation was generated (T0, left panels), and then were treated for 10-day (T10) intraperitoneal administration (right panels), as indicated.

(C) Mouse hind paw swelling as determined with a caliper. Data are represented as mean ± SEM with at least six mice per treatment. The statistical significance as compared to the Dex treatment was calculated by student t test. (*) $p<0,05$; (ns) indicates that the difference observed between Dex-treated, CpdX-treated and CpdX-D3-treated mice are not significant.

(D) Q-RT-PCR for RNA transcripts of pro-inflammatory genes in hind paws of mice treated as indicated. T_h17- and T_h1-specific pro-inflammatory interleukins are highlighted. Data are represented as mean ± SEM with at least six mice per treatment.

Fig. 3

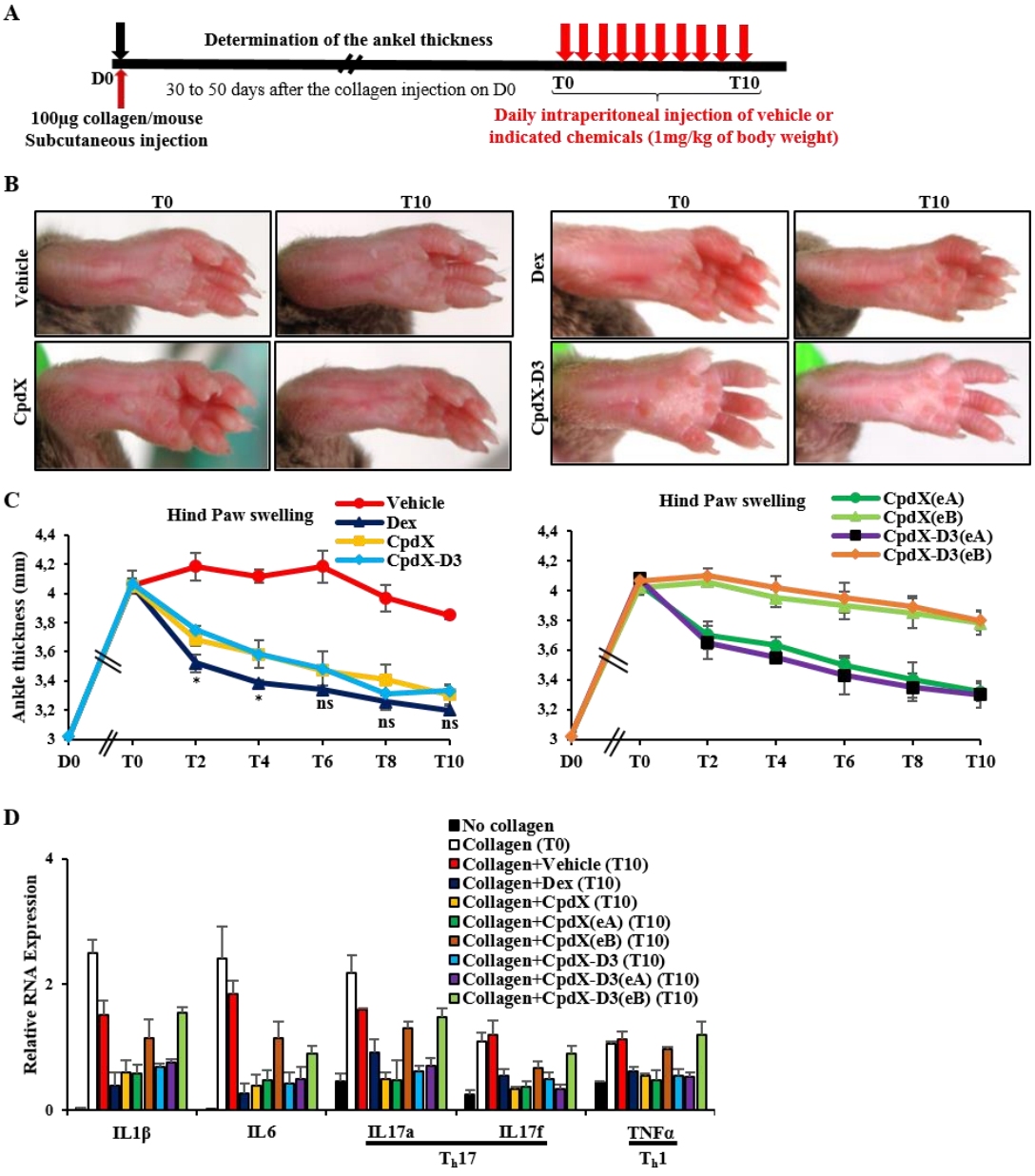
A
Determination of the ankel thickness
D0
30 to 50 days after the collagen injection on D0
T0
T10
100µg collagen/mouse
Subcutaneous injection
Daily intraperitoneal injection of vehicle or
indicated chemicals (1mg/kg of body weight)
B
T0
T10
Vehicle
Dex
CpdX
CpdX-D3
C
Hind Paw swelling
Vehicle
Dex
CpdX
CpdX-D3
Ankle thickness (mm)
4,4
4,2
4
3,8
3,6
3,4
3,2
3
D0
T0
T2
T4
T6
T8
T10
*
*
ns
ns
ns
Hind Paw swelling
CpdX(eA)
CpdX(eB)
CpdX-D3(eA)
CpdX-D3(eB)
D
No collagen
Collagen (T0)
Collagen+Vehicle (T10)
Collagen+Dex (T10)
Collagen+CpdX (T10)
Collagen+CpdX(eA) (T10)
Collagen+CpdX(eB) (T10)
Collagen+CpdX-D3 (T10)
Collagen+CpdX-D3(eA) (T10)
Collagen+CpdX-D3(eB) (T10)
Relative RNA Expression
4
2
0
IL1β
IL6
IL17a
IL17f
Th17
TNFα
Th1

Fig. 4 CpdX, CpdX-D3 and their enantiomers are as efficient as Dexamethasone at curing a Dextran Sodium Sulfate (DSS)-induced Th17 ulcerative colitis.

(A) Experimental protocol for DSS-induced colitis.

(B) Hematoxylin and eosin staining of colon sections. Solid arrows: mucosal inflammatory cell infiltration; dotted arrows: submucosal inflammatory cell infiltration; arrow head: ulceration. Scale bar represents 50 µm or 20 µm respectively.

(C) Q-RT-PCR for transcripts of pro-inflammatory genes in colons of mice treated as indicated. T_h17- and T_h2-specific pro-inflammatory interleukins are highlighted. Data are represented as mean ± SEM of at least three independent experiments with at least four mice per treatment.

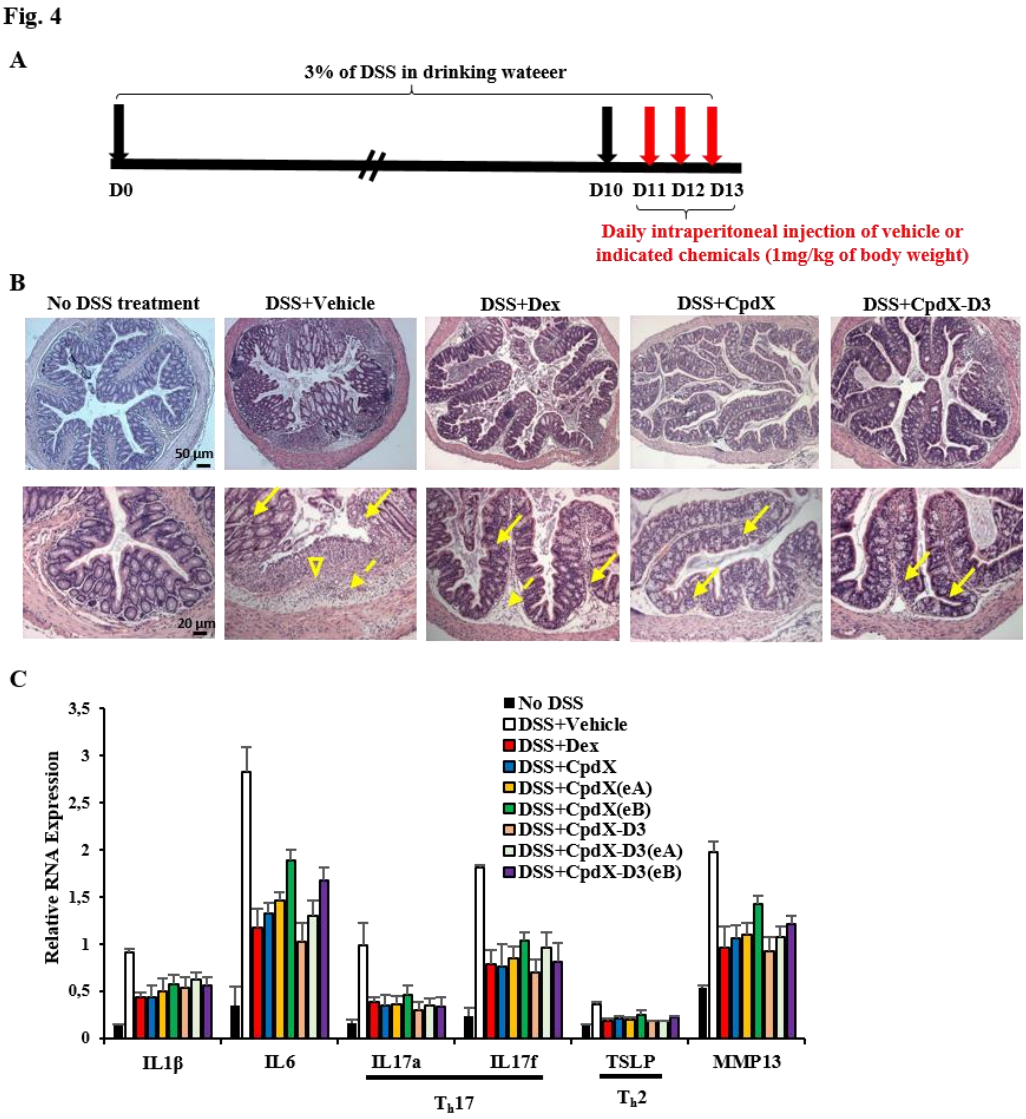

Fig. 5 CpdX, CpdX(eA), CpdX(eB), CpdX-D3, CpdX-D3(eA) or CpdX-D3(eB) alleviate as efficiently as Dexamethasone (Dex) an ovalbumin (OVA)-induced allergic conjunctivitis

(A) Experimental protocol for generation of an OVA-induced allergic conjunctivitis. (B) Photographs of mouse eyes taken 20 minutes after the last treatment on day 24. (C) Clinical scores (conjunctival hyperemia, lid edema and tearing) of treated mouse eyes as indicated were evaluated as under (B). The data were expressed as mean ± SEM with at least four mice per treatment.

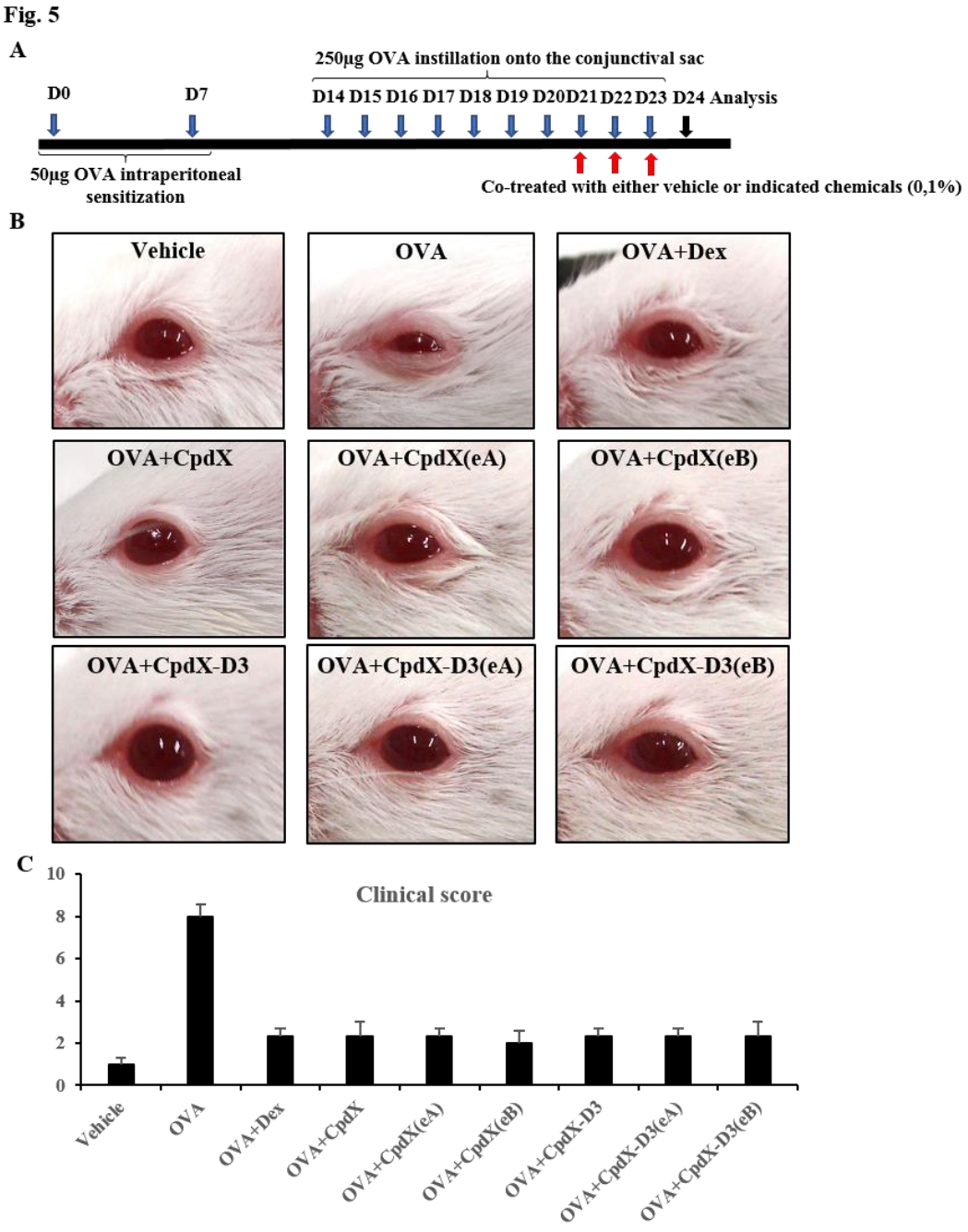

7. Supplementary figures & legends

Fig. S1 CpdX and CpdX-D3 are as efficient as Dexamethasone (Dex) at decreasing skin inflammations.

(A) Experimental protocol for TPA-induced irritant contact dermatitis-like inflammation.

(B) Experimental protocol for Aldara-induced psoriasis-like inflammation.

(C) Hematoxylin and eosin staining of ear section. Scale bar represents 20 µm.

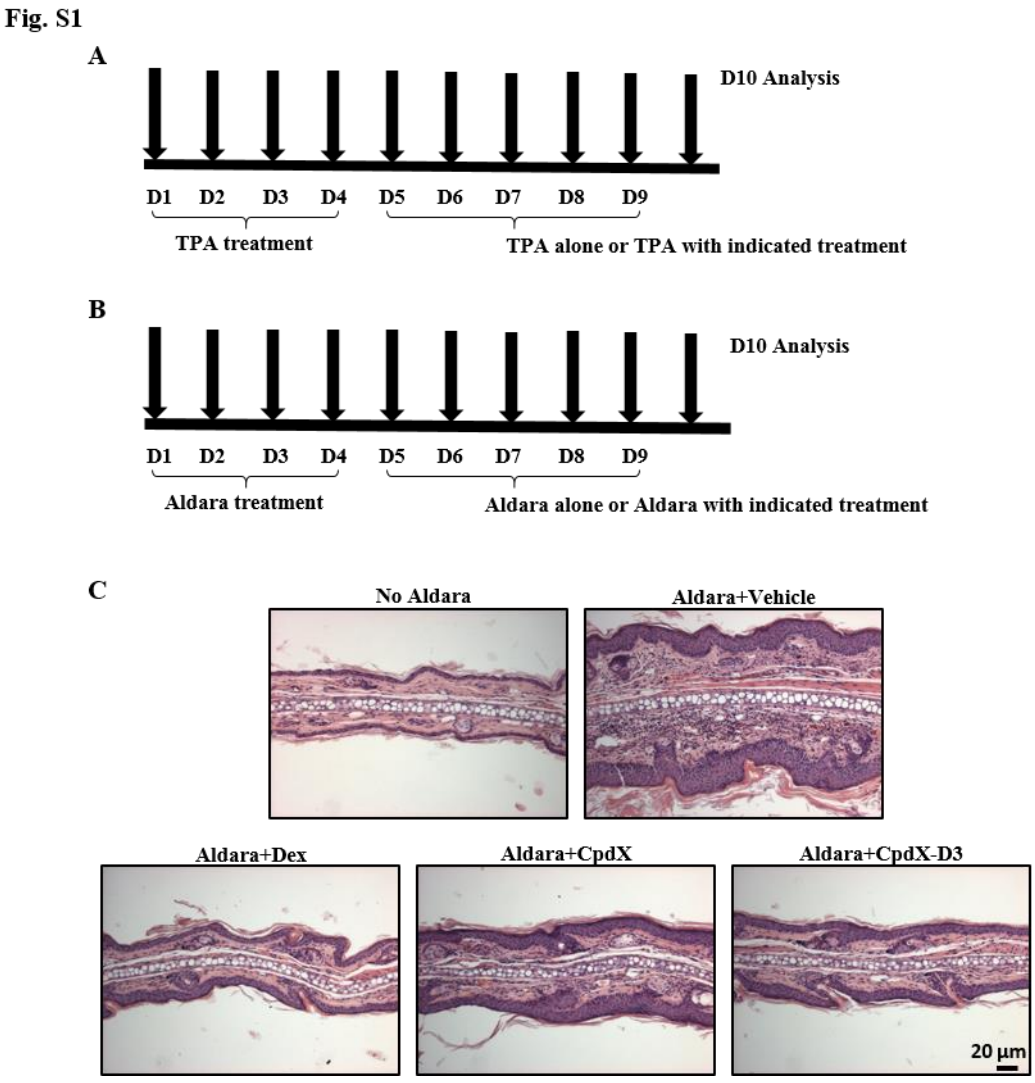

Fig. S2 CpdX, CpdX(eA), CpdX-D3 and CpdX-D3(eA), but not CpdX(eB) nor CpdX-D3(eB), are as efficient as Dexamethasone (Dex) at decreasing an HDM-induced asthma-like lung allergic inflammation.

(A) Immunohistochemistry analyses of lung sections using the eosinophils specific antibody MBP. Scale bar represents 40 µm.

(B) As in (A) but using the neutrophil specific antibody R14.

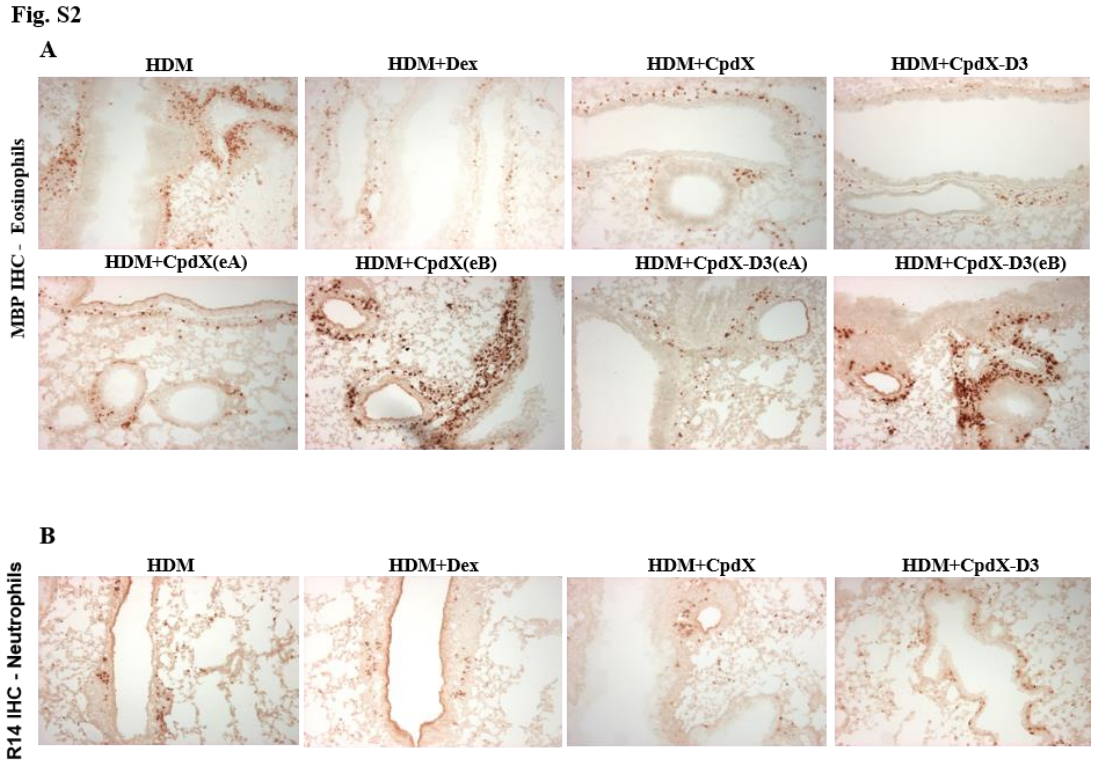

PART II

(Manuscript in preparation)

CpdX and CpdX-D3 and their respective enantiomers do not exhibit the multiple long-term undesirable effects of present day synthetic glucocorticoids, such as Dexamethasone, while keeping their beneficial anti-inflammatory functions

CpdX and CpdX-D3 and their respective enantiomers do not exhibit the multiple long-term undesirable effects of present day synthetic glucocorticoids, such as Dexamethasone, while keeping their beneficial anti-inflammatory functions.

Guoqiang Hua[a], Naimah Zein[a], Laetitia Paulen[a], Nadia Jessel[b], and Pierre Chambon[a,c,d,1]

[a]Institut de Génétique et de Biologie Moléculaire et Cellulaire, CNRS UMR7104, INSERM U964, Illkirch, 67404, France;
[b]INSERM (French National Institute of Health and Medical Research), UMR 1260, Regenerative Nanomedicine laboratory, Faculté de Médecine, FMTS, Strasbourg Cedex F-67085, France;
[c]University of Strasbourg Institute for Advanced Study, Illkirch, 67404, France;
[d]Collège de France, Illkirch, 67404, France;

[1]Correspondance: chambon@igbmc.fr (P.C.)

PART II

CpdX and CpdX-D3 and their respective enantiomers do not exhibit the multiple long-term undesirable effects of present day synthetic glucocorticoids, such as Dexamethasone, while keeping their beneficial anti-inflammatory functions

1. Introduction

Glucocorticoids (GC) have been extensively used to treat patients with inflammatory disorders since the late forties of the last century (1). In spite of several adverse effects, synthetic GCs have been increasingly used in the treatment of numerous inflammatory and allergic conditions thanks to their anti-inflammatory and immunosuppressive properties. The GC functions are transduced by a single receptor, the glucocorticoid receptor (GR). Which upon GC binding exerts either one of its three main functions by regulating the transcription of target genes through: (i) (+)GRE-mediated direct transactivation (2), (ii) IR nGRE-mediated direct transrepression (3, 4) and (iii) indirect tethered transrepression of transcriptional activators (e.g. NFκB, AP1, STAT3) (5–7). The beneficial anti-inflammatory effects of GR have been mainly ascribed to tethered transrepression, whereas there has been increasing evidence that the GC undesirable side-effects are related to both direct transactivation (1) and direct transrepression (3, 4). This led to searches for "dissociated" Selective Glucocorticoid Receptor Agonistic Modulators (SEGRAMs) which would preferentially induce tethered transrepression, while being devoid of both direct transactivation and direct transrepression activities. Several such synthetic non-steroidal putative SEGRAMs have been identified during the last decade and claimed to exhibit the GC anti-inflammatory properties, while being mostly devoid of their undesirable effects (8–10). On our side, we reported the identification of such a possible SEGRAM (named CpdX) that selectively exerts the GR indirect transrepression activity (7).

We now report that the racemic non-steroidal CpdX (7), its racemic deuterated form CpdX-D3, as well as their respective enantiomers, selectively and efficiently exert the anti-inflammatory activities of synthetic glucocorticoids (e.g. Dexamethasone) in several mouse inflammatory models. However, whether CpdX or CpdX-D3 are better drugs for clinical treatments remains unknown.

We report here that in marked contrast to a treatment with a synthetic GC (e.g. Dexamethasone), a long-term treatment with either CpdX, CpdX-D3, or one of their enantiomers, does not induce the ''classical'' GC undesirable side-effects, while keeping their therapeutically beneficial anti-inflammatory activity.

2. Results

In marked contrast to Dexamethasone (Dex) and Mapracorat, a topical treatment of skin with CpdX or CpdX-D3 or either one of their enantiomers does not induce a skin epidermal atrophy

Skin atrophy is a severe limitation to topical treatments with glucocorticoids (11). To investigate whether, similarly to Dex, a topical administration of CpdX could result in a skin atrophy, Balb/C mice were shaved on the dorsal skin. Ethanol (vehicle), Dex, CpdX, its "deuterated" form CpdX-D3 or either one of their enantiomers CpdX(eA), CpdX(eB), CpdX-D3(eA) or CpdX-D3(eB), were daily topically applied onto the dorsal skin for 8 days. Upon completion of the treatments, mice were sacrificed, and a histological analysis of the dorsal skin was performed. A hematoxylin and eosin staining revealed that in contrast to an application of CpdX or its deuterated form CpdX-D3, or of any of their enantiomers, a Dex application severely induces a marked epidermal atrophy (Fig. 1A). Morphometric analyses showed that the epidermal thickness decreases by 65 % upon a Dex treatment, whereas the epidermal thickness was not decreased by a CpdX, a CpdX(eA), a CpdX(eB), a CpdX-D3, a CpdX-D3(eA) or a CpdX-D3(eB) treatment (Fig. 1B).

As it was reported that the loss of the Kindlin-1 protein resulted in an epidermal skin atrophy (12), while the loss of the Redd1 protein prevented a GC-induced skin atrophy (13, 14), RNA transcripts were extracted from dorsal skin samples and the

transcripts of Kindlin-1 and REDD1 genes were analyzed by q-RT-PCR. The transcription of the Kindlin-1 gene (which contains putative nGREs: -9884 bp CTCCcaGGAGg; - 6414 bp CTCCTGAGa; - 5964 bp CTCCtTGAG) was strongly decreased by a Dex topical treatment, but not by either a CpdX, CpdX(eA), CpdX(eB), CpdX-D3, CpdX-D3(eA) or CpdX-D3(eB) treatment (Fig. 1C left panel). Conversely, the transcription of the REDD1 gene (which contains a +GRE) (13) was significantly increased by a Dex, but not by a CpdX, a CpdX(eA), a CpdX(eB), a CpdX-D3, a CpdX-D3(eA) nor a CpdX-D3(eB) treatment (Fig. 1C, right panel).

A "dissociated" synthetic non-steroidal ligand, namely Mapracorat (also named ZK245186 or BOL-303242-X), has been reported to be a promising anti-inflammatory drug in skin diseases (9). However, a short 8-day topical treatment with Mapracorat induced a significant dorsal skin epidermal atrophy (Fig. 1A). Thus, the transcription of the Kindlin-1 gene was decreased by Mapracorat, while the transcription of the REDD1 gene was increased by Mapracorat (Fig. 1C).

These results clearly demonstrate that, in marked contrast with a Dex, or a Mapracorat topical treatment of the skin, a topical treatment with either CpdX or its deuterated form CpdX-D3, or with any of their enantiomers [CpdX(eA), CpdX(eB), CpdX-D3(eA) and CpdX-D3(eB)], does not result in an epidermal skin atrophy, indicating that CpdX and CpdX-D3, as well as their enantiomers, can be safely used in skin treatments.

In marked contrast to Dexamethasone, a three-month mouse treatment with either CpdX, CpdX-D3 or any of their enantiomers does not affect bone formation.

Osteoporosis is a common undesirable side effect of long-term glucocorticoid clinical treatments (15). To study whether a long-term CpdX treatment could induce such an osteoporosis, 8-week-old B6 male mice were daily subjected for three months to either a subcutaneous injection of vehicle (NaCl 0,9%), Dex, CpdX, CpdX(eA), CpdX(eB), CpdX-D3, CpdX-D3(eA) or CpdX-D3(eB) (1 mg/kg body weight, diluted in NaCl 0,9%). From each animal included in these experiments, one femur and the

ipsilateral tibia were dissected and preserved in 70% ethanol for further bone microstructure analysis by micro-CT.

As expected, after a three-month Dex treatment, osteoporosis-like phenotypes were observed in the mouse tibia cortical bone: the bone volume was significantly decreased as compared to the total volume (Fig. 2A), the cortical thickness was drastically decreased (Fig. 2B) and the bone area, but not the marrow area, was also reduced (Figs. 2C-D). Surprisingly, but in agreement with a previous report (16), a Dex-treatment increased the mouse trabecular bone volume due to a higher in number of trabecula and to a decrease of the trabecular spacing, with no change in the trabecular thickness (data not shown). Importantly, in marked contrast to a Dex treatment, a three-month administration of CpdX or CpdX-D3, as well as of either one of their enantiomers CpdX(eA), CpdX(eB), CpdX-D3(eA) or CpdX-D3(eB), did not affect the bone formation in cortical and trabecular bones (Figs. 2A-E and S2A-E, and data not shown).

The expression of the WNT16 gene has been reported to affect the bone mineral density, the cortical bone thickness, the bone strength, and to an increase the risk of osteoporotic fracture (17). Q-RT-PCR analyses of WNT16 transcripts in mouse tibia samples demonstrated that the transcription of the WNT16 gene was decreased by 50% upon a Dex treatment, but not upon either a CpdX, CpdX(eA), CpdX(eB), CpdX-D3, CpdX-D3(eA) or CpdX-D3(eB) treatment (Fig. 2F).

These results indicate that CpdX, and CpdX-D3, as well as any of their enantiomers [CpdX(eA), CpdX(eB), CpdX-D3(eA) or CpdX-D3(eB)], could be safely used for clinical treatments of inflammatory diseases, since unlike synthetic glucocorticoids such as Dex, they do not affect bone formation.

In marked contrast to Dexamethasone, a three-month treatment with either CpdX, CpdX-D3 or any of their enantiomers does not lead to a loss of body weight, a change in body composition nor to undesirable tissue-specific "toxic" side-effects

A dual-energy x-ray absorptiometry (DEXA) machine (18) was used to determine the mouse lean mass and fat mass after three-month treatments, as described above. All mice treated with either vehicle, CpdX, CpdX-D3 or any of their enantiomers, exhibited similar increases of body weight (Fig. 3A, and data not shown), as well as a commensurate increase in fat mass (Fig. 3B, and data not shown) and lean percentage (Fig. 3C, and data not shown). In contrast, mice treated with Dex exhibited a net loss in total body weight (Fig. 3A), together with a disproportional increase in fat (Fig. 3B) and a decrease of lean mass (Fig. 3C).

Glucocorticoids are well known to induce a drastic thymus apoptosis (19). Accordingly, after a three-month treatment, no thymus was found in sixteen out of nineteen mice treated with Dex. In marked contrast, a treatment with either CpdX, its deuterated form CpdX-D3, or their enantiomers CpdX(eA), CpdX(eB), CpdX-D3(eA) or CpdX-D3(eB) did not result in any significant thymus apoptosis (Fig. 3D). The spleen weight was decreased by more than 50 % in Dex-treated mice, whereas it was not decreased in CpdX-, CpdX(eA)-, CpdX(eB)-, CpdX-D3-, CpdX-D3(eA)- or CpdX-D3(eB)-treated mice (Fig. 3E). A weak, but significant loss of the kidney weight was also selectively observed in mice treated with Dex (Fig. 3F). Interestingly, the weight of the adrenal gland, in which corticosterone synthesis takes place, was decreased by a Dex treatment, whereas it was significantly increased by a treatment with either CpdX, CpdX(eA), CpdX(eB), CpdX-D3, CpdX-D3(eA) or CpdX-D3(eB) (Fig. 3G).

A long-term daily subcutaneous injection of Dexamethasone inhibits corticosterone synthesis which, in marked contrast, is increased upon a similar treatment with either CpdX, CpdX(eA), CpdX(eB), CpdX-D3, CpdX-D3(eA) or CpdX-D3(eB)

Corticosterone is synthesized in the fasciculata zone of the cortex layer of the adrenal gland. Histological sections of adrenal gland showed that upon a three-month

treatment with Dex, the cortex layers (see double-headed arrow in upper panels), most notably the fasciculata zone (see bold double-headed arrow in lower panels) of the adrenal glands were drastically decreased (Fig. 4A), whereas they were markedly increased upon administration of CpdX or its deuterated form CpdX-D3, or either one of their enantiomers CpdX(eA), CpdX(eB), CpdX-D3(eA) or CpdX-D3(eB) (Fig. 4A and data not shown). Transcriptional analyses from mouse adrenal glands samples demonstrated that the transcripts of the Cyp11a, Cyp11b1 and HSD3β genes which are involved in the corticosterone synthesis pathway (20), were inhibited by Dex treatment due to the presence of nGREs in these genes (underline in Fig 4B), whereas being increased by CpdX, CpdX(eA), CpdX(eB), CpdX-D3, CpdX-D3(eA) or CpdX-D3(eB) treatments (Fig. 4C). As compared to control mice (Vehicle), Dex-treated mice exhibited a much lower corticosterone levels in plasma at both 10 a.m. and 6 p.m. whereas, in marked contrast, CpdX-, CpdX(eA)-, CpdX(eB)-, CpdX-D3-, CpdX-D3(eA)- and CpdX-D3(eB)-treated mice exhibited a much higher corticosterone level at 10 a.m. (Fig. 4D).

Interestingly, transcriptional analyses from mouse adrenal glands samples also showed that the transcript of the Cyp11b2 gene, which is involved in the aldosterone synthesis pathway, was inhibited by Dex treatment, but not by CpdX, CpdX(eA), CpdX(eB), CpdX-D3, CpdX-D3(eA) or CpdX-D3(eB) treatment (Fig. 4C). In agreement with this result, histological analyses revealed that the glomerulosa zone (outermost zone of the cortex layer, see the small empty double-headed arrows in the lower panels of Fig. 4A), which produces aldosterone, was drastically decreased by Dex treatment, but not by either CpdX, CpdX(eA), CpdX(eB), CpdX-D3, CpdX-D3(eA) or CpdX-D3(eB) treatment (Fig. 4A and data not shown).

Most interestingly, these data indicate that the beneficial anti-inflammatory effects of CpdX and of its deuterated form CpdX-D3 [as well as any of their enantiomers CpdX(eA), CpdX(eB), CpdX-D3(eA) and CpdX-D3(eB)], which all occur through repression of pro-inflammatory genes, result from both (i) the direct binding of CpdX or CpdX-D3 to the GR, which activates its tethered indirect transrepression function, and (ii) a further activation of this indirect transrepression function due to a CpdX- or

CpdX-D3-induced increase of the blood corticosterone level, most notably during the rest period when the ACTH level is the lowest.

In marked contrast to Dexamethasone, a three-month treatment with either CpdX, CpdX-D3 or any of their enantiomers does not induce a type 2 diabetes syndrome nor a fatty liver

Upon a long-term glucocorticoid administration, hyperglycemia is a common undesirable side effect (21). After a three-month treatment, the overnight fasting blood glucose level in Dex-treated mice was significantly higher than in mice treated with either saline (vehicle), CpdX, CpdX(eA), CpdX(eB), CpdX-D3, CpdX-D3(eA) or CpdX-D3(eB) (Fig. 5A). An intraperitoneal glucose tolerance test (IPGTT) showed that, upon glucose injection, a significant higher blood glucose level was observed during a two-hour period in Dex-treated mice, whereas there was no significant difference between these levels in control, CpdX-, CpdX(eA)-, CpdX(eB)-, CpdX-D3-, CpdX-D3(eA)- or CpdX-D3(eB)-treated mice (Fig. 5B). These results indicated that, in contrast to Dex, a treatment with CpdX, CpdX(eA), CpdX(eB), CpdX-D3, CpdX-D3(eA) or CpdX-D3(eB) does not induce a hyperglycemia.

A chronic exposure of humans to glucocorticoids (GC) is well known to result in a whole-body insulin-resistance (22). After a three-month treatment, the blood insulin level revealed a hyperinsulinemia in Dex-treated mice, but not in mice treated with either saline (vehicle), CpdX, CpdX(eA), CpdX(eB), CpdX-D3, CpdX-D3(eA) or CpdX-D3(eB) (Fig. 5C). The hyperglycemia which was observed in Dex-treated mice (Fig. 5A-B), taken together with an intraperitoneal glucose insulin tolerance test (IPITT) test which disclosed a significant impaired response to insulin (Fig. 5D), could be due to insulin resistance in these mice (22). In keeping with this suggestion, western-blot analyses from liver extracts showed in Dex-treated mice, but not in vehicle-, CpdX- or CpdX-D3-treated mice, a decrease in phosphorylated insulin receptor substrate 1 (p-IRS1 S318) (Fig. 5E). As expected, the phosphorylation of the insulin-stimulated protein kinase B (p-AKT S473) was also decreased in Dex-treated mice (Fig. 5E). We

conclude that, in contrast to Dexamethasone, a treatment with CpdX, its deuterated form CpdX-D3, or any of their enantiomers [CpdX(eA), CpdX(eB), CpdX-D3(eA) or CpdX-D3(eB)], does not induce the insulin resistance characteristic of a type 2 diabetic syndrome.

Liver samples were also harvested at the end of these three-month treatments. 5% Red oil staining of frozen sections revealed a marked lipid deposition in livers from mice subjected to a daily subcutaneously administration of Dex, but not in liver from mice treated with either CpdX or CpdX-D3, their enantiomers or Vehicle (Fig. 5F). Accordingly, an increase in RNA transcripts of fatty acid synthase (FASN) and Stearoyl-CoA desaturase 1 (SCD1), which are both critically involved in liver lipogenesis (23), was observed in liver of Dex-treated mice, but not in vehicle-, CpdX-, CpdX(eA)-, CpdX(eB)-, CpdX-D3-, CpdX-D3(eA)- or CpdX-D3(eB)-treated mice (Fig. 5G). Hypercholesterolemia is a main cause of non-alcoholic fatty liver diseases (NAFLDs) (24) and cholesterol is converted in the liver into bile acids. Accordingly, a high level of bile acids was observed in patients exhibiting fatty liver diseases (25). As expected, Dex-treated, but not CpdX-, CpdX(eA)-, CpdX(eB)-, CpdX-D3-, CpdX-D3(eA)- or CpdX-D3(eB)-treated mice, exhibited a clear increase in blood cholesterol and bile acids' levels (Figs. 5H-I).

Taken altogether the above results demonstrate that a three-month in vivo treatment with either CpdX or its deuterated form CpdX-D3, or with any of their enantiomers [CpdX(eA), CpdX(eB), CpdX-D3(eA) or CpdX-D3(eB)], does not induce a type 2 diabetes syndrome, nor a fatty liver disease, in marked contrast with a similar treatment with Dexamethasone.

3. Conclusion

Barker et al., showed that the compound that we named CpdX, could be selectively docked *in vitro* into the GR Ligand binding domain using an "Agreement Docking" method (26). We have firstly characterized CpdX as a potential "dissociated" Selective Glucocorticoid Receptor Agonist (SEGRA) (7), and more recently we reported that CpdX, its deuterated form CpdX-D3, as well as their respective enantiomers, can indeed be used to treat as efficiently as the synthetic glucocorticoid, Dexamethasone, several mouse inflammatory models. In this paper, we demonstrate that, unlike a Dex treatment, an *in vivo* treatment with either CpdX, CpdX-D3, or any of their enantiomers, does not induce a skin epidermal atrophy, an osteoporosis-like phenotype, a loss of body weight, an apoptosis of the thymus and the adrenal gland, a fatty liver and a type 2 diabetes syndrome.

4. Materials & Methods

Mice

Wild type BALB/c female mice and C57BL/6J male mice were purchased from Charles River Laboratories. They were maintained under institutional guidelines, in a temperature and humidity controlled animal facility, with a 12 hours light/dark cycle and free access to water and food. Experimental manipulation of mice were approved by the animal care and use committee of the IGBMC/ICS.

Materials

Dexamethasone (Dex) and Glucose were from Sigma Aldrich. Insulin (Humulin R; Eli Lilly) was from Eurobio ingen. Pan AKT (C67E7), pAKT S473 (9271L), IRS-1 (D23G12) and pIRS-1 S318 (D51C3) antibodies were from Cell Signaling.

Histology

Mouse samples were fixed overnight at 4°C in 4% paraformaldehyde and embedded in paraffin. Sections (5µm) were stained with hematoxylin and eosin.

For the liver, lipid deposition was revealed by 5% Red oil staining of frozen sections.

RNA extraction and quantitative RT-PCR

Total RNA was extracted from either mouse dorsal skin, tibia, adrenal gland or liver with Trizol reagent (Invitrogen) according to standard protocol. RNA was reverse transcribed by using random oligonucleotide hexamers and amplified by means of quantitative PCR with a LightCycler 480 (Roche Diagnostics) and the SYBR Green kit (Roche), according to manufacturer's instructions. Relative RNA levels were calculated with hypoxanthine phosphoribosyl- transferase (HPRT) as an internal control. For analysis of each set of gene expression, an arbitrary value of 1 was given to the samples exhibiting the highest level, and the remaining samples were plotted relative to this value. PCR primers are available upon request.

Micro-CT analysis

From each animal included in the experiments, one femur and the ipsilateral tibia have been dissected and preserved in 70% ethanol. The FX Quantum micro-CT scanner (Perkin Elmer) was used to perform measurements at the distal femur and midshaft tibia. All scans were performed with an isotropic voxel size of 10 µm, 160 µA tube current and 90 kV tube voltage. Gray scale images were initially pre-processed using ImageJ software. Morphological 3D measurements were further performed using the CTAn software (Bruker). Cortical bone parameters were measured in the tibia midshaft and included measures of cortical thickness, bone area fraction, total area, bone area and marrow area. The region of interest was selected from below the distal tibial crest and continued for 20 slices toward the proximal end of the tibia. Trabecular bone parameters were measured in the distal metaphysis of the femurs and included bone volume fraction, trabecular thickness, trabecular number and trabecular separation. The region of interest was selected from below the distal growth plate where the epiphyseal cap structure completely disappeared and continued for 100 slices toward the proximal end of the femur.

Determination of plasmatic parameters

Blood was collected at 10 a.m. and 6 p.m. by retro-orbital puncture in lithium-heparin coated vials, and the plasmatic level of corticosterone, insulin, total cholesterol and bile acids were determined.

Intraperitoneal glucose tolerance test (IPGTT)

Mice were fasted for 14 hours before test. Mouse blood glucose concentration was measured at 10 a.m. before (T_0) and during two hours (T_{120}) after glucose i.p. injection (2 mg/kg body weight).

Intraperitoneal insulin tolerance test (IPITT)

Mice were fasted for 6 hours before test. The blood glucose concentration was measured both before (T0) and during a one- hour period after insulin i.p. injection (0,75 U/kg body weight).

Western Blot

Liver samples were harvested and lysed in the RIPA buffer (20 mM Tris pH 8, 150 mM NaCl, 10% glycerol, 1% NP-40 and 2 mM EDTA). Antibodies from Cell Signaling were used to assess by Western-Blotting the relative level of p-IRS1 (S318), IRS-1, p-AKT (S473) and AKT.

5. References

1. Clark AR, Belvisi MG (2012) Maps and legends: the quest for dissociated ligands of the glucocorticoid receptor. *Pharmacol Ther* 134(1):54–67.
2. Meijsing SH, et al. (2009) DNA binding site sequence directs glucocorticoid receptor structure and activity. *Science* 324(5925):407–410.
3. Surjit M, et al. (2011) Widespread negative response elements mediate direct repression by agonist-liganded glucocorticoid receptor. *Cell* 145(2):224–241.
4. Hua G, Paulen L, Chambon P (2016) GR SUMOylation and formation of an SUMO-SMRT/NCoR1-HDAC3 repressing complex is mandatory for GC-induced IR nGRE-mediated transrepression. *Proc Natl Acad Sci USA* 113(5):E626-634.
5. Ratman D, et al. (2013) How glucocorticoid receptors modulate the activity of other transcription factors: a scope beyond tethering. *Mol Cell Endocrinol* 380(1–2):41–54.
6. Langlais D, Couture C, Balsalobre A, Drouin J (2012) The Stat3/GR interaction code: predictive value of direct/indirect DNA recruitment for transcription outcome. *Mol Cell* 47(1):38–49.
7. Hua G, Ganti KP, Chambon P (2016) Glucocorticoid-induced tethered transrepression requires SUMOylation of GR and formation of a SUMO-SMRT/NCoR1-HDAC3 repressing complex. *Proc Natl Acad Sci USA* 113(5):E635-643.
8. Baiula M, et al. (2014) Mapracorat, a selective glucocorticoid receptor agonist, causes apoptosis of eosinophils infiltrating the conjunctiva in late-phase experimental ocular allergy. *Drug Des Devel Ther* 8:745–757.
9. Schäcke H, et al. (2009) Characterization of ZK 245186, a novel, selective glucocorticoid receptor agonist for the topical treatment of inflammatory skin diseases. *Br J Pharmacol* 158(4):1088–1103.
10. Ripa L, et al. (2018) Discovery of a Novel Oral Glucocorticoid Receptor Modulator (AZD9567) with Improved Side Effect Profile. *J Med Chem* 61(5):1785–1799.
11. Schoepe S, Schäcke H, May E, Asadullah K (2006) Glucocorticoid therapy-induced skin atrophy. *Exp Dermatol* 15(6):406–420.
12. Ussar S, et al. (2008) Loss of Kindlin-1 causes skin atrophy and lethal neonatal intestinal epithelial dysfunction. *PLoS Genet* 4(12):e1000289.
13. Baida G, et al. (2015) REDD1 functions at the crossroads between the therapeutic and adverse effects of topical glucocorticoids. *EMBO Mol Med* 7(1):42–58.
14. Britto FA, et al. (2014) REDD1 deletion prevents dexamethasone-induced skeletal muscle atrophy. *Am J Physiol Endocrinol Metab* 307(11):E983-993.
15. Canalis E (2003) Mechanisms of glucocorticoid-induced osteoporosis. *Curr Opin Rheumatol* 15(4):454–457.
16. Grahnemo L, et al. (2015) Possible role of lymphocytes in glucocorticoid-induced increase in trabecular bone mineral density. *J Endocrinol* 224(1):97–108.
17. Zheng H-F, et al. (2012) WNT16 influences bone mineral density, cortical bone thickness, bone strength, and osteoporotic fracture risk. *PLoS Genet* 8(7):e1002745.

18. Champy M-F, et al. (2008) Genetic background determines metabolic phenotypes in the mouse. *Mamm Genome* 19(5):318–331.
19. Cohen JJ (1992) Glucocorticoid-induced apoptosis in the thymus. *Semin Immunol* 4(6):363–369.
20. Boucher E, Provost PR, Tremblay Y (2014) Ontogeny of adrenal-like glucocorticoid synthesis pathway and of 20α-hydroxysteroid dehydrogenase in the mouse lung. *BMC Res Notes* 7:119.
21. Clore JN, Thurby-Hay L (2009) Glucocorticoid-induced hyperglycemia. *Endocr Pract* 15(5):469–474.
22. Geer EB, Islam J, Buettner C (2014) Mechanisms of glucocorticoid-induced insulin resistance: focus on adipose tissue function and lipid metabolism. *Endocrinol Metab Clin North Am* 43(1):75–102.
23. Wang J-C, Gray NE, Kuo T, Harris CA (2012) Regulation of triglyceride metabolism by glucocorticoid receptor. *Cell Biosci* 2(1):19.
24. Kim EJ, et al. (2014) Cholesterol-induced non-alcoholic fatty liver disease and atherosclerosis aggravated by systemic inflammation. *PLoS ONE* 9(6):e97841.
25. Aranha MM, et al. (2008) Bile acid levels are increased in the liver of patients with steatohepatitis. *Eur J Gastroenterol Hepatol* 20(6):519–525.
26. Barker M, et al. (2005) Design and synthesis of new nonsteroidal glucocorticoid modulators through application of an “agreement docking” method. *J Med Chem* 48(14):4507–4510.

6. Figures & legends

Fig.1 In marked contrast to Dexamethasone (Dex) and Mapracorat, a topical treatment of skin with CpdX or CpdX-D3 or either one of their enantiomers does not induce a skin epidermal atrophy.

(A) Hematoxylin and eosin staining (left panels) and DAPI staining for nucleus (right panels) of sections of mouse ears treated as indicated. Scale bar represents 20 µm.

(B) Morphometric analysis of the epidermal thickness (in µm) from H&E stained ear sections as under (A).

(C) Q-RT-PCR for transcripts of Kindlin-1 and REDD1 genes in mouse ears treated as indicated. Data are represented as mean ± SEM of at least three independent experiments with at least three mice per treatment.

Fig. 1

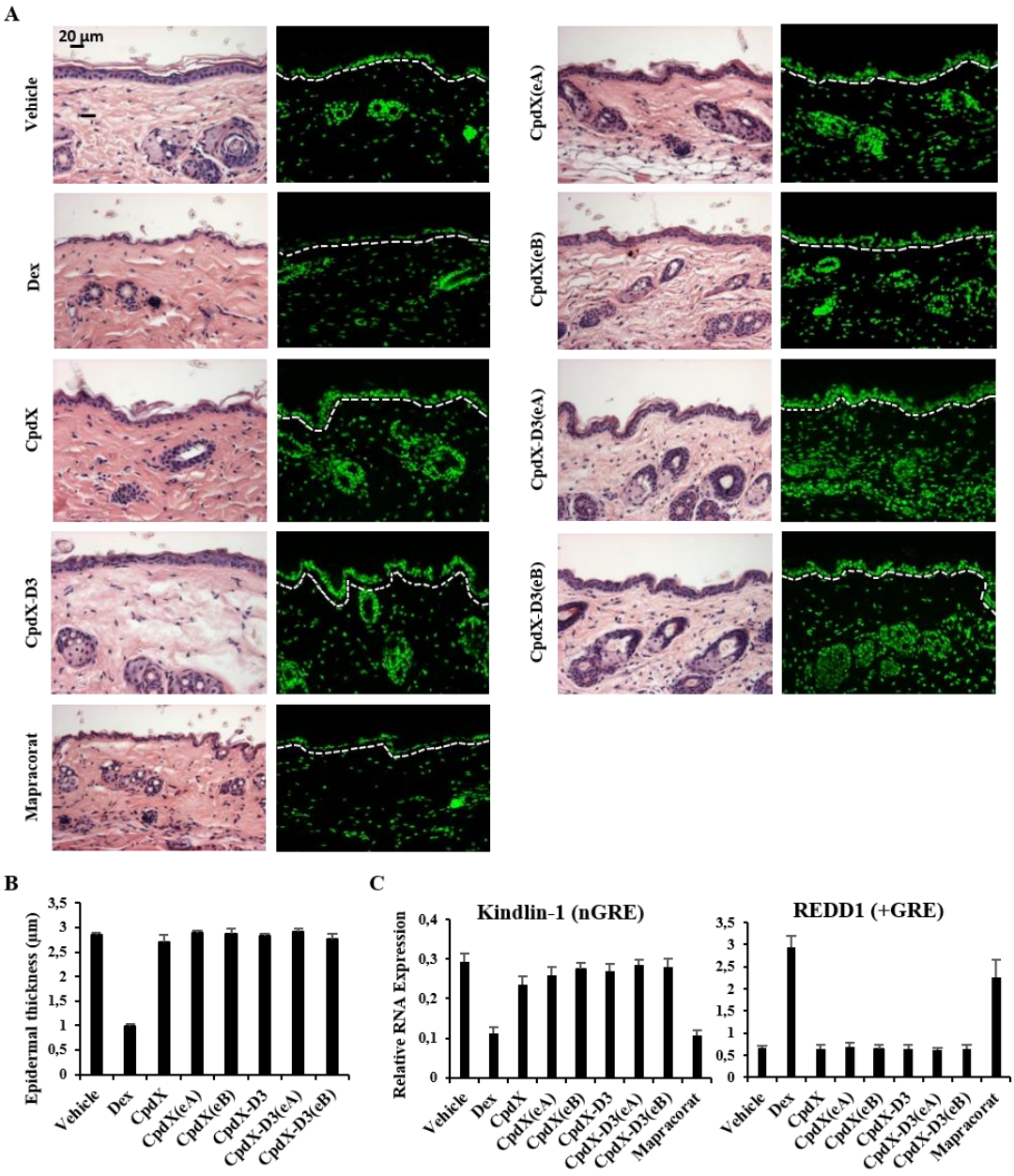
A
20 µm
Vehicle
Dex
CpdX
CpdX-D3
Mapracorat
CpdX(eA)
CpdX(eB)
CpdX-D3(eA)
CpdX-D3(eB)
B
Epidermal thickness (µm)
3,5
3
2,5
2
1,5
1
0,5
0
Vehicle
Dex
CpdX
CpdX(eA)
CpdX(eB)
CpdX-D3
CpdX-D3(eA)
CpdX-D3(eB)
C
Kindlin-1 (nGRE)
Relative RNA Expression
0,4
0,3
0,2
0,1
0
Vehicle
Dex
CpdX
CpdX(eA)
CpdX(eB)
CpdX-D3
CpdX-D3(eA)
CpdX-D3(eB)
Mapracorat
REDD1 (+GRE)
3,5
3
2,5
2
1,5
1
0,5
0
Vehicle
Dex
CpdX
CpdX(eA)
CpdX(eB)
CpdX-D3
CpdX-D3(eA)
CpdX-D3(eB)
Mapracorat

Fig. 2 In marked contrast to Dexamethasone, a three-month mouse treatment with either CpdX, CpdX-D3 or any of their enantiomers, does not affect bone formation. Five cortical bone parameters were measured by microCT: (A) bone volume/total volume (%); (B) cortical thickness (mm); (C) bone area (mm^2), (D) marrow area (mm^2) and (E) total area (mm^2); The data correspond to the mean (as pointed by arrow heads) ± SEM for at least six mice per treatment. The statistical significance compared to vehicle treatment was calculated through One-way ANOVA test followed by Dunnett's multiple comparison test (*) p<0,05; (**) p<0,01 (***) p<0,001; (****) p<0,0001; (ns): not significant. (F) Q-RT-PCR for transcripts of WNT16 gene in tibia from mice treated as indicated. Data are represented as mean ± SEM with at least six mice per treatment. The statistical significance was calculated by student t test; (***) p<0,001.

Fig. 2

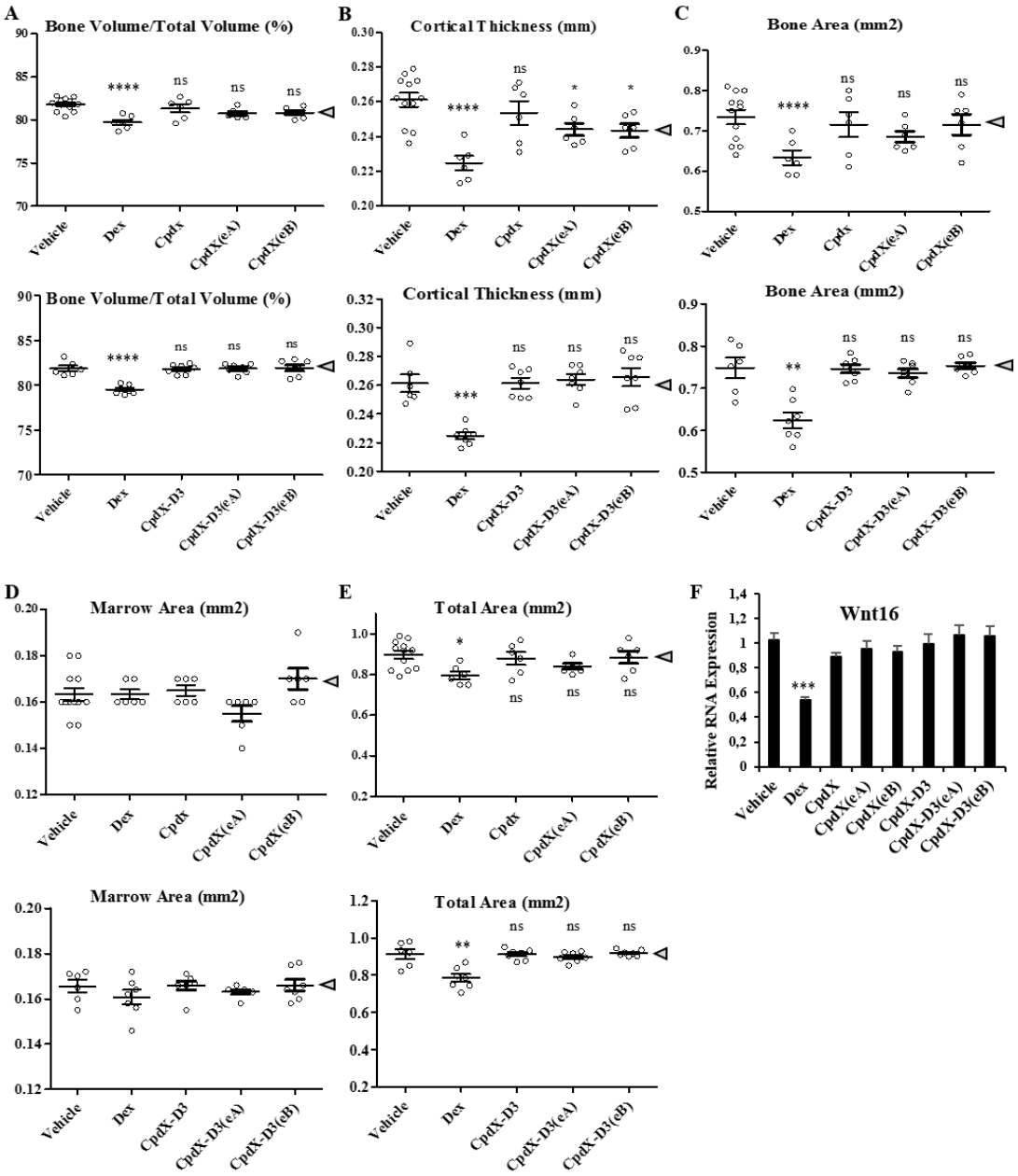
A
Bone Volume/Total Volume (%)
B
Cortical Thickness (mm)
C
Bone Area (mm2)
Vehicle
Dex
Cpdx
CpdX(eA)
CpdX(eB)
Bone Volume/Total Volume (%)
Cortical Thickness (mm)
Bone Area (mm2)
CpdX-D3
CpdX-D3(eA)
CpdX-D3(eB)
D
Marrow Area (mm2)
E
Total Area (mm2)
F
Wnt16
Relative RNA Expression
Marrow Area (mm2)
Total Area (mm2)

Fig. 3 In marked contrast to Dexamethasone, a three-month treatment with either CpdX, CpdX-D3 or any of their enantiomers does not lead to a loss of body weight, a change in body composition, nor to undesirable tissue-specific "toxic" side-effects.

(A) Change of body weight after a 3-month treatment as indicated. (B) Fat percentage and (C) Lean mass percentage for mice treated for 3-month, as indicated. The data correspond to the mean (as pointed by arrow heads) ± SEM for at least nine mice per treatment. The statistical significance was calculated through Krustal-Walis test followed by Dunn's multiple comparison test; (*) p<0,05; (**) p<0,01 (***) p<0,001. (D) The weight (in grams) of thymus, (E) spleen, (F) kidney and (G) adrenal gland in mice treated for 3-monthes as indicated. Data are represented as mean ± SEM for at least nine mice per treatment. The statistical significance of the data as compared to vehicle treatment was calculated by student t test; (*) p<0,05.

Fig. 3

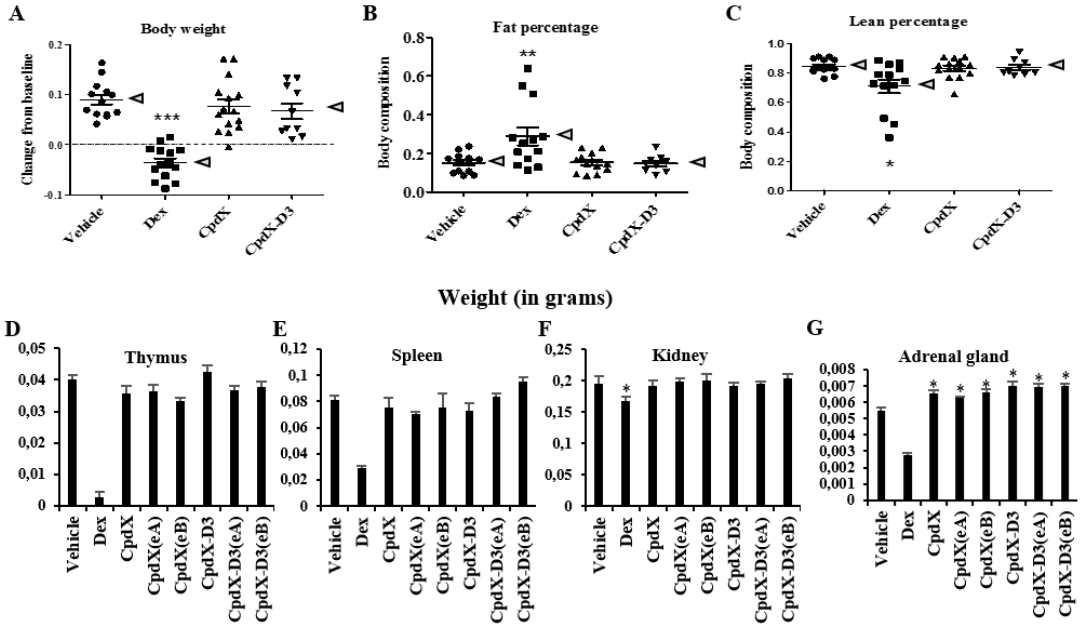

Fig. 4 A long-term daily subcutaneous injection of Dexamethasone inhibits corticosterone synthesis which, in marked contrast, is increased by a similar treatment with either CpdX, CpdX(eA), CpdX(eB), CpdX-D3, CpdX-D3(eA) or CpdX-D3(eB).

(A) Hematoxylin and eosin staining of adrenal gland sections. The cortex layer of the adrenal gland is indicated in left panels by double-headed arrows, while the fasciculata and the glomerulosa zones of the cortex are indicated by long bold double-headed arrows and small empty double-headed arrows in right panels, respectively. Scale bar represents 50 µm and 25 µm, respectively.

(B) Locations of putative nGRE present in the promoter regions of Cyp11a, Cyp11b, HSD3β and Cyp11b2 genes.

(C) Q-RT-PCR for transcripts of Cyp11a, Cyp11b1, HSD3β and Cyp11b2 genes in adrenal glands of mice treated for 3-monthes, as indicated. Data are represented as mean ± SEM for at least nine mice per treatment.

(D) Plasmatic corticosterone levels at 10 a.m. and 6 p.m. in mice treated for 3-monthes, as indicated. Data are represented as mean ± SEM with at least nine mice per treatment.

Fig. 4

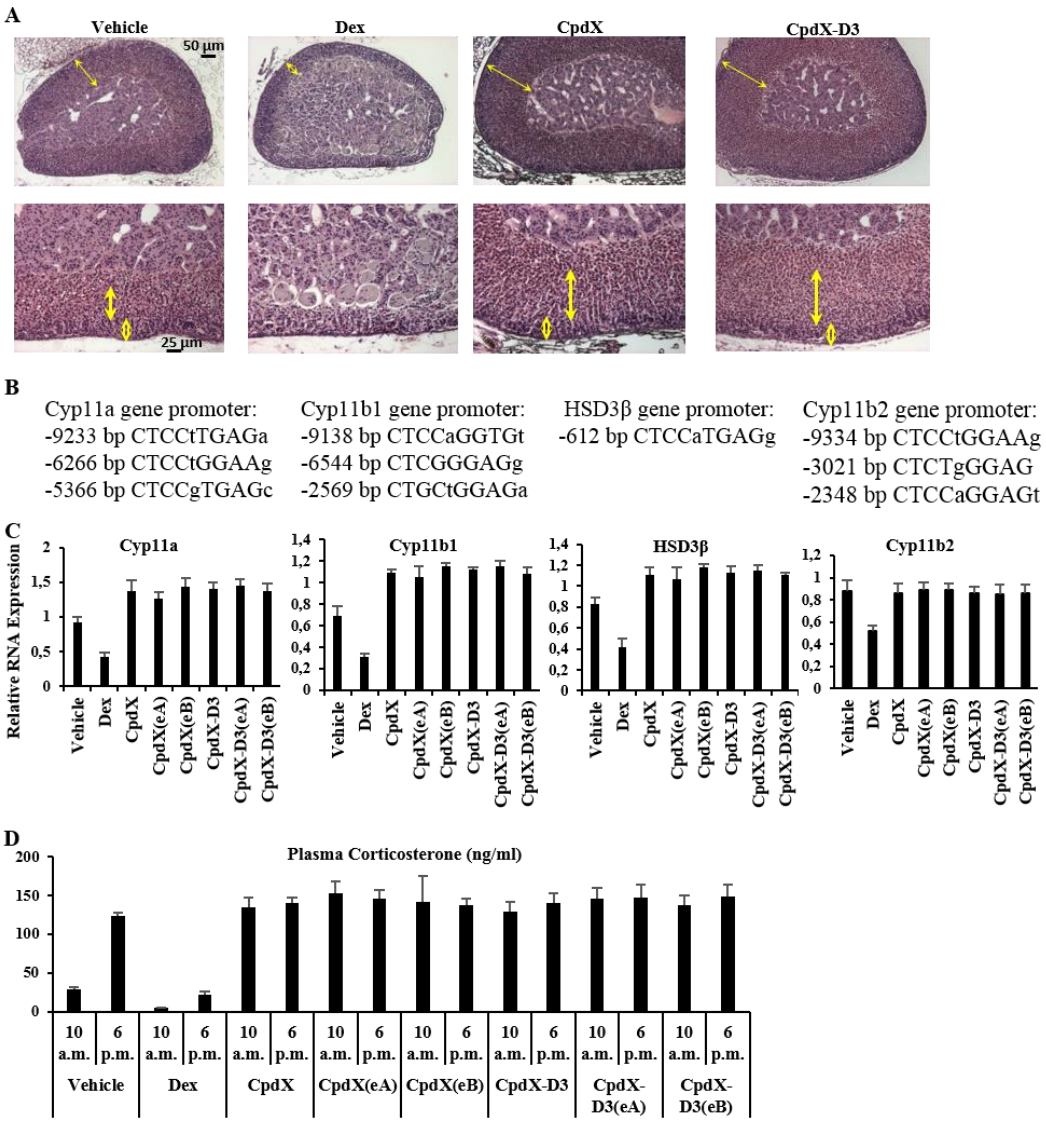
A
Vehicle
Dex
CpdX
CpdX-D3
50 µm
25 µm
B
Cyp11a gene promoter:
-9233 bp CTCCtTGAGa
-6266 bp CTCCtGGAAg
-5366 bp CTCCgTGAGc
Cyp11b1 gene promoter:
-9138 bp CTCCaGGTGt
-6544 bp CTCGGGAGg
-2569 bp CTGCtGGAGa
HSD3β gene promoter:
-612 bp CTCCaTGAGg
Cyp11b2 gene promoter:
-9334 bp CTCCtGGAAg
-3021 bp CTCTgGGAG
-2348 bp CTCCaGGAGt
C
Relative RNA Expression
Cyp11a
Cyp11b1
HSD3β
Cyp11b2
Vehicle
Dex
CpdX
CpdX(eA)
CpdX(eB)
CpdX-D3
CpdX-D3(eA)
CpdX-D3(eB)
D
Plasma Corticosterone (ng/ml)
10 a.m.
6 p.m.
Vehicle
Dex
CpdX
CpdX(eA)
CpdX(eB)
CpdX-D3
CpdX-D3(eA)
CpdX-D3(eB)

Fig. 5 In marked contrast to Dexamethasone (Dex), a three-month treatment with either CpdX, CpdX-D3 or any of their enantiomers does not induce a type 2 diabetes syndrome, nor a fatty liver.

(A) Plasmatic glucose levels after an overnight 14-hour fasting of mice treated for 3-monthes, as indicated. Data are represented as mean ± SEM for at least nine mice per treatment, as indicated. (B) 2-hour intraperitoneal glucose tolerance test (IPGTT) after a glucose i.p. injection (2 mg/kg body weight). Data are represented as mean ± SEM for at least six mice per treatment, as indicated. The statistical significance of the data as compared to vehicle treatment was calculated by student t test; (*) $p<0,05$; (**) $p<0,01$. (C) Blood insulin levels (µg/L) at 10 a.m. in mice treated for 3-monthes, as indicated. Data are represented as mean ± SEM for at least nine mice per treatment. (D) 1-hour intraperitoneal insulin tolerance test (IPITT) after an intraperitoneal injection of 0,75 U Insulin/kg body weight. Data are represented as mean ± SEM with at least six mice per treatment. The statistical significance as compared to vehicle treatment, was calculated by student t test, * $p<0,01$. (E) Western blot analyses of liver samples of mice treated for 3-monthes, as indicated for phospho-insulin receptor substrate-1 phosphorylated at serine 318 (p-IRS1 S318), pan-insulin receptor substrate-1 (IRS total), phospho-protein kinase B phosphorylated at serine 473 (p-AKT S473) and pan-protein kinase B (AKT total) proteins. (F) 5% red oil staining of frozen liver sections from mice treated for 3-monthes, as indicated. (G) Q-RT-PCR for transcripts of FASN and SCD1 genes in livers of mice treated for 3-month as indicated. The data correspond to the mean ± SEM for at least nine mice per treatment. The statistical significance was calculated by student t test; (**) $p<0,01$; (***) $p<0,001$. (H) The total cholesterol level (mmol/L) and bile acids levels (µmol/L) in blood collected at 10 a.m. from mice treated for 3-monthes, as indicated. Data are represented as mean ± SEM for at least nine mice per treatment.

Fig. 5

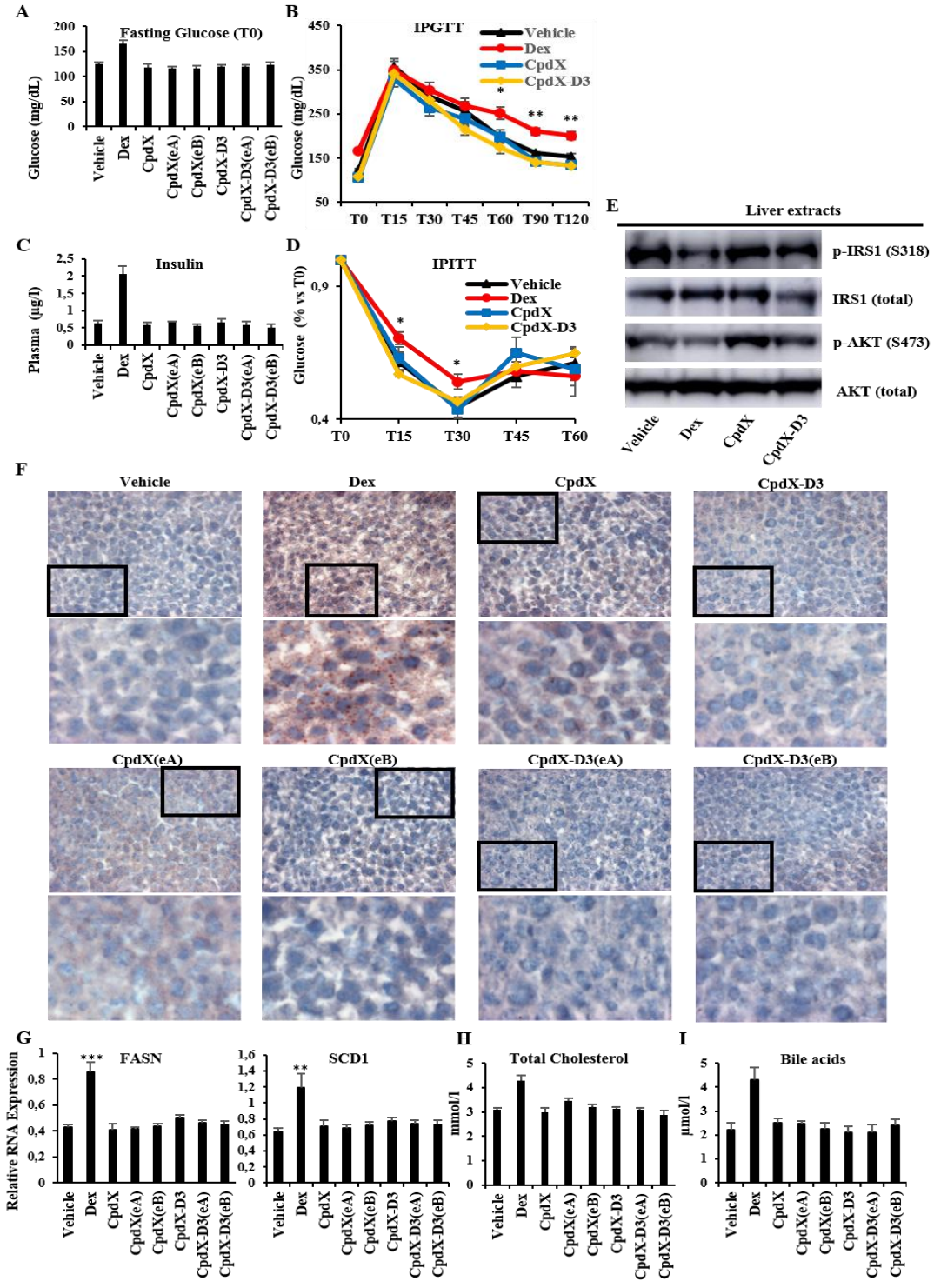
A
Fasting Glucose (T0)
Glucose (mg/dL)
200
150
100
50
0
Vehicle
Dex
CpdX
CpdX(eA)
CpdX(eB)
CpdX-D3
CpdX-D3(eA)
CpdX-D3(eB)
B
IPGTT
Glucose (mg/dL)
450
350
250
150
50
Vehicle
Dex
CpdX
CpdX-D3
T0
T15
T30
T45
T60
T90
T120
C
Insulin
Plasma (µg/l)
2,5
2
1,5
1
0,5
0
D
IPITT
Glucose (% vs T0)
0,9
0,4
T0
T15
T30
T45
T60
E
Liver extracts
p-IRS1 (S318)
IRS1 (total)
p-AKT (S473)
AKT (total)
Vehicle
Dex
CpdX
CpdX-D3
F
Vehicle
Dex
CpdX
CpdX-D3
CpdX(eA)
CpdX(eB)
CpdX-D3(eA)
CpdX-D3(eB)
G
FASN
SCD1
Relative RNA Expression
H
Total Cholesterol
mmol/l
I
Bile acids
µmol/l

UNIVERSITÉ DE STRASBOURG

Naimah ZEIN

igbmc institut de génétique et de biologie moléculaire et cellulaire

"CpdX", a non-steroidal Selective Glucocorticoid Receptor Agonistic Modulator (SEGRAM) selectively triggers the beneficial anti-inflammatory activity of glucocorticoids, but not their long-term debilitating effects

Résumé

Lors de la liaison d'un glucocorticoïde (GC) naturel ou synthétique (par exemple, la Dexaméthasone) au récepteur des glucocorticoïdes (GR), les GCs régulent l'expression de gènes cibles soit par (i) transactivation par liaison ''directe'' à un élément de liaison à l'ADN de type ''(+)GRE'', (ii) transrépression ''directe'' par liaison à un élément de type ''nGRE'' ou (iii) transrépression ''indirecte'' par interaction physique directe avec des facteurs de transcription pro-inflammatoires tels que AP-1 et NF-κB. Les effets anti-inflammatoires bénéfiques des GCs sont généralement attribués à la transrépression indirecte, alors que nombre de leurs effets secondaires pathologiques indésirables paraissent liés à la transactivation et/ou à la transrépression directe. Notre laboratoire a récemment découvert qu'un composé non-stéroïdien dénommé CpdX ainsi que ses dérivés deutérés, ne présentent ni la fonction de transactivation, ni celle de transrépression directe du GR, tout en stimulant son activité bénéfique de transrépression indirecte. Notre projet a consisté à caractériser un composé non-stéroïdien dit CpdX, ainsi que ses dérivés, quant à leurs activités thérapeutiques et à démontrer qu'elles sont semblables à celles des glucocorticoïdes anti-inflammatoires, couramment utilisés, tout en étant débarrassés de leurs effets pathologiques secondaires, tels que l'ostéoporose, l'atrophie cutanée et le syndrome métabolique. Pour atteindre nos objectifs, nous avons utilisés des modèles de souris présentant soit les affections cutanées (dermatites de contact ou atopique, psoriasis), l'asthme, l'arthrite rhumatismale, la colite ulcérative ou la conjonctivite allergique, associés à des études d'immunologie et de biologie moléculaire et cellulaire. Mon travail de thèse a démontré que CpdX, et certains de ses dérivés deutérés, présentent une activité anti-inflammatoire dans le traitement de ces modèles ''souris'' (Partie I). Nous avons aussi montré que le traitement par CpdX et ses dérivés n'induit pas les effets secondaires pathologiques des glucocorticoïdes (Partie II), ouvrait ainsi la vue à une nouvelle ère dans le traitement à long-terme de maladies inflammatoires, sans provoquer les effets pathologiques indésirables des traitements actuels aux glucocorticoïdes

Mots clés: glucocorticoïdes, récepteur des glucocorticoïdes, médicaments anti-inflammatoires, effets secondaires débilitants à long-terme, CpdX

Abstract

Upon binding of natural or synthetic glucocorticoids (GCs) (e.g. Dexamethasone) to their glucocorticoid receptor (GR), GCs regulate the expression of target genes either by (i) direct transactivation through direct binding to "(+)GRE" DNA binding sites (DBS), (ii) direct transrepression through binding to "IR nGRE" DBSs or (iii) tethered indirect transrepression mediated through interaction with transactivators, such as NFkB, AP1, or STAT3 bound to their cognate DBSs. The beneficial anti-inflammatory effects of GCs have been generally ascribed to tethered transrepression, whereas many of their long-term undesirable side-effects could be due to transactivation and/or direct transrepression. Our laboratory recently reported that a non-steroidal compound, named CpdX, selectively lacks both direct transactivation and direct transrepression functions, while still exerting an indirect transrepression activity. The goal of our project was to characterize CpdX and some of its derivatives as effective anti-inflammatory drugs similar to glucocorticoids, but lacking their main deleterious side-effects, e.g. osteoporosis, skin atrophy and metabolic disorders. To this end, we have used experimental mouse model for skin disorders (atopic dermatitis, contact dermatitis, and psoriasis), asthma, rheumatoid arthritis, ulcerative colitis and allergic conjunctivitis, combined with immunology, molecular and cellular biology. My thesis studies have demonstrated that in mouse models, CpdX and its derivatives exhibit anti-inflammatory activities, which are similar to those of glucocorticoids (Part I). Importantly, we further show that CpdX and its derivatives do not exhibit the long-term debilitating side-effects of glucocorticoids (Part II). Thereby paving the way to a new era in the long-term therapy of major inflammatory diseases.

Keywords: glucocorticoids, glucocorticoid receptor, anti-inflammatory drugs, long-term debilitating side-effects, CpdX